

ENVIRONMENT FRIENDLY CROSSLINKING OF BIOPOLYMERS AND
FABRICATION OF GREEN NANOCOMPOSITES

A Dissertation

Presented to the Faculty of the Graduate School

of Cornell University

In Partial Fulfillment of the Requirements for the Degree of

Doctor of Philosophy

by

Trina Ghosh Dastidar

May 2013

© 2013 Trina Ghosh Dastidar

ENVIRONMENT FRIENDLY CROSSLINKING OF BIOPOLYMERS AND FABRICATION OF GREEN NANOCOMPOSITES

Trina Ghosh Dastidar, Ph. D.

Cornell University 2013

Majority of the conventional plastics and composites used today are derived from petroleum, a non-renewable resource. A very high percentage of these materials end up in the landfills causing significant end of life disposal problem. Plant based natural polymers offer a sustainable, yearly renewable and environment friendly solution to the current plastic waste problem. Biodegradable polymers such as polysaccharides and proteins obtained from plants, animals and microbes are convenient and offer several advantages over petroleum-derived synthetic polymers.

In the present research environment friendly processes were developed to crosslink starches to achieve higher mechanical properties as well as lower hydrophilicity. Thermoset starch based polymer resins were developed using polycarboxylic acids as crosslinking agents, utilizing a completely 'green' water based processes. The reactivity of starches varied owing to the inherent differences in the internal structure of the starches depending on their origin.

Nanocomposites were fabricated by incorporating micro/nanofibrillated cellulose (MFC) in thermoset starch based resin. Incorporation of MFC showed significant enhancement in tensile properties (strength, stiffness and toughness) of the nanocomposites. The starch based resins were characterized for their adhesive properties for bonding wood. It was observed that the shear strength of the adhesive increased with increase in amylopectin content as well as with the increase in

crosslinking of the starch based adhesive. Studies were compared to commercially available Tite Bond 2 adhesive which is considered a superior adhesive for wood.

The research was also conducted on soy protein which also is an abundantly available biopolymer. Soy proteins are available commercially as defatted soy flour (SF), soy protein isolate (SPI) and soy protein concentrate (SPC). Of all these varieties SF, which contains about 55% protein and 32% carbohydrate, is the most easily available and inexpensive material and was used for this research. A novel, clean crosslinking reaction scheme was developed to separate the carbohydrates, modify them and use to crosslink the separated soy protein in soy flour. This process completely avoided the use of any external crosslinker. The resulting crosslinked protein was shown to have enhanced mechanical, thermal and moisture absorption properties comparable to commercially available plastics and composites.

BIOGRAPHICAL SKETCH

Trina was born and raised in Kolkata, the city of joy, in India. Inspired by her father's devotion towards science she developed a yearning for knowledge and passion for reading and learning at a very young age. Under the care and attention of parents and teachers she managed to excel in her field of study, Chemistry. She completed her undergraduate (B.S. and M.S.) in Chemistry and decided to pursue higher education. The concept of interdisciplinary research to her was extremely fascinating and she aspired to work on interdisciplinary chemistry and material science in a premier university to gradually carve out a niche for herself in the scientific community. This brought her to the Materials Science and Engineering department, Cornell University, in January 2007.

Her master's thesis comprised of work on the synthesis of monodisperse 'bent' trimer polystyrene colloidal building blocks, 1-2 μm in the largest dimension, using multi-stage seeded emulsion polymerization. Nonspherical building blocks have been shown in theoretical reports to self assemble into complex phases with strong light-matter interactions leading to the desired control of optical properties. The self assembly of these non spherical building blocks was examined using optical and confocal microscopy. She earned her M. S. degree from Materials Science and Engineering department, in 2009 under the guidance of Prof. Liddell. Trina always had a strong passion for developing polymer materials with unique properties and potential commercial applications. Her doctoral thesis focused on developing an environment friendly process to crosslink biopolymers as potential replacements for commercial petroleum based plastics and composites. Under the supervision of Prof. Netravali; she completed her doctoral work in the fall of 2012.

ACKNOWLEDGEMENTS

It has been a great privilege for me to work under the guidance of my advisor, Prof. Anil N. Netravali. His constant counsel, encouragement and unending energy level were a great motivation. I also thank my special committee members, Prof. Estroff and Prof. Wiesner for their advice and helpful suggestions that helped me sharpen the focus of my research. I am also grateful to Prof. Van Dover for his constant support and assistance.

I acknowledge support, help, and feedback from my colleagues in the Netravali group. I thank the Cornell Center for Material Science (CCMR) facility managers for their assistance in using different materials characterization facilities. I have been blessed with wonderful friends, too many to name, who have provided me with support, strength, entertainment and enlightenment over the years. My husband receives a special mention, not only has he been a dear friend and a constant source of support, he has also been a mentor to me. I have learnt much from him and this thesis would not be complete without mentioning his selfless efforts and dream to watch me succeed. Finally, I thank my parents for their infinite patience and unconditional love.

TABLE OF CONTENTS

BIOGRAPHICAL SKETCH.....	iii
ACKNOWLEDGEMENTS	iv
LIST OF FIGURES.....	vi
LIST OF TABLES	viii
LIST OF SCHEMES.....	viii
CHAPTER 1.....	1
CHAPTER 2.....	4
CHAPTER 3.....	21
CHAPTER 4.....	67
CHAPTER 5.....	90
CHAPTER 6.....	113
CHAPTER 7.....	126
APPENDIX	147

LIST OF FIGURES

Figure 1. The chemical structure of lignin is complex and an example of possible lignin structure ¹⁰	5
Figure 2. (A) PHA formation reaction catalyzed by polyester synthase (B) Copolymer of PHB and PHV (PHBV). ¹⁵	8
Figure 3. Maltotriose units forming pullulan. ³	11
Figure 4. Typical polymerization routes for PLA. ⁷	12
Figure 5. Triglyceride composed of one molecule of glycerol and three molecules of fatty acids. ⁶	15
Figure 6. Structure of chitin. ^{1,2}	17
Figure 7. Chemical structure of a typical poly ϵ - caprolactone ¹²	17
Figure 8. The chemical structure of mandelic acid	19
Figure 9. α -D-glucopyranose.....	23
Figure 10. Chemical structures of (a) amylose and (b) amylopectin molecules. ¹³	24
Figure 11. Structures of the A- and B-granules of starch. ¹⁸	26
Figure 12. Cross-section of a starch granule showing the orientation of amylopectin double helices. ¹⁴	27
Figure 13. Topographic image of native starch showing growth rings ⁴	28
Figure 14. Unit cell of retrograded amylose film. ⁹	30
Figure 15. Mechanism of dry crosslinking of cellulose with polycarboxylic acid. ¹⁶	35
Figure 16. Mechanism of reaction of starch with epichlorohydrin. ¹⁷	37
Figure 17. Mechanisms of starch phosphorylation showing (A) formation of monostarch phosphates ¹¹ and (B) crosslinking by formation of distarch phosphates. ¹⁹	40
Figure 18. Structure for hydroxypropylated starch.	52
Figure 19. Proposed scheme for crosslinking starch with MA.....	69
Figure 20. (A) The ATR-FTIR spectra of gelatinized PS, MA, blend of native PS and MA and PS crosslinked (cured at 120°C at 2000 lb for 20 min) with 37.5% MA (B) Extent of esterification of PS and CS as a function of initial MA content, using the internal calibration curve.....	76
Figure 21. DS of (A) precured PS and CS as a function of MA concentration (B) PS (precured with 37.5% MA at 90°C for 60 min) as a function of curing temperature.	77
Figure 22. WXR patterns of native PS and CS powders, MA and gelatinized and crosslinked CS.....	80
Figure 23. (A) the swelling power of crosslinked PS (cured at 120°C and 0.1 MPa for 20 min) with 15%, 25% and 37.5% initial MA concentration, in water (B) the swelling power of crosslinked PS (cured at 120°C and 0.1 MPa for 20 min) with 15%, 25% and 37.5% initial MA concentration, in DMSO and (C) the gel fraction of crosslinked PS (cured at 120°C and 0.1 MPa for 20 min) with 15%, 25% and 37.5% initial MA concentration, DMSO.	83
Figure 24. (A) DSC thermograms of MA and native, precured and cured PS heated from 25°C to 260°C at 25°C/min (B) DSC enthalpy values for moisture absorption for PS specimens	

precured with different MA concentrations (C)Thermal degradation behavior of MA and (D) TGA of PS powder and cured PS (with 37.5% MA).	84
Figure 25. Tensile stress-strain curves of (A) gelatinized CS and PS, (B) gelatinized, precured and cured PS.....	87
Figure 26. A) FTIR of WMS, BTCA and ester of WMS formed with BTCA; (B) Extent of esterification of WMS as a function of initial BTCA content, using the internal calibration curve.....	98
Figure 27. Swelling power of WMS crosslinked with BTCA in water and DMSO as a function of BTCA concentration.....	100
Figure 28. Stability of crosslinked composite in water.....	101
Figure 29. Tensile properties of WMS resin and composite.....	102
Figure 30. SEM images of A. Pregelatinized WMS granules B. MFC fibers. ⁸	107
Figure 31. SEM images (A). Fracture surface of crosslinked WMS, (B). BTCA wetting MFC network and (C). Schematic of MFC-WMS composite showing the network structure of MFC incorporated in starch based resin.....	108
Figure 32. SEM images of MFC-WMS crosslinked composites.....	109
Figure 33. DTGA of WMS. Crosslinked WMS, MFC (15%)-crosslinked WMS composite.....	111
Figure 34. (A) Surface wetting and Contact angle (B) Wetting of starch on the surface of wood substrate.....	116
Figure 35. The adhesive (A) shear and (B) tensile strength test specimens (C) Picture of modified clip binder as a holder for Instron. ⁵	118
Figure 36. Effect of starch variety on the adhesion strength in shear	120
Figure 37. (A) Diagram showing how application of weight helps in penetration and spreading of adhesive (B) Effect of application of weight on the strength of the gelatinized WMS based adhesive.....	122
Figure 38. Increase in shear strength with increase in curing temperature.....	124
Figure 39. FTIR spectra of sugars (glucose, sucrose and SFE) and oxidized sugars.....	138
Figure 40. FTIR spectra of SPI and SPI+oxidized sucrose (crosslinked SPI).....	139
Figure 41. FTIR spectra of SF resin and crosslinked SF resin.....	140
Figure 42. Changing of color from pale yellow (beige) to dark red color with the progression in Maillard reaction between amine groups in amino	141
Figure 43. Results of the sol-gel test: SF film, disintegrated, (right) and crosslinked SF, only partially disintegrated, (left).....	142
Figure 44. TGA of SF and crosslinked SF.....	143
Figure 45. Epoxy functionalized silica nanoparticles.....	148
Figure 46. Starch like crosslinking of WMS chains with surface functionalized nanoparticles.....	149
Figure 47. NMR spectra comparing WMS epoxy functionalized silica nanoparticles (GlymoNP), nanocomposite (or hybrid) of WMS and GlymoNP, physical mixture of WMS and glymo NP.....	154

Figure 48. ATR-FTIR spectra comparing neat WMS resin, GlymoNP(1%)-WMS and GlymoNP(5%)-WMS nanocomposites.	155
Figure 49. Solution of (A) neat resin (WMS) and (B) nanocomposite: both transparent indicating homogeneous distribution of nanoparticles and no clustering or coagulation (C) WMS resin and GlymoNP(1%)-WMS composite film soaked in water: WMS resin is completely soluble while GlymoNP(1%)-WMS nanocomposite is insoluble indicating crosslinking or formation of strong network structure.	156
Figure 50. TEM image of GlymoNP(1%)-WMS and GlymoNP(5%)-WMS nanocomposites.	157
Figure 51. (A) TGA, (B) DTGA for WMS resin and GlymoNP-WMS nanocomposite films.	159
Figure 52. DSC thermograms DSC plots for WMS resin and GlymoNP-WMS nanocomposite films.	160

LIST OF TABLES

Table 1. The tensile properties such as Young's modulus, tensile stress at maximum load and strain (%) at maximum load of gelatinized CS and PS, precured and cured PS films.	86
Table 2. Mechanical properties of WMS and MFC-WMS (crosslinked) composites as a function of sorbitol (%).	103
Table 3. Mechanical properties of MFC-crosslinked WMS composites as a function of MFC loading.	103
Table 4. Tensile strength of gelatinized and crosslinked WMS based adhesives.	124
Table 5. Initial degradation temperatures of SF and crosslinked SF.	143
Table 6. Young's modulus, fracture stress and fracture strain of SF and crosslinked SF resin films.	144

LIST OF SCHEMES

Scheme 1. Crosslinking of SF using a novel three step process	129
Scheme 2. Proposed reactions for oxidation of glucose.	134
Scheme 3. Proposed reactions for oxidation of sucrose.	135
Scheme 4. Crosslinking reaction of WMS with epoxy functionalized silica nanoparticles. ...	153

CHAPTER 1

INTRODUCTION

Majority of the conventional plastics and composites are derived from petroleum, a non-sustainable resource. They may also utilize hazardous and toxic synthetic procedures that could be harmful to humans as well as nature. At the end of their life over 90% of these plastics and composites are discarded in landfills. Plant based natural polymers, on the other hand, offer a sustainable, yearly renewable and environment friendly solution to the problem of plastic waste. Biodegradable polymers such as polysaccharides and proteins obtained from plants, animals and microbial sources are convenient and offer several advantages over petroleum-derived synthetic polymers.

This dissertation investigates the fabrication of crosslinked biopolymers (starches and soy protein) based resins and composites. Chapters one and two provide comprehensive literature review on green resins and the physical and chemical modification of native starches for improving resin and film forming properties.

Chapter three and four describe the fabrication of crosslinked starch based resins and composites based on them. An environment friendly process has been developed to crosslink starches to achieve the desired higher mechanical properties as well as lower hydrophilicity. The appropriate processing conditions for the fabrication of starch based composites have been identified and optimized by studying the fundamental structure and property relationships of starch based resins. The effects of starch variety (rice, corn, potato, etc.), starch granule morphology, crystallinity and molecular composition of the polymers on the mechanical, rheological and water absorption properties were also investigated. Crosslinked starch resins were developed using polycarboxylic acid based crosslinking agents - particularly malonic acid (MA) and 1, 2, 3, 4- butane tetracarboxylic acid (BTCA). These acids are nontoxic, relatively inexpensive and were used instead of commercially available toxic and synthetic crosslinkers such as epichlorohydrin. The reactivity of starches varied owing to the inherent differences in the internal structure of different starch varieties. Crosslinking was confirmed by various

techniques such as calculation of gel (crosslinked) fraction, swelling power measurements and mechanical testing. Young's modulus of potato starch crosslinked with MA was close to 2.7 GPa which is much higher than the earlier reported values for starch crosslinked with epichlorohydrin (≈ 100 MPa) and was comparable to commercially available epoxy based resins.

In order to fabricate starch based nanocomposites with enhanced mechanical properties, waxy maize starch (WMS) was crosslinked with BTCA. WMS is a genetically modified starch variety with high amylopectin content which leads to better reactivity and film forming properties (defect free, smooth, continuous and transparent films). Nanocomposites were prepared by dispersing halloysite nanotubes (HNT) and micro/nanofibrillated cellulose (MFC), separately. A critical step in this process was to obtain a nanocomposite with nanoparticles uniformly dispersing in the resin using various methods that included surface modification of the nanoparticles, high speed mechanical shearing and ultrasonication. As expected, incorporation of MFC showed significant enhancement of mechanical properties owing to the chemical compatibility of starch and cellulose resulting in excellent bonding between them. Other properties, such as high fracture stress and Young's modulus (140 GPa) of the MFC fibrils as well as their high aspect ratio, network like structure and broad range of size distribution of the fibers contributed to improving the mechanical properties. Crosslinking of WMS helped in reducing the hydrophilicity and swelling power of the resin as well as increased the stability of the resins in water as was expected. However, tensile testing of the crosslinked WMS films without the presence of a plasticizer (such as glycerol or sorbitol) was impossible, owing to the brittleness of the films, which is common to highly crosslinked polymer systems. Incorporation of MFC as reinforcing fillers assisted in the fabrication of stiff and strong nanocomposite films even without the use of a plasticizer. Addition of plasticizer increased the fracture strain of the polymer films but also reduced the Young's modulus and glass transition temperature by adding free volume to the polymer network. Incorporation of MFC improved the toughness of the composite films without compromising the Young's modulus.

Chapter five presents the adhesive properties of starch based resins on wood and paper. The adhesive shear strength of these bioadhesives was tested to develop polymeric adhesive from renewable resources. Studies were conducted to optimize conditions to replace commercially available urea formaldehyde and phenol formaldehyde based resins with the biopolymer based adhesives. It was observed that the shear strength of starch based adhesives increased with increase in the amylopectin content as well as with increase in crosslinking.

Chapter 6 presents a novel crosslinking reaction scheme to crosslink the soy protein present in soy flour, without using any external crosslinker resulting in improved mechanical properties and stability in water. Soy protein is an abundant and worldwide available biopolymer. Soy products are commercially available as defatted soy flour (SF), soy protein isolate (SPI) and soy protein concentrate (SPC). Of all the different varieties of soy products SF, which contains about 55% protein and 32% carbohydrate, is the most easily available and least costly variety and was used for this research. Soy protein consists of 18 different polar and nonpolar amino acids. Polar amino acids like cysteine, arginine, lysine and histidine can be used for chemically crosslinking the proteins to improve the material properties such as mechanical strength, thermal properties as well as reduce water solubility and hydrophilicity. It has been reported that soy protein undergoes crosslinking with aldehydes including formaldehyde, glutaraldehyde (GA), glyoxal and glyceraldehyde using Maillard-type chemistry. However, owing to the cytotoxicity of the above mentioned aldehydes, there is always a search for a greener alternative. In the present research a novel, clean crosslinking reaction scheme was developed to crosslink the soy protein present in soy flour, by modifying the carbohydrates (sugars) present in soy flour. For this, the first step consisted of separating protein in soy flour from carbohydrates. The second step consisted of chemically modifying the carbohydrates to obtain aldehyde and carboxyl groups and the final step consisted of reacting the modified carbohydrates with the separated protein. The crosslinked protein resulted in significantly enhanced mechanical and thermal properties as well as reduced moisture absorption. These enhanced properties were comparable to commercially available plastics and composites.

CHAPTER 2

BIOPOLYMERS AS RESINS FOR FABRICATION OF FILMS AND NANOCOMPOSITES

Green resins

Majority of the conventional plastics and composites that are used in day-to-day applications are derived from petroleum based resources utilizing hazardous and toxic synthetic procedures that are harmful to nature. Plant based natural polymers offer a renewable and environment friendly solution to the problem of plastic waste. Biodegradable polymers such as polysaccharides and proteins obtained from renewable resources such as plants, animals and microbial sources are convenient, environment friendly and offer several advantages over petroleum-derived synthetic polymers.

Green resins are polymers derived from sustainable plant based materials and processed using green technology. Their properties can be enhanced using sustainable and non-toxic chemicals as plasticizers, crosslinkers and other additives. Plant based sources for polymers are widely available throughout the world and are plentiful as well. Most of these sources are also considered to be carbon neutral. Further, it should be possible in the future to process them using energy derived from sustainable sources to make them 'truly green' in every sense. Such green resins usually tend to be both biodegradable and compostable. So they need not end up in landfills at the end of their life as most of the petroleum based resins do.

Green resins can be divided into three categories depending on the way they are derived, as briefly described in this chapter. The first category consists of plant synthesized biopolymers that are naturally available in the polymeric form. Starch, cellulose, hemicellulose, lignin, rubber and proteins are primary examples of this category. The resins in the second category are produced from microorganisms through fermentation. Microorganisms used in such fermentation processes are commonly fed with naturally occurring polymers such as cane and other sugars and starch or compounds such as lipids that are derived from plants and malt waste

as inexpensive carbon sources. Polyhydroxyalkanoates (PHAs), their copolymers and pullulan are examples of biopolymers produced using microbial fermentation technologies. Cellulose has also been produced using *Acetobacter xylinum* that secretes nanocellulose fibers during the fermentation using simple sugars. The third category of resins consists of biopolymers that are produced by polymerization of naturally occurring monomers or low molecular weight molecules that are derived from plant based sources. Polylactic acid (PLA) (from cane sugar, corn, etc.) and polymers derived from triglycerides (oils) are examples of such polymers. Some commonly used green polymer resins including lignin, PHAs, PLA and polybutylenesuccinate, are briefly described in this chapter. Starch based resins and their modifications are described in much greater depth in the next chapter.

Lignin

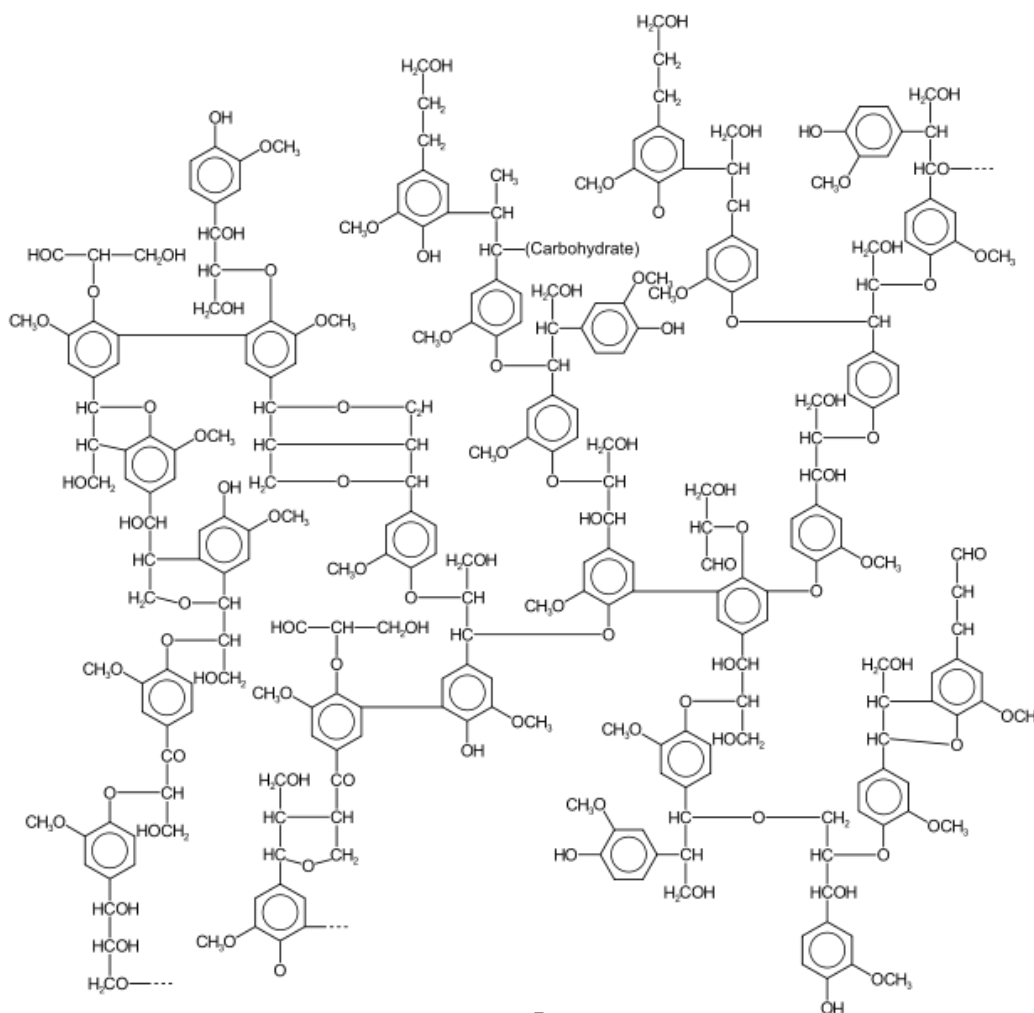


Figure 1. The chemical structure of lignin is complex and an example of possible lignin structure¹⁰

Lignin, as an integral part of the secondary cell walls of plants, makes up about 20% of a typical plant. It is the second most abundant component of woody material after cellulose and constitutes from 25 to 33% of the dry woody mass. The chemical structure of lignin is complex and an example of possible lignin structure is provided in **Figure 1**.¹⁰ While this is a possible structure, it should be made clear that a wide range of structures are possible.

Lignin is relatively hydrophobic and aromatic in nature. However, it can be seen from **Figure 1** that it does contain hydroxyl groups, which are necessary for bonding with cellulose, hemicellulos, pectin, etc., which are also present in the wood and together for a composite structure. It is resistant to biodegradation because of its highly crosslinked structure, aromatic nature as well as internal H-bonding. Three monolignol molecules; p-coumaryl alcohol, coniferol alcohol and sinapyl alcohol, methoxylated to various degrees, are incorporated in various ratios to form the complex structure of lignin. It is considered as a family of heterogeneous biopolymers resulting from the enzymatic polymerization of the above mentioned coniferous alcohol monomers giving rise to complex, amorphous and three dimensional polymers.²⁰ Being largely complex and crosslinked hydrocarbonaceous structure it is mostly amorphous. Lignins bind, stiffen and fortify the secondary plant cell walls within the xylem tissues providing mechanical support and stiffness to the plant cells by binding the cellulose microfibrils within the dense crosslinked matrix as in composites.²¹ Lignin also provides protection of the plant carbohydrates against attack by microorganisms or insects due to its phenolic and aliphatic composition. Being hydrophobic lignin also protects plants from the water damage. Since all plants contain lignin it is a common byproduct of chemical manufacturing of paper from cellulose. As a result, it is an abundantly available biomaterial. About 1.1 million metric tons of lignin is produced globally every year¹⁰. While most of it is burned as fuel, a small amount is used for industrial applications from adhesives to concrete mixtures.²² It has also been extensively used as an adhesive for wood.²³

Commercially used lignosulfates are derived as coproducts of wood-pulping industries and are a mixture of sulfonated lignins and other wood derivatives. They can be chemically or

physically modified to produce specialty materials for industrial purposes. Some specialty uses involve pesticide formulations, retarders in oil well cements, as stucco dispersants in the manufacture of gypsum boards, dispersants in water based paints and ink, dispersants and scale deposit inhibitors in water treatment, as emulsion stabilizers and as industrial cleaners.²⁰

Kraft lignin produced during the conversion of wood to pulp for paper production has also been used for making thermoplastic polymers.²⁴ The conversion of lignin into plastic products depends on their phenolic group and the frequency of hydroxyl groups which is their main functionality. However, since the structure of lignin itself is very complex, as seen in **Figure 1**, it is not so easy to derivatize lignin to form polymeric materials with reproducible properties. In a recent study alkylated 100% kraft lignin polymers were shown to possess promising mechanical properties such as Young's modulus of 1.9 GPa and tensile strength in the range of 37 MPa.²⁴ These properties are better than the commonly used polyethylene and comparable to polypropylene properties.²⁵ Tecarno, a German company, has refined the technique to produce plastic like pellets from kraft lignin by forming a composite with fibers and wax. These composite materials behave like melted plastic in a high pressure environment and can be processed using injection molding techniques.²⁵ Chemically modified (methyolated) lignin has been used to substitute phenol formaldehyde as adhesives for wood pulp. Lignin and its derivatives are also used for coating and forming composites because of the small particle size, hydrophobicity and ability to form stable mixtures.²⁶

Polyhydroxyalkanoates

Polyhydroxyalkanoates (PHAs) are linear aliphatic polyesters produced by bacterial fermentation in a medium containing excess of carbon source.²⁷ Polyester synthases are key enzymes for catalyzing the biosynthesis of PHA. PHA formation reaction catalyzed by polyester synthase is shown as **Figure 2 (A)**.²⁷ The polyesters are deposited as cytoplasmic inclusions from different gram-positive and gram-negative bacteria.²⁷ In the absence of nitrogen, phosphorus and oxygen in the culture medium, PHAs are accumulated as reserve food materials and account for up to 90% of the dry weight of the microbes. Bacteria synthesizing PHA can be

broadly subdivided into two groups. The first group of bacteria that includes *Acalegenis eutropus* synthesizes short chain PHAs with C3-C5 monomers and the second group that includes *Pseudomonas oleovorans* synthesizes C6-C14 monomers. While polyhydroxybutyrate (PHB) is the most commonly produced PHA, copolymers of different PHAs consisting of monomers with different carbon chain lengths have also been produced.¹⁵ The carbon chain length of the monomer (typically C3-C5) depends on the type and quantity of carbon sources supplied to the growth media.

Addition of propionic acid or valeric acid to the growth media containing glucose leads to formation of random copolymer of 3-hydroxybutyrate (3-HB) and 3-hydroxyvalerate (3-HV).¹⁵ Biopol is a commercial polymer composed of random copolymer of 3-HB and 3-HV.¹⁵ Such copolymer structure of PHB and PHV (PHBV) is shown in **Figure 2 (B)**.¹⁵

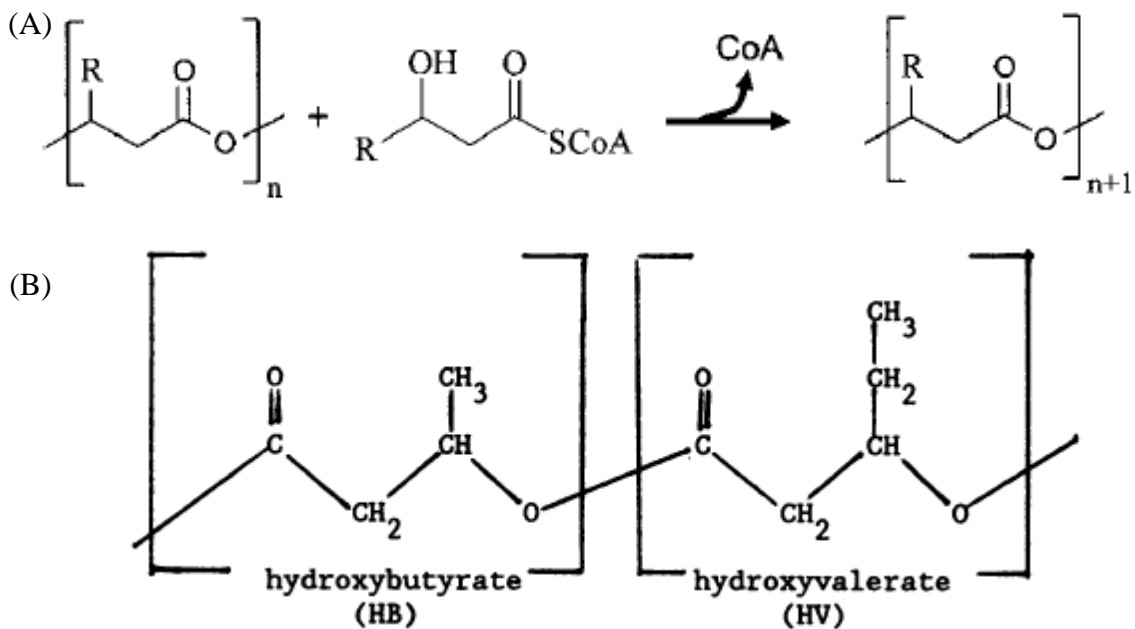


Figure 2. (A) PHA formation reaction catalyzed by polyester synthase
(B) Copolymer of PHB and PHV (PHBV).¹⁵

For industrial production of PHA, waste water or sludges activated with microbes are being considered as alternative sources of fermentation. Such methods are expected to reduce the cost of production significantly and promote their use. Mixed cultures of bacteria that can grow in low intensity aeration and produce high quantity of PHA in a short time are being studied at present.⁶ Companies such as Metabolix in Cambridge, MA, are commercializing the production of PHA from renewable feedstocks such as cornstarch, cane sugar, cellulose hydrolysate, and vegetable oil.²⁸ Tephra Inc., a biomedical device company based in Lexington, MA, has developed and commercialized innovative technologies (e.g. recombinant fermentation) to produce PHAs using microorganisms.¹ PHAs are used in medical devices such as surgical sutures, meshes and films, composite meshes and devices for ligament repair, intracardiac defect closure, and absorbable cardiovascular stents.¹

While PHAs are biodegradable thermoplastics and are comparable to polypropylene in properties, PHB is stiff and brittle. PHB and PHBV have tensile strengths of about 40 MPa, comparable to that of polypropylene (38 MPa). The melting point (T_m) of PHB and polypropylene are also similar being 176°C for PHB and 175°C for polypropylene.²⁹ Being a saturated ester, PHB is hydrophobic, water insoluble and resistant to hydrolytic degradation.¹⁵ PHB also has good UV resistance. However, it is soluble in chloroform and other chlorinated hydrocarbons.¹⁵ Combining PHV and PHB to form a copolymer leads to reduction in crystallinity, stiffness and increase in toughness.²⁹ Addition of 24% PHV to PHB was also shown to significantly increase the impact strength from 25 J/m to 300 J/m.³⁰ However, PHBV has a glass transition temperature (T_g) around room temperature that results in changes in its crystallinity when aged at room temperature.³¹ Due to these changes the mechanical and physical properties change as well. Copolymers of PHB and PHV (PHBV) are easier to process and therefore used commercially. However, because of their high cost, they are used only in niche applications.

PHBV has been processed using injection molding, blow molding, extrusion and also to produce extruded sheets, films, paper coatings and fibers. Typically PHBV with 10% HV show a T_m of 140°C, crystallinity of 60%, tensile strength of 25 MPa, flexural modulus of 1.2 GPa, 20% fracture strain and Notched izod impact strength of 110 J/m.³⁰ PHBV is completely biodegradable in microbially active environments such as compost.^{30, 32} As a result, paper plates, cups, bowls, etc., coated with thin PHBV film have been tried successfully as 'green' compostable replacement for Styrofoam and other non-degradable plastic based plates and bowls. Rate of biodegradation of PHBV depends on surface area, microbial activity of disposal environment, pH, temperature, moisture level and presence of other nutrient materials.³⁰ Based on these results it is clear that PHVB can biodegrade in environments such as normal soils, river water, sea water, aerobic and anaerobic sewer sludges. The biocompatibility of PHVB allows it to be blended with other biopolymers such as polycaprolactone to enhance their properties further while retaining their biodegradability. PHBV and blended polymers may be used as resins to form 'green' composites using different naturally available cellulose fibers as reinforcing agents.³¹⁻³⁴ Owing to its biodegradability PHVBs are also used as packaging materials and its biocompatibility allows it to be used in biomedical applications like reconstructive surgery.

Pullulan

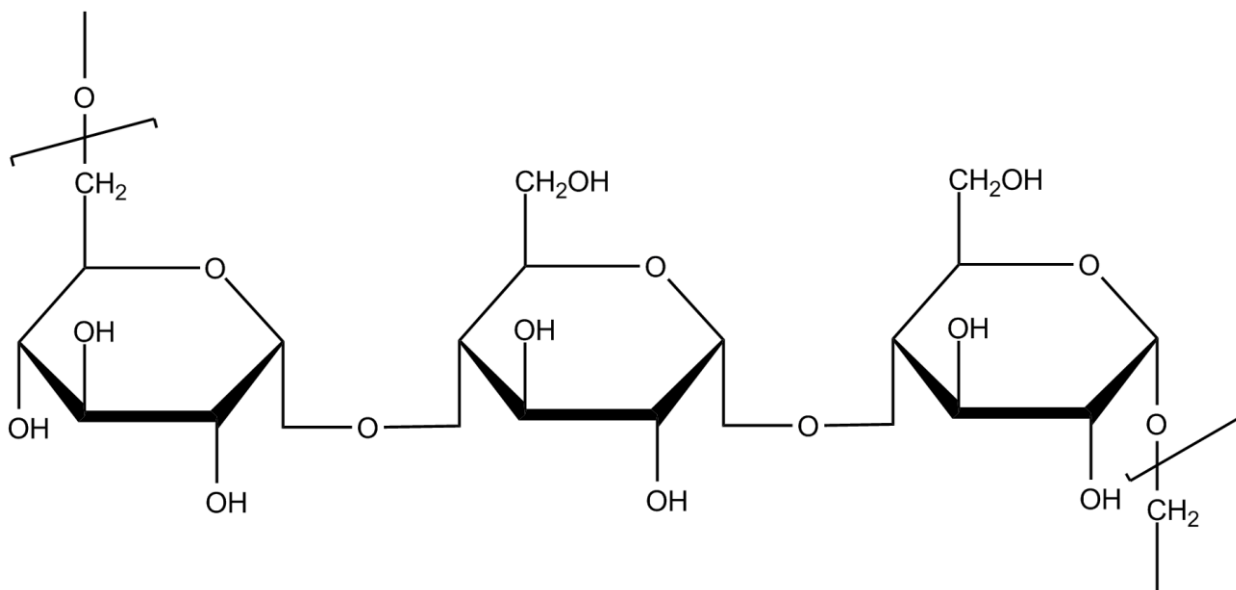


Figure 3. Maltotriose units forming pullulan.³

Figure 3 shows maltotriose units forming pullulan.³ It is a polysaccharide produced by yeast like fungus called *Aureobasidium pullulans*, from starch.³ *A. pullulans* exhibit phenotypic plasticity which means these organisms can change in response to change in the environment.³⁵ The variations depend on the type of carbon sources (sugars or alcohols), age of the fungus colony, incubation temperature, light cycle and carbon source type. Pullulan is mainly used as a food additive to enhance its bulk and texture. However, it can also be used as a resin for molded products.³⁶ Because of its water sensitivity, in such applications it needs coating of water insoluble thermosetting resins (such as polyurethanes, unsaturated polyester, epoxy resin, etc.). In this application, properties of pullulan such as transparency, toughness, gas impermeability and non-toxicity are retained.³⁶ Pullulan has been blended with polymers such as PVA to improve the mechanical properties. The tensile strength was found to increase with increase in PVA content from 20% (20 MPa) to 80% (100 MPa).³⁷

Poly(lactic acid)

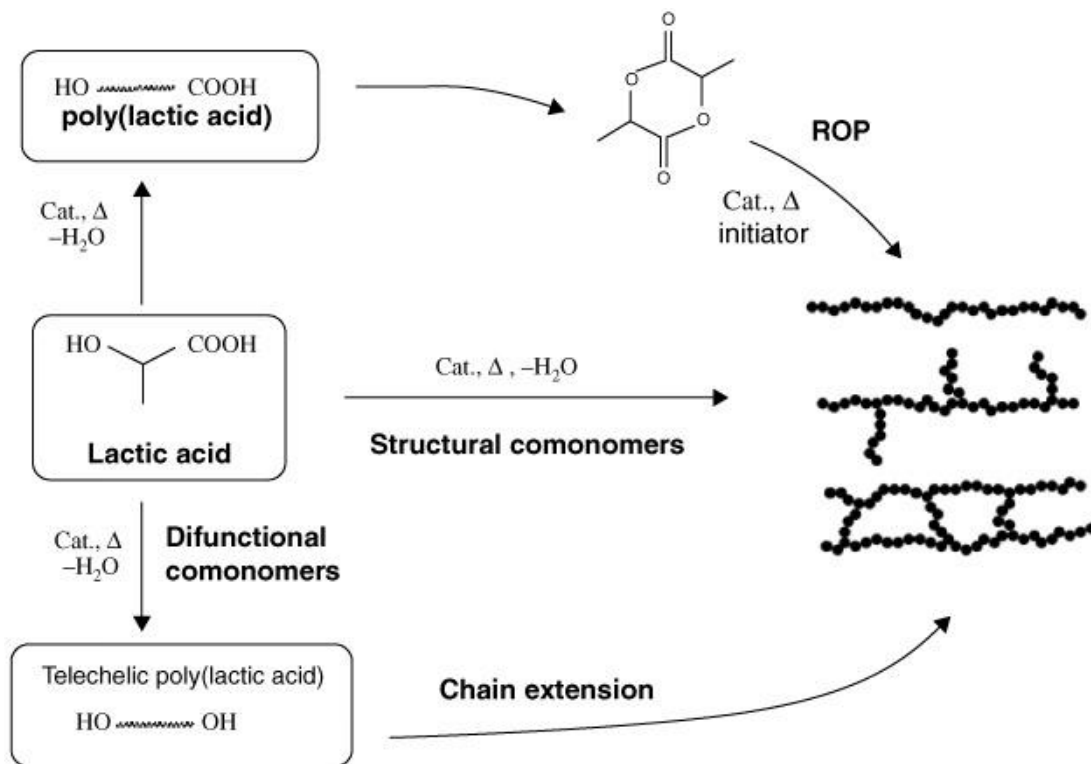


Figure 4. Typical polymerization routes for PLA.⁷

Poly(lactic acid) (PLA) is a biopolyester prepared using lactic acid as the monomeric unit. Lactic acid itself is made by fermentation process of renewable resources such as sugar obtained from corn and sugarcane. The preparation of PLA involves either direct condensation of lactic acid into a polymer and/or opening of the cyclic lactide dimer.⁷ Typical polymerization routes for PLA are presented in **Figure 4**.⁷

Lactic acid (α -hydroxypropionic acid) is a hydroxyacid that exists in enantiomeric form due to presence of an asymmetric carbon atom.³⁸ The L-stereoisomer (PLLA) is the one most commonly occurring in nature while the D-stereoisomer (PDLA) is produced synthetically.³⁹ Lactic acid is produced by bacteria, fungi or yeast.^{40, 41} Commercially high yield of lactic acid is obtained through bacterial fermentation of renewable sources including carbohydrates such as corn starch, tapioca products and sugarcane using *lactobacillus*. Lactic acids can form PLA by reaction between the hydroxyl and carboxyl groups of lactic acid forming an ester group and

eliminating water (condensation product). Condensation polymerization is an equilibrium reaction and removing water is important for the equilibrium reaction to proceed only in the forward direction.⁴²

Condensation polymerization of lactic acid to PLA involves three stages. However, a fourth stage may be used to obtain polymer with higher molecular weight. In the first stage, to convert lactic acid to PLA, the free water that may be present in the feed stock is removed, usually by evaporation. Due to occurrence of depolymerization (equilibrium between lactic acid and water) reaction there is difficulty in achieving high molecular weight polymers in the presence of water. In the second stage, water is removed when the lactic acid is converted to low molecular weight PLA or oligomeric species of lactic acid. In the commercial processes catalysts are commonly used to increase the rate of the reaction. Traditionally, strong acids and organometallic compounds are used as catalysts for condensation reactions. The third stage involves melt polycondensation by removal of water to obtain high molecular weight PLA.^{43, 44} The rate determining step of this reaction is the removal of water which can be aided by carrying out the reaction in vacuum or maintaining an inert atmosphere. Removal of water is critical to drive the reaction in the forward direction as well as to ensure polycondensation reaction instead of transesterification reaction.^{43, 44, 42}

Sometimes, to obtain higher molecular weight PLA, a fourth stage is used in which the melt-polycondensate PLA is cooled below its melting temperature and allowed to crystallize.⁴² This leads to separation of the solidified PLA into two phases, crystalline and amorphous. The reactive groups and the catalysts are thus concentrated in the amorphous phase leading to an enhancement of the reaction rate.⁴²

Another method, the azeotropic dehydration method, is often used to replace the melt polycondensation stage in the PLA synthesis.⁴² In the azeotropic dehydration method, the polycondensation reaction is performed in a solution containing dry organic solvents such as methanol, ethanol, acetic acid or pyruvic acid. The water generated during the reaction along with the organic solvent is removed by drying agents such as molecular sieves, phosphorus

pentoxide or metal hydrides.⁴² The advantage of using this method is that the synthesis can be performed in a lower viscosity medium due to presence of the solvent. On the other hand, in the melt polycondensation method, due to formation of the high molecular weight PLA, special apparatus is required to handle the high viscosity mass.⁴²

In order to make high molecular weight PLA, ring opening polymerization (ROP) in the presence of a catalyst may be a more preferred method.^{42, 45} In this method, lactic acid dimer known as lactide is polymerized through ROP to produce PLA. As precise control on the chemistry is possible in the ROP method, the properties of the resulting polymers can be varied in a precise manner as desired. This process has been commercialized by NatureWorks LLC (Blair, Nebraska) which produces 300×10^6 lbs of PLA/year, under the trade name of Ingeo, mainly for making fibers (apparel and carpet), silverware and packaging materials.⁴⁵⁻⁴⁸ It can be thermoformed and foamed. PLA is a promising material to reduce environmental pollution by reducing the waste disposal problem owing to its biodegradability and compostability. Other than packaging, PLA has also been used for agricultural, engineering and compostable product application where, biodegradability is needed. Commercially, PLA has also been used for biomedical applications.⁴⁶ While PLA is fully biodegradable, it has relatively strong mechanical properties which make it suitable for applications like medical implants. Semicrystalline PLA has a tensile modulus in the range of 3 GPa, tensile strength of 50–70 MPa, flexural modulus of 5 GPa, flexural strength of 100 MPa and an elongation at break of about 4%.^{46, 49} PLA is a versatile material and can be processed into different grades of resin for a variety of products. PLA can be processed using drying, extrusion, injection molding, film and sheet casting, blow molding and electrospinning techniques into nanofibers.⁴²

PLLA, has a crystallinity of 37% and a tensile modulus of PLLA varies between 2.7-16 GPa. It has a low T_g of around 65°C and T_m of around 175°C. As a result, cups made using this material cannot withstand hot liquids. The T_m of PLLA can be increased by about 45°C by physically blending PDLA and PLLA.⁵⁰ Together they form a highly regular stereocomplex with increased crystallinity. The temperature stability is maximized when a 50:50 blend is used.

However, even at substantially lower concentrations of 3-10% of PDLA, significant improvement can be obtained. When present in low concentrations, PDLA is seen to act as nucleating agent, thereby increasing the crystallization rate.⁵⁰ However, the rate of biodegradation is reduced as the crystallinity is increased. Stereocomplex blends of PDLA and PLLA are stable and transparent and are used for the manufacture of microwavable trays and engineering plastics (by blending with other rubber like polymers like acrylonitrile butadiene styrene). PLA is fully biodegradable and hence finds application in production of bioplastics, compostable bags, nonwoven textiles and disposable garments. PLA is currently also used in several biomedical applications such as sutures, stents, dialysis media and drug delivery devices.⁵⁰

Polymers of triglycerides

Triglyceride is an ester obtained from one molecule of glycerol and three molecules of fatty acids.⁶ **Figure 5** presents triglyceride composed of one molecule of glycerol and three molecules of fatty acids.⁶

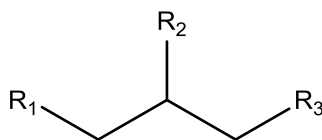


Figure 5. Triglyceride composed of one molecule of glycerol and three molecules of fatty acids.⁶

Triglycerides are the main constituents of vegetable oil and animal fat. Vegetable oils are lipids extracted from plants, mostly seeds. Commonly used triglyceride oils for synthesis of oil-modified resins are linseed, sunflower, castor, soybean, palm and rapeseed oils.⁶ Fatty acids are 14-22 carbons in chain length and may or may not contain double bonds. There are different kinds of fatty acids, saturated (no double bond), unsaturated (with double bonds), conjugated (double bond alternate between carbon atoms) or isolated (double bonds are separated by at least two carbon atoms in the carbon chain).²⁸ Additionally some fatty acids may contain hydroxyl, epoxy, oxo groups or triple bonds leading to a vast array of structural differences and a wide

range of properties .^{6, 28} The polymers of triglycerides usually exhibit modulus in the range of 1-2 GPa and glass transition temperature of 70-120°C.²⁸ The biggest uses of triglyceride oil based polymers are in the coating industry.

Chitin

Chitin is a polysaccharide, a glucose derivative. It is a long chain polymer consisting of N-acetylglucosamine units.^{1, 2} These units form covalent β -1,4 linkages (similar to the linkages between glucose units forming cellulose). Therefore, chitin may be described as cellulose with one hydroxyl group on each monomer substituted with an acetyl amine group. This allows for increased hydrogen bonding between adjacent polymers, giving the chitin-polymer matrix increased strength.⁵² The structure of chitin is shown in **Figure 6**.^{1, 2} Chitin is a biopolymer found in the skeletal tissue of marine crustaceans, cell walls of fungi, exoskeleton of insects and other arthropods and aquatic animals such as shrimp and crabs. In its unmodified form, chitin is translucent, pliable, resilient, and quite tough. Major applications of chitin include biomedical applications like wound healing and antitumor agent, cosmetics, biotechnology and environmental uses. Chitosan is a commercially important derivative of chitin obtained by base catalyzed deacetylation reaction.

Chitin is added to food and pharmaceuticals as thickener and stabilizer; it is also added as a binder to dyes and adhesives. Chitin is strong, flexible and biodegradable which makes it a perfect candidate for surgical threads that wear away or biosorbed as the wound heals.⁵²

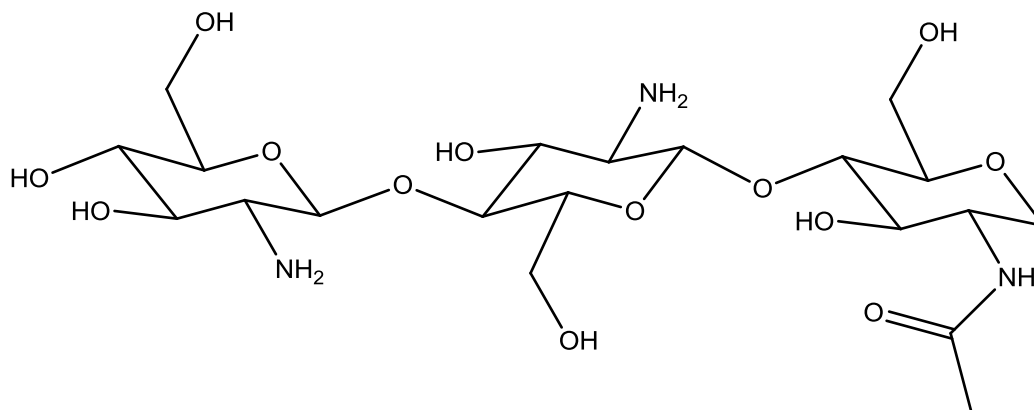


Figure 6. Structure of chitin.^{1,2}

Poly ϵ -caprolactone

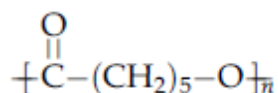


Figure 7. Chemical structure of a typical poly ϵ - caprolactone¹²

Poly ϵ -caprolactone (PCL) is a linear aliphatic polyester synthesized by either condensation of 6-hydroxyhexanoic acid or the ring opening polymerization of ϵ -caprolactone.¹² The chemical structure of a typical caprolactone is shown in **Figure 7**. The polycondensation of caprolactone is carried out in vacuum by removing water to drive the equilibrium reaction in the forward direction.²³ Ring opening polymerization (ROP) involves several mechanisms depending on the catalyst. The mechanisms include anionic ROP (formation of anionic species that attacks the carbonyl carbon of monomer), cationic ROP (formation of cationic species that attacks the carbonyl carbon of monomer), monomer activated ROP (activation of monomer molecules by catalyst) and coordination insertion ROP (reaction proceeds through coordination of the monomer with the catalyst).^{23, 26, 53} Polymerization is generally catalyzed by organometallic catalysts as well as alkanolamine.¹² PCL has a low Tm of about 52°C and low Tg of -62°C. PCL has been used in drug delivery due to its biodegradability. Drugs such as disodium norcantharidate can be encapsulated with polycaprolactone microspheres employing a solvent evaporation technique for controlled drug release. During the drug release there is a rapid release phase (55% in 2 hours) due to diffusion and osmotic pressure followed by a slow

release phase (85% in 16 hours) governed mainly by diffusion. PCL is also used as a polymer scaffold in tissue engineering, because of its relatively low biodegradability, non-toxicity and compatibility with tissues.⁵⁴ Poly ϵ -caprolactone allows successful cell attachment, proliferation and functioning. PCL can also be copolymerized with other polymers such as cyclic butylene terephthalate³², starch^{21, 33} and lauryl lactum³¹ PCL with molecular weight in the range of 530-630000 gmol^{-1} (M_n) have Young's modulus ranging from 0.21-0.44 GPa. Copolymerization of Poly ϵ -caprolactone with cyclic butylene terephthalate helps in reducing the crystallinity and brittleness of the polymer and helps in processing.³² Copolymerization of PCL with native corn starch helps in reducing the melting temperature of PCL from 58°C to 45°C.²¹ PCL is easily degraded by hydrolysis of its ester linkages in physiological conditions. As a result, it has been used as an implantable biomaterial. Food and Drug Administration (FDA) has approved PCL for many applications in the human body including drug delivery device, suture or adhesion barrier.⁵⁵ Because of the low melting temperature, PCL has also been used as hand moldable plastic and for rapid prototyping.

Poly(butylene succinate)

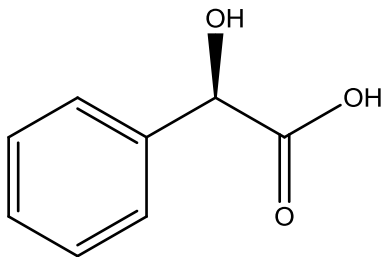


Figure 8. The chemical structure of mandelic acid

Polybutylene succinate (PBS) is a white, crystalline thermoplastic aliphatic polymer with excellent biodegradability.^{34, 35, 37} PBS is made from polycondensation of 1, 4-butanediol (BD) and succinic acid (SA) and high molecular weight polymers can be obtained by effective use of esterification catalysts and high vacuum techniques.³⁶ It has a T_m between 90-120°C (similar to low density polyethylene) and T_g between -45 to 10°C (similar to polyethylene and polypropylene).^{34, 35, 37} The mechanical, thermal and biodegradable properties of PBS can be enhanced by copolymerization with other diacids and diols. For example, copolymerization of PBS with polypropylene succinate (PBS co PPS) leads to lowering of the T_m from 113°C (pure PBS) to 63°C for PBS where the feed ratio of BS/PS was 50/50.⁵⁶ Jin et al.⁵⁶ studied the effect of a phenyl side chain on the properties of PBS by copolymerization of PBS with mandelic acid (MA). The chemical structure of mandelic acid is given in **Figure 8**. It was observed that the crystallinity of PBS decreased from 58.9% (measured by WAXD) to 39.4% on copolymerization with mandelic acid. The T_m also decreased from 115.9°C for PBS to 108.5°C for the feed composition of BD/SA/MA 1.33/ 1.00/ 0.11, due to decrease in crystallinity. However, the T_g increased from -36.6°C to -32.4°C due to increase in the degree of branching. For the same reason the tensile modulus increased from 268 MPa to 388.7 MPa on copolymerization of PBS with MA. PBS can be processed using injection, extrusion, compression and lamination molding techniques. PBS is recyclable and is produced by polymerization of butanediol and succinic acid which may be available from renewable sources.^{34, 35, 37}

Several companies like Stonyfield farms, Pepsico and Papermate have started replacing petroleum based products with green resins. Stonyfield farms have replaced polystyrene plastics cup with PLA and Papermate introduced a PHA based biodegradable pen.

Pepsico, one of the largest food and beverage companies, has developed a polyethylene terephthalate (PET) plastic that has been synthesized using ethylene glycol made from switch grass, pine bark and corn husks, making the PET partly sustainable. They have already begun using this PET for their soda bottles. Producers like Dupont are focusing on biomass for food stocks to lower the cost of green resins. Dow and Braskem have already announced plans to produce polyethylene from ethanol derived from sugarcane feedstock in Brazil. Braskem also has plans to produce polypropylene from plant (sugarcane) based sustainable raw materials.

Accepted as:

Ghosh Dastidar, T., Netravali, A. N; Green Resins; Lancaster: DESTech Publications, 2012,
Netravali A. N., Pastore C, eds. Sustainable Composites and Advanced Materials

CHAPTER 3

IMPROVING RESIN AND FILM FORMING PROPERTIES OF NATIVE STARCHES BY PHYSICAL AND CHEMICAL MODIFICATION

Abstract

Starch is a yearly renewable and biodegradable source of polysaccharides produced by plants and is the second most available biomaterial in nature, next to only cellulose. This has provided an incentive to a growing number of researchers, scientists and engineers to prepare starch based materials as ‘green’ alternatives to plastics and resins obtained from petroleum based resources. Through these research efforts, in recent years, significant progress has been made in understanding the relationship between structure and functionality of starches obtained from various sources. Various chemical and physical modifications of starch have helped in synthesizing biobased green materials with tunable properties that are suitable for a myriad of industrial applications. Starch has also been modified for use as resin and film forming. Starch based resin with improved mechanical, thermal, electronic and/or optical properties, compared to those of petroleum based resins, could be easily used with natural fibers for ‘green’ composite manufacturing. At the end of their life they could be easily disposed of or composted instead of putting into landfills. In addition, depending on the modification, the starch based resins may have the advantage of exhibiting biocompatibility. This review presents a comprehensive discussion on starch and their chemical and physical modifications and fundamental structure-property relationships as well as various applications.

Published as:

T. Ghosh Dastidar and A. N. Netravali, *Journal of Biobased Materials and Bioenergy*, 2012, **6**, 1-124.

Introduction

Plastics and fiber reinforced plastics (composites) have become one of the most important classes of materials for consumer goods as well as sophisticated and diverse applications ranging from aerospace to housing and from automobile to packaging.⁵⁷⁻⁵⁹ Composites have been increasingly replacing metals in these applications because of their low density and excellent mechanical properties combined with their ability to be engineered to obtain the required properties. Most of the currently available plastics and resins e. g., epoxies, polymethylmethacrylate (PMMA), polyimides, polyetherketones, polyurethanes (PU), polyesters, nylon, polypropylene (PP), etc., and fibers, e.g. Aramid, ultra high molecular weight polyethylene (UHMWPE), graphite, etc., that are used to fabricate composites are derived from petroleum. These composites have excellent mechanical, physical and chemical properties for the intended applications. However, they suffer significantly from their end-of-life disposal problems. Since they are not biodegradable and cannot be recycled or reused easily, most of them end up in landfills at the end of their life. By some estimates we are consuming petroleum at 100,000 times the rate at which the earth can produce.^{60, 61} Biodegradable polymers such as polysaccharides and proteins obtained from renewable resources such as plants, animals and microbes are convenient, environment friendly and offer several advantages over petroleum-derived synthetic polymers. Among all polysaccharides investigated as potential alternatives for petroleum-derived products, starch has received considerable attention. This is because starch is an inexpensive, yearly renewable plant based polysaccharide. It is produced worldwide in sufficiently large quantities and can be used as a raw material to produce biodegradable materials. Thus starch can be an environment-friendly solution to the current plastic waste issues.⁶² Starch based polymers have been used in diverse applications including drug delivery system, hydrogels, bone cement, bone fixation devices and tissue engineering.⁶²⁻⁶⁵ Diverse applications, however, require different properties. As a result, starch has been modified in many different ways including physical, chemical and enzymatic methods to produce low water sensitive materials with desired thermal and mechanical properties. Chemical modifications, in

general, can introduce functional groups into starch molecules which change their physico-chemical, morphological, mechanical, thermal and rheological properties.⁶⁶ In this article we review the most relevant literature exploring the factors that affect the properties of native starches as well as how different chemical and physical modifications can impart properties desirable for different applications as resins and/or films.

Properties of native starch with respect to film and resin formation

The supramolecular structure of starch has been studied using a broad range of characterization techniques including X-ray diffraction (XRD), small angle X-ray scattering (SAXS), differential scanning calorimetry (DSC), thermogravimetric analysis (TGA), electron microscopy, etc.^{67, 68} Knowledge of the network structure and related properties of starch gels has provided critical input for the industrial applications of these materials. Such knowledge has enabled scientists to process starch and modify them to meet specific demands of the industry. Factors that affect properties of starch based resins such as the detailed microscopic structure, biological source, effect of hydrothermal treatments on the structure, dependence of properties on the content of amylose and amylopectin, retrogradation (development of crystallinity with aging) of starch films, effect of plasticizers and blending with compatible polymers on structure and properties of starch films are briefly explored in this section.

Native starch

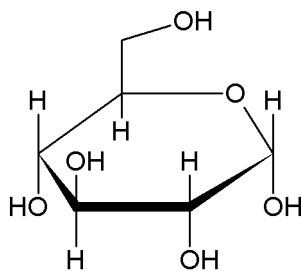


Figure 9. α -D-glucopyranose

Starch is a polysaccharide and is composed of two polymers of D-glucopyranose (**Figure 9**), amylose and amylopectin. Amylose is a linear molecule formed by glucose units joined by 1, 4 glycosidic linkages and with molecular weight ranging from 10^5 - 10^6 g/mol. Amylopectin, on the other hand, is a highly branched macromolecule formed by glucose units joined by both the 1, 4 and the 1, 6- glycosidic linkages with much higher molecular weight of around 10^7 - 10^9 g/mol. Chemical structures of amylose and amylopectin molecules are shown in **Figure 10**.⁶⁹

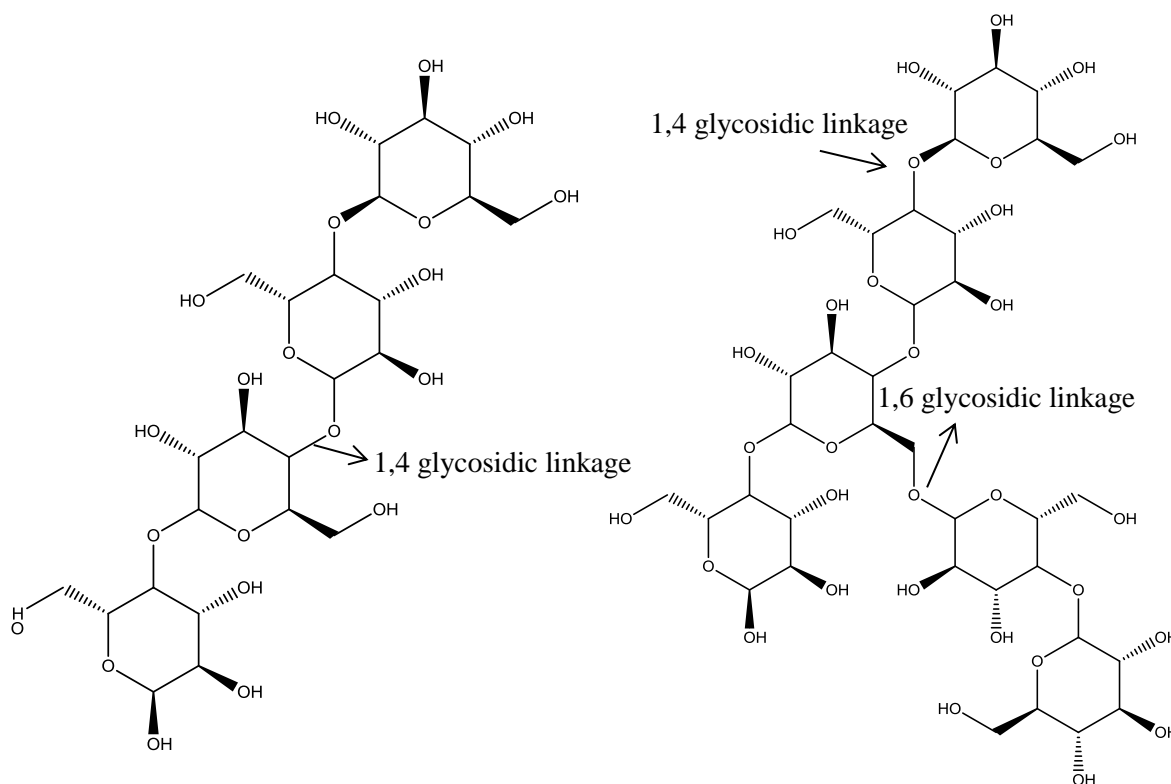


Figure 10. Chemical structures of (a) amylose and (b) amylopectin molecules.¹³

Amylose and amylopectin together form about 98-99% of the dry weight of the starch granules. The remainder consists of lipids, minerals and phosphorus. Phosphorus is present in the form of phosphates esterified to the hydroxyl group of starch molecules. Because of the hydroxyl groups, under normal conditions, starch also absorbs about 10% moisture.⁷⁰ The conventional model of starch consists of, the crystalline and amorphous lamellae which together form the crystalline growth rings and the amorphous growth rings.⁷¹

Structure and composition of starch are a function of biosynthetic pathway which involves different types of enzymes like adenosine-di-phosphate (ADP) phosphorylases, starch synthetases, starch branching enzymes and starch debranching enzymes.⁷² It is known that crystallization of starch depends on the molecular weight, branching, concentration and temperature of the solvent used.⁷³ Starch is classified into cereal starches (maize, wheat, sorghum, and rice), tuber or root starches (potato, tapioca, arrowroot and sweet potato starches) and waxy or high amylopectin starches (waxy maize, waxy sorghum and waxy rice) based on the sources. The starches obtained from different sources have different semi-crystalline structures which give rise to differences in their properties.⁷³ For example, corn starch has lower solubility (1.01%) and absorbs and retains lesser moisture (7.92 g/g H₂O) than potato starches (1.21% solubility and 10.44 g/g H₂O). This is because of the compact semi-crystalline arrangement of the cereal starches as compared to root starches which leads to lesser availability of hydroxyl groups to form hydrogen bonds and covalent bonds with the rest of the starch chains.⁷³ The extent of crystallinity in starch granules also varies with the content of amylose, being 15% in high amylose starches and 45% in waxy starches. Common starch properties such as swelling and pasting as well as thermodynamic properties (e.g., gelatinization, crystallization and glass transition temperatures) have been found to be affected by the amylose content and the interaction between the amylose (linear) and amylopectin (branched) contents of the starch granules.^{4, 74, 75}

Starch granules differ in sizes and shapes based on the organization of amylose and amylopectin, degree of crystallinity and branching of amylopectin.¹⁸ For example, wheat, triticale (a hybrid of wheat and rye) and barley endosperms consist of; A-granules that are large and disk shaped and measure around 10-35 µm in diameter and B-granules that are smaller and spherical and measure around 2 µm in diameter. Structures of the A- and B-granules of starch are shown in **Figure 11**.¹⁸ Normally, the B-granules possess higher crystallinity than the larger A-granules as illustrated in **Figure 11**.¹⁸

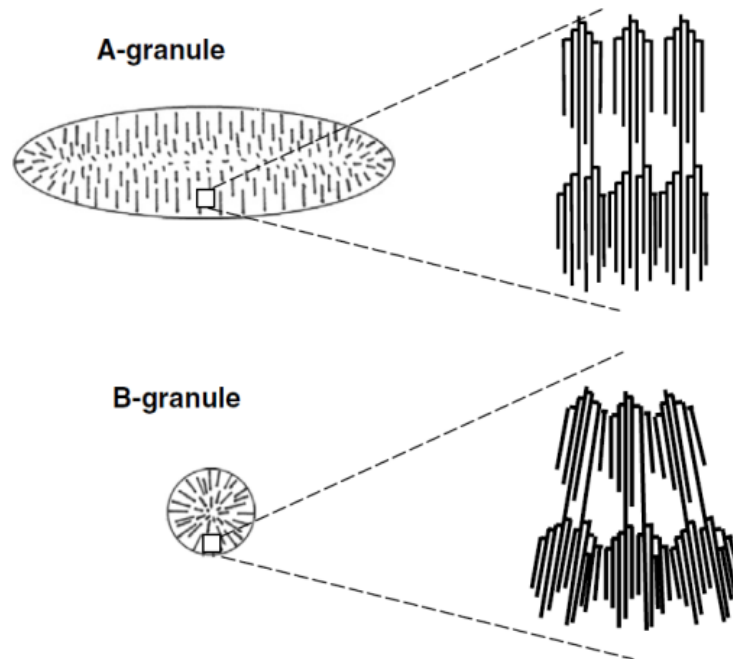


Figure 11. Structures of the A- and B-granules of starch.¹⁸

B-granules which consist of less amylose, amylopectin and have more lipids show higher gelatinization temperature (around 99°C) and pasting temperature (95°C) than A-granules. Normal gelatinization temperatures for A-granules are around 98°C and pasting temperatures are around 85°C.¹⁸ Cross-section of a starch granule showing the orientation of amylopectin double helices is presented in **Figure 12**.⁷⁶ Typically the granules consist of multiple layers of growth rings extending from the hilum towards the surface of the granules, giving it a hierarchical structure.⁷⁶

The hilum is the point of initiation of the granule and is positioned at the center of the elliptically shaped granules or on the axis of symmetry at the fat end of pear shaped granules.¹⁴ The amylose and amylopectin are arranged radially with their molecular axis aligned perpendicular to the growth rings and to the granule surface.⁴ The concentric rings consist of alternating crystalline and amorphous layers. Amylopectin is found in the form of double helices

with A-type and B-type crystal structures, with the packing being more compact in the A-type than in the B-type, as explained below.⁴

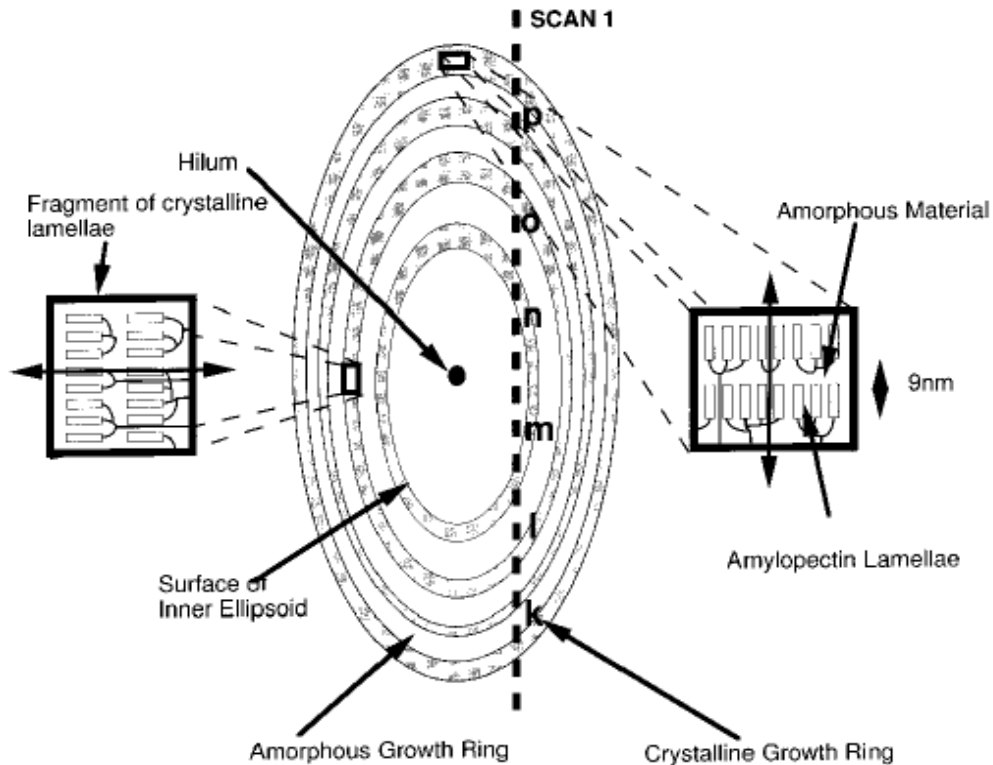


Figure 12. Cross-section of a starch granule showing the orientation of amylopectin double helices.¹⁴

Topographic image of native starch showing growth rings are shown in Figure 13.⁴ The proposed structure for A-type crystal consists of a parallel stranded double helix packed in an antiparallel arrangement in the unit cell.⁷⁷ The chains in B-type crystal are also arranged in the form of double helices but with a hexagonal unit cell.⁷⁸ A third type of crystal structure found in starches - the C-type crystal- is regarded as a mixture of A-type and B-type crystal structures. It is easier for the branched chains of amylopectin to form these double helices whereas the branch points are located in the amorphous region.⁷⁷ Amylose-lipid complexes formed by adding 3%

(w/w) stearic acid to autoclaved starch films gave a new V-type crystal structure in which amylose chains formed a helical conformation and the diameter of the helix depended on the complexing ligand.⁷⁹

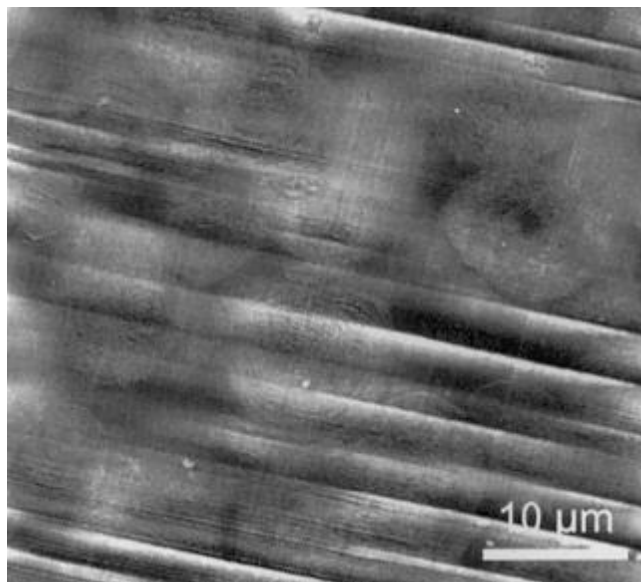


Figure 13. Topographic image of native starch showing growth rings⁴

Heat-moisture treatment

Heat-moisture treatment which refers to limiting the molecular mobility of starch by limiting the amount of moisture absorption have been shown to cause microstructural changes in starches.⁸⁰ Studies have involved heating starch from various sources such as barley (cereal), red millet (cereal), triticale (cereal), arrowroot (tuber) and cassava (tuber) with moisture content between 18 and 27% for 16 hr at 100°C in an air circulating oven and then air-dried to 7.5% moisture content. In general, results have shown that crystal structure in tuber starches (cassava and arrowroot) changed from original C-type to A-type while no change was observed for cereal starches with heat-moisture treatment.⁸⁰ This transformation was attributed to dehydration and transformation of amorphous amylose to helical form. In native tuber starches there are intergranular water at the core that forms bridges giving rise to the B-type crystal structure. However, with the heat-moisture treatment the water is lost and the structure is converted to a more compact A-type structure usually predominant in cereal starches. This leads to a change in

their functional properties. For example, with heat-moisture treatment, solubility of wheat starch increased from 0.9% to 2.11% at 60°C with increase in moisture content from 0% to 27%, since there was no change in the crystal structure.⁸⁰ On the other hand, under similar conditions, solubility of potato starch decreased from 3.0% to 1.55% since there was a change in crystal structure from B-type crystal structure to the more compact A-type crystal structure. The swelling factor (ratio of volume of swollen starch granules to the volume of dry starch) of native potato starch at 95°C reduced from 93.1 to 13.4 after heat-moisture treatment. The swelling factor of wheat starch reduced from 27.6 (native) to 17.2 (heat-moisture treated). The drastic change in the swelling factor of potato starch with heat-moisture treatment was due to the polymorphic transformation of potato starch from B-type to the compact A-type crystal structure. No changes in the crystal structure of wheat starch were observed under similar conditions.^{81, 82}

Annealing

Conventionally, annealing of polymers is defined as heating a polymer to temperatures below its melting temperature for extended periods of time to induce larger crystal size, the perfection of crystals or a change to more stable crystal structures.³ In case of starches, annealing is defined as the physical organization of starch granules in water at temperatures above glass transition temperature but below the gelatinization temperature. Differential scanning calorimetry (DSC) of rice and corn starches with different amylose contents also showed that gelatinization temperature for starches increased with higher amylose content.⁸³ Gelatinization temperature for starches with amylose content as high as 26% was around 76.4°C while gelatinization temperature for the starches containing 4.47% amylose was around 69.8°C. Starches with high amylose content consist of more amorphous and less crystalline region.⁸³ Amylose forms the amorphous region of the starch and the stability to disruption decreases with increase in the amorphous content. Corn starches with different amylose and amylopectin ratios have been subjected to annealing at different temperatures.⁸⁴ These experiments showed that annealing at 30°C has no effect on the gelatinization endotherm of the native starch.⁸⁴ However, the gelatinization endotherm shifted to higher temperature and became narrower after annealing

at 50°C indicating a change in microstructural arrangement of the corn starch. These results also mean that the helical length of amylopectin is affected by annealing in amylose rich corn starches.⁸⁴

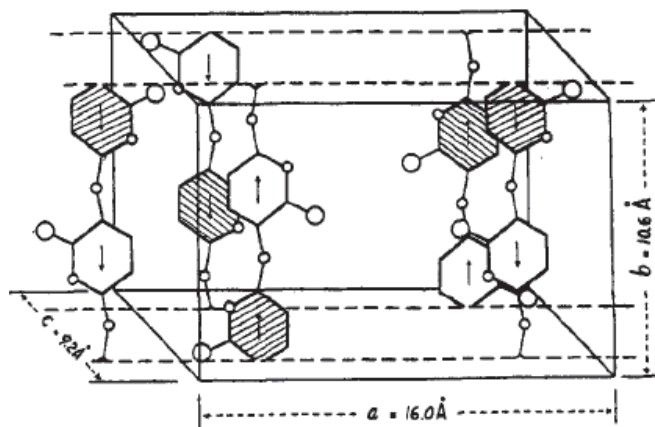


Figure 14. Unit cell of retrograded amylose film.⁹

Crystal structure of high amylose corn starch film formed through aqueous medium was shown to be a function of the drying temperature.⁸⁵ The study showed that the strength and elasticity of films formed by amylose rich corn starch were greatly affected by the temperature of the film formation.⁸⁵ The results also illustrated that films formed at low (10°C) temperature were completely amorphous whereas films formed at high (80°C) temperature were crystalline, discontinuous and cloudy with low mechanical strength.⁸⁵ The microstructure of amylose gel in a film has been investigated with electron microscopy and acid hydrolysis methods.⁸⁶ The microstructure of amylose gel consisted of a macroporous arrangement with filaments in a B-type crystal structure resulting from association of amylose chains. The gel also consisted of an amorphous region that existed as a dangling chain from the macroporous structure.⁸⁶ Amylose films of a few hundredths of a millimeter thickness have been prepared by evaporating a hot solution containing 5% amylose very slowly.⁹ X-ray diffraction patterns of films showed a unit cell with $a_0 = 16.0 \text{ \AA}$, $b_0 = 10.6 \text{ \AA}$, $c_0 = 9.2 \text{ \AA}$ having an orthorhombic structure.⁹ **Figure 14** shows a unit cell in a retrograded amylose film.⁹

Amorphous potato starch stored in a humid condition absorbed moisture and retrograded to form a crystalline gel with the crystalline structure depending upon the amylopectin molecules.⁸⁷ Two types of long range orders were observed in the crystalline gel. One of the structures was spherulitic that consisted of an amylopectin molecule at the center and radially outgoing lamellae of either amylose or amylopectin molecules. The other one was a nanostructure of concentric crystalline spherical cells made of pure amylopectin separated by amorphous layers.⁸⁷ While these structures can be expected to result in different mechanical properties, the authors did not characterize them.

Plasticizing and blending

Thermoplastic starch produced by plasticization of native starch is an attractive material owing to its ease of production using traditional plastic processing techniques besides its low cost and biodegradability. Plasticization of starch commonly involves application of mechanical shear stresses and heat in the presence of a suitable plasticizer to obtain complete and/or partial destruction of the crystalline structure.⁸⁸ In the presence of the plasticizer the molecular chains in the starch gain mobility due to added free volume and is usually accompanied by the variation of rheological and mechanical properties of the starch/plasticizer mixture. The effect of the chemical nature of the plasticizer and its concentration on the properties of thermoplastic starch has been discussed in this section. Zullo and Iannace⁸⁸ reported the thermo-mechanical destruction of the structure of starches from different botanic origins (maize and potato) and with different plasticizer contents. They prepared a variety of thermoplastic starches and characterized them to correlate the material composition, thermoplastic modification conditions and external rheology. Studies were focused on the composition and the procedures used to obtain biodegradable starch films using film blowing technology.⁸⁸ The elongational properties of thermoplasticized starches were evaluated by studying the melt spinning of fibers.⁸⁸ The polymer melt strand extruded from a capillary die was gripped between two counter rotating wheels. The haul off force (cN) was measured as a function of draw ratio until the strand broke. The material composed of high amylose starch thermoplasticized with 30% urea formamide

showed better elongational viscosity (4×10^9 Pa.s for strain rate of 0.001 s^{-1}), high melt strength (40 cN and break at 3.5 draw ratio) and strain hardening behavior than starch plasticized with glycerol (19 cN and break at 2.3 draw ratio).⁸⁸ With the aim of understanding the structural difference of amylose and amylopectin films and their correlation with functional properties, X-ray diffraction patterns of amylose and amylopectin films with 0, 10 and 30% glycerol and stored at 0, 54 and 91% relative humidity (RH) were studied by Myllarinen et al.⁸⁹ The study revealed that pure amylopectin film was generally amorphous and the plasticized amylopectin film (with 30% glycerol) was shown to have B-type crystals that developed with aging at 20°C for a month.⁸⁹ It was also concluded from the experiments that amylose films plasticized with water only or water and glycerol mixture had a stable B-type crystal structure. The crystallinity increased from 6-14% at dry conditions to 20% at 54% RH and to 32% at 92% RH. The results demonstrated that amylose films had stable crystal structures while amylopectin films were unstable and changed their amorphous structure to B-type crystallinity upon aging.⁸⁹ Lourdin et al.⁹⁰ have conducted research focused on blending starch, particularly amylopectin with plasticizers, to understand the impact of amylose content on the solid properties of these materials.⁹⁰ Their experiments demonstrated that mechanical properties improve with increase in amylose content. For example, elongation at break increased from 4.2% for films containing 0% amylose to 6.5% for those containing 100% amylose. Also, the tensile strength (fracture stress) increased from 38 MPa for pure amylopectin films to 69 MPa for pure amylose films. Regardless of the amylose content the stress-strain curves for these materials showed characteristically brittle behavior. In plasticized films the positive effect of amylose was masked by glycerol so that increase in amylose content did not lead to an increase in the tensile stress or breaking elongation. Amylopectin films were found to be more sensitive to the addition of plasticizer and plasticized amylopectin films showed ductile behavior with breaking elongation of 25% and fracture stress of 5 MPa.⁹¹ External plasticizers such as glycerol and water are small molecules that blend easily with hydrophilic starch materials and become part of the system, reducing their rigidity.

Blending is an important way to enhance mechanical and barrier properties of starches while ensuring their biodegradability.⁹² Chillo et al.⁹² blended tapioca starch and glycerol (50 g of each one) with chitosan, to study their influence. The tensile strength at break increased to 22 MPa for starch film blended with 1% chitosan and 0.5% glycerol from a tensile strength of 2 MPa for starch film blended with 0.3% chitosan and 0.5% glycerol. Introduction of chitosan reduced the availability of the number of hydrophilic groups due to hydrogen bonding interaction between chitosan and starch chains. However, adding too much chitosan led to phase separation. Mechanical properties and swelling of starch/PVOH blend mixed with glycerol, sorbitol, succinic acid, maleic acid, tartaric acid and citric acid were studied to compare the effect of carboxylic acid and hydroxyl groups on the properties.^{93, 94} The results verified that the presence of carboxyl and hydroxyl groups increase the flexibility of the films. The elongation at break (%) increased from 10% for starch/PVOH films to up to 190% for starch/PVOH films blended with sorbitol. Addition of agar has also shown to improve the microstructure of potato starch based films owing to better interactions through hydrogen bonding as a result of the compatibility between the two.⁹⁵ The tensile stress at break increased from 5 MPa to 13 MPa with addition of 30% agar for films stored at 50% relative humidity for 48 hours. Even though agar is very hydrophilic and absorbs a large quantity of moisture which may act as plasticizer for the starch molecules this effect is countered by the ability of agar to form a three dimensional network structure which restrains the motion of the polysaccharide chains. Blending starch with compatible polymers led to modification of the microstructure of starch influencing the mechanical properties.

Chemical modifications of starch and their effect on structure and properties of resins and films

The physicochemical properties of starch that are commonly affected by chemical modifications are moisture absorption, swelling power, solubility and the resultant light transmittance. Morphological properties which involve increase or decrease in granule size and internal structure of granules also depend on the type of modification. The functional properties

affected by chemical modification of starches are thermal properties (gelatinization, crystallization, crystal melting and thermal degradation), rheological properties, retrogradation (development of crystallinity with aging) properties, syneresis (separation or expulsion of water from starch gel upon standing) and freeze thaw stability (the ability of a product to maintain its composition after going through repeated cycles of freezing and being in ambient temperature). All these properties can be characterized and provide detailed quantitative and qualitative understanding of the effect of different modifications and the degree of substitution on the properties of modified starches and thus their usefulness as resins and/or films.

As described earlier, polysaccharides have a complex chemical structure and most of their chemical reactions involve cleavage of the carbon-oxygen bond or reaction at the hydroxyl group. Carbohydrate monomer, α -D-glucopyranose, as shown in Fig. 1, has three reactive hydroxyl groups. However, their reactivity depends on their respective position on the glucose ring. The free primary hydroxyl group is more reactive whereas the other two secondary hydroxyl groups on the ring are less reactive due to steric hindrance.⁹⁶

Starches can be modified to form either thermosets or thermoplastics. Some of the common modification methods used for starches are chain cleavage (thermoplastic modification), ether formation (thermoplastic modification), ester formation (thermoplastic modification) and crosslinking (thermosetting modification) and involve treating starch with specific chemical reagents for esterification, etherification, oxidation and hydrolysis.⁶⁶ Major chemical modifications of starches and their influence on their properties are discussed briefly in this section.

Crosslinking

Crosslinking of starch with bi or polyfunctional reagents is a key modification technique widely utilized in industrial applications such as preparation of wet-rub-resistant starch paper coatings, permanent textile sizes and water resistant adhesives.⁹⁷ Crosslinking interconnects the starch molecules by covalent bonding, thus it not only increases the molecular weight but also increases the modulus (stiffness) and often its tensile strength, depending on the decrease in the fracture

strain.¹⁶ Crosslinking is also expected to improve the water resistance. The most widely used crosslinking agents include polycarboxylic acids like citric acid, polyphosphates like sodium trimetaphosphate, sodium tripolyphosphate as well as epichlorohydrin, phosphorus oxychloride and 1, 2, 3, 4-diepoxybutane.^{16, 17, 98-102}

Crosslinking with polycarboxylic acid

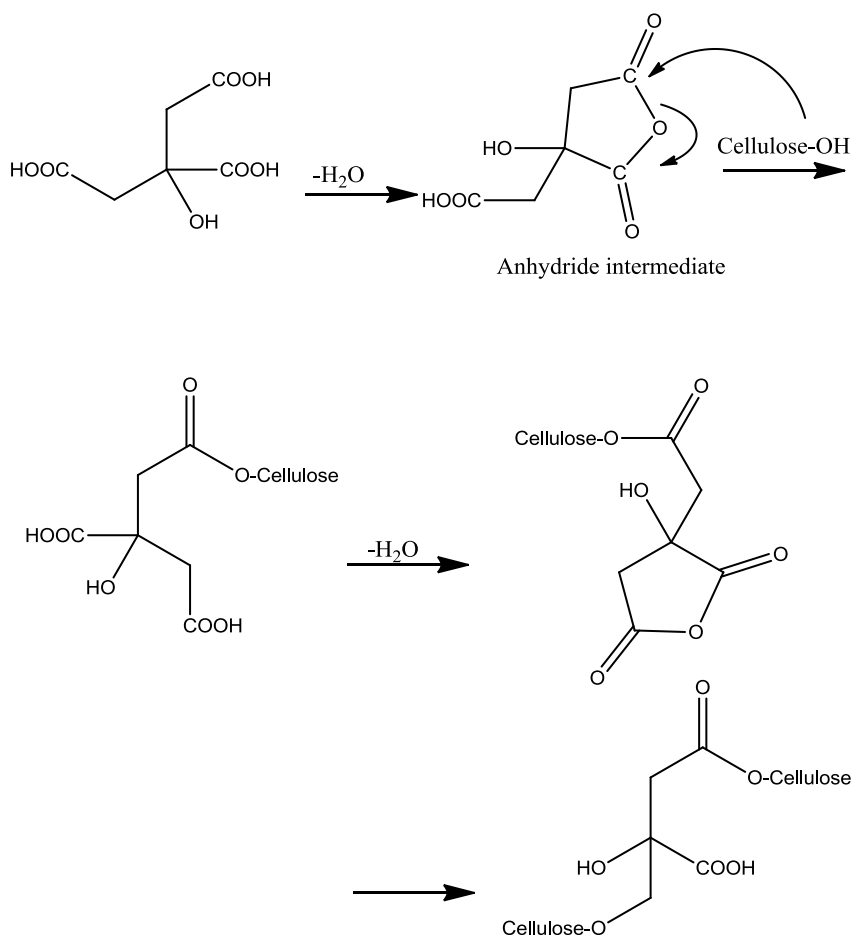


Figure 15. Mechanism of dry crosslinking of cellulose with polycarboxylic acid.¹⁶

Polycarboxylic acids such as citric acids are nontoxic and inexpensive materials that have been used to improve the appearance, wrinkle resistance, mechanical properties and water resistance of cellulose and protein fibers in the textile industry.¹⁰³⁻¹⁰⁵ Mechanism of dry crosslinking of cellulose (CF-OH) with polycarboxylic acid is shown in **Figure 15**. It is postulated that crosslinking of starch with polycarboxylic acid follows the same mechanism due to similarity between starch and cellulose structures.¹⁶ Reddy and Yang⁵³ used citric acid to

crosslink starch which improved the mechanical properties and reduced dissolution in water and formic acid by forming ester bonds with the hydroxyl groups of starch molecules. In their experiments citric acid and sodium hypophosphite (50% w/w, on weight of citric acid used), were dissolved in the starch solution that was held at 90°C for 20 min and then cooled to 65°C. Required amount of glycerol was added before pouring the slurry on to Teflon[®] coated plates to obtain films. The starch slurry in film form was air dried for 48 hr and then treated in the hot air oven at 165°C for various periods of time. After heating, the films were transferred to conditioning chamber and maintained at 23°C and 50% relative humidity. Crosslinking starch films with citric acid increased the tensile strength of the film by 150% to about 24 MPa.¹⁶ The citric acid crosslinked films also showed 20% lower weight loss than non-crosslinked films after heating to 600°C.¹⁶ Further, the films that were not crosslinked started showing weight loss at around 70°C while for crosslinked films weight loss started at around 120°C.¹⁶ Such improvements can increase the applications of crosslinked starches.

Films made from corn starch crosslinked with epichlorohydrin had strength ranging between 12 and 16 MPa as compared to 24 MPa for the films crosslinked with citric acid. The crosslinked starch films lost only about 25% of their weight in water as compared to non-crosslinked films that lost about 75% of their weight in water at 50°C after 35 days of soaking at pH 7.2.¹⁶ These data suggested that crosslinking not only increased the strength of the film but also made a more dense structure which decreased the regions accessible to water leading to an improvement in water resistance. Weight loss of starch films in water and in an organic solvent such as formic acid also decreased after crosslinking. Glycerol was added to the crosslinked films to fine tune the mechanical properties of the films. A glycerol concentration of 15% provided the highest tensile strength (24 MPa) and was used to study all the mechanical properties of the films. The films were brittle when concentration of glycerol was below 10%. At concentrations above 15% the plasticizing effect was pronounced and the films showed high elongation and low tensile strength. At even higher concentrations, the plasticizer molecules were seen to aggregate and exist in free form reducing its effectiveness. These results suggest

that an optimum level of glycerol (or any plasticizer) is needed to be added, based on the desired mechanical properties.^{16, 106}

Crosslinking with epichlorohydrin

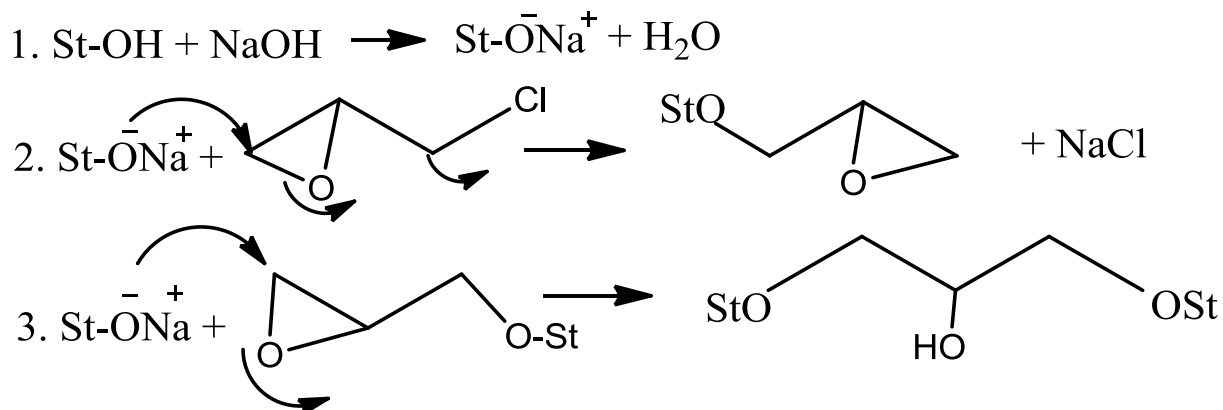


Figure 16. Mechanism of reaction of starch with epichlorohydrin.¹⁷

Crosslinking starch with epichlorohydrin is another common modification technique used in the polysaccharide chemistry. Reaction of starch with epichlorohydrin leads to the formation of distarch glycerols which are highly resistant to pH and mechanical shear due to the formation of ether linkages with the starch hydroxyl groups. Mechanism of starch and epichlorohydrin reaction is shown in **Figure 16**.¹⁰⁷

Epichlorohydrin reacts with starch to produce mono- and di-ethers (**Figure 16**)¹⁰⁷ by the reaction of the epoxy groups with hydroxyl groups on the starch molecules and crosslinking occurs when the newly generated epoxy group (step 2 in **Figure 16**) can react with another molecule of starch (step 3 in **Figure 16**).^{107, 108, 17, 109} Crosslinking reinforces the granules and prevents granule rupture and loss in viscosity after hydration in water. This property is important for applications such as surgical dusting powder, carriers, absorbents and ion-exchange resins that require swelling of the starch granules in water. Cassava starch was crosslinked with epichlorohydrin in three different media; water, water in the presence of a phase transfer catalyst and dimethyl formamide at 45°C for 2 hours in alkaline pH.¹⁷ At the end of the reaction the pH

of the slurry was maintained at 6.0 using 0.1 M HCl and the final product was filtered and washed. In order to determine the degree of crosslinking the starch slurry (10% by weight) was heated from 50 to 95°C at 12°C/min at 160 rpm, and was then held at 95°C for 2 min and finally cooled to 50°C at 12°C/min and kept at 50°C for 2 min. The peak viscosity of the starch specimens were recorded using a Rapid Visco Analyser (RVA). The degree of crosslinking was calculated as follows:

$$\text{Degree of crosslinking} = \frac{A - B}{A} \times 100$$

where, A is the peak viscosity in RV units of the native starch and B is that of the crosslinked starch. At higher levels of crosslinking a decrease in the peak viscosity was observed due to reinforcement of the starch granules that prevented their rupture. The setback viscosity was also lower since after rupturing the crosslinking provided sufficient granule integrity to keep the swollen granules intact and minimize or prevent loss in viscosity. Crosslinked starches also showed lower swelling volumes (8.8 mL/g) as compared to native starches (27 mL/g). This is again attributed to the fact that with the increase in the degree of crosslinking the starch granules become more compact preventing both swelling and solubility.¹⁷ As reported in many technical articles^{17, 107, 108, 110-114} crosslinking of starch using epichlorohydrin has been carried out in heterogeneous medium.¹¹¹ This essentially implies that swollen starch granules representing the solid phase were reacted with an alkali solution containing the epichlorohydrin which represented the liquid phase.¹¹¹ Hamerstrand et al.¹¹¹ observed that the yield of insoluble crosslinked starch increased with increasing concentration of starch and decreased with increasing the sodium hydroxide concentration.¹⁰⁷ The yield increased from 96% to 102% as the molar ratio of starch/epichlorohydrin increased from 0.1 to 0.5. Further increase in NaOH concentration resulted in a decrease in the yield from 102 to 95% for a molar ratio of 1.0. This is because the glycerol mono-ether starch bonds formed were proportional to the starch concentration used. Yield of crosslinked starch was independent of the

reaction temperature which only affected the speed of the reaction. Under both heterogeneous and homogeneous conditions epichlorohydrin was reported to have a side reaction with starch. About 5-10% of epichlorohydrin was found to form a glycerol mono-ether derivative with starch.¹⁰⁷

Phosphorylation and crosslinking

Phosphorylation of starch is another important and useful modification. Starch phosphate hydrogels have been used in applications such as cosmetics and sanitary products where mechanically stable gels with high water storing capacity and swelling power are desired.^{102, 115, 116} Phosphorylated starches have shown superior viscosity, improved gel-hardness as well as better water retention, increased swelling power and solubility as compared to the native starches due to the polar nature of the phosphate group.¹¹⁷⁻¹²⁰ In nature, only potato starch consists of 0.06 to 0.08% phosphorus bound to the anhydroglucose unit. Chemically, phosphorylation of starch is accomplished by esterification of native starch with phosphorylating agents such as orthophosphates, metaphosphates or phosphoryl chlorides. Mechanisms of starch phosphorylation showing (A) formation of monostarch phosphates¹¹ and (B) crosslinking by formation of distarch phosphates¹⁹ are presented in **Figure 17**. Typical mechanism of starch phosphorylation producing monostarch phosphates under acidic conditions is shown in **Figure 17(A)**.¹¹ The degree of substitution (DS) of phosphate groups affects properties such as solubility, swelling capacity, rheomechanical characteristics, stability of dispersions, retrogradation, syneresis and transparency of solutions and dispersions.^{120, 121}

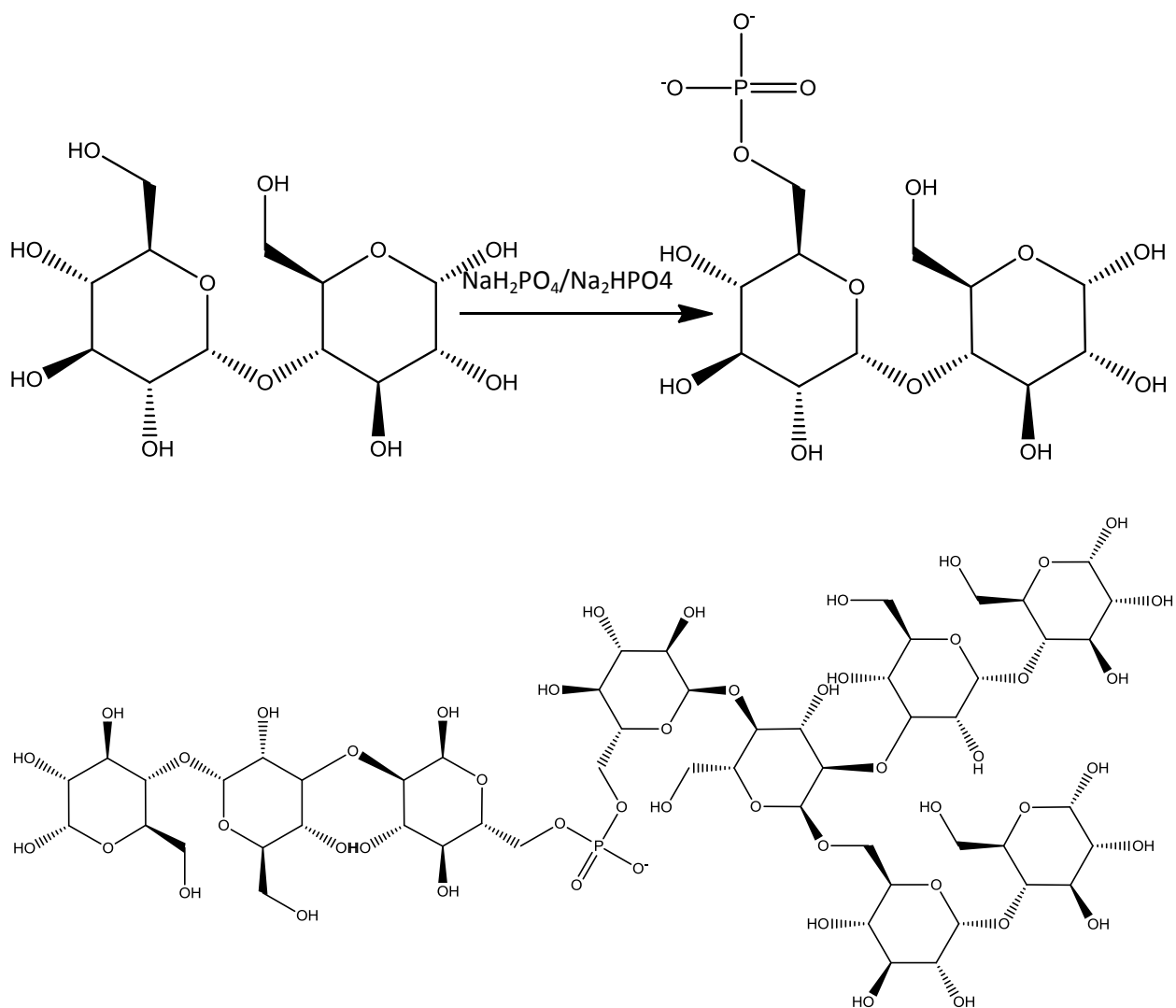


Figure 17. Mechanisms of starch phosphorylation showing (A) formation of monostarch phosphates¹¹ and (B) crosslinking by formation of distarch phosphates.¹⁹

Kulicke et al.¹⁹ crosslinked starch with sodium trimetaphosphate (STMP) in alkaline pH obtained through NaOH.^{19, 102} The reaction mechanism for crosslinking of starch with STMP via formation of distarch phosphates is shown in (B).¹⁹ The DS increased from 0.03 to 0.25 with the increase in concentration of phosphates from 15% to 21.1% (w/w).⁶³ As the crosslinking increased with increasing concentrations of both NaOH and STMP in the starch hydrogels, the swelling capacity and the storage modulus reduced due to the denser structure as well as effective entanglements between the crosslinked molecules, both of which reduced the water

uptake. At a very high concentration of NaOH (0.7 M) hydrolysis of the diester bonds was observed which lead to an increase in swelling capacity (300 g H₂O/g polymer). In these experiments dilute solution of NaCl (10⁻⁴ M) was used for the reactions. Swelling capacity was found to decrease from 150 g H₂O/g polymer to 50 g H₂O/g polymer as the salt concentration increased from 10⁻⁵ to 10 moles/l. This was shown to be the result of shrinkage of ionic gels in the presence of the salt.⁶⁴ Gui-Jie et al.¹²² reacted starch with phosphorus salts in acidic conditions to form monostarch phosphates. They found that microwave irradiation increased the DS of starch crosslinked with STMP in the presence of sodium carbonate at a temperature lower than the decomposition temperature of starch, which is around 350°C. Microwave heating was found to increase the kinetic energy of the molecules rapidly by dissipating heat inside the medium.¹²³ Consequently, in this unconventional heating method more molecules get energized than traditional heating. Addition of salts increased the conductivity of the medium leading to more absorption of heat and a dramatic increase in the rate of heating. Reacting starch intermittently led to a higher degree of substitution because starch was below the decomposition temperature for longer which allowed the reaction to proceed while preventing degradation. As the STMP concentration increased from 0 to 80%, the DS increased from 0.01 to 0.07 until a point was reached when the concentration of STMP was too high to dissolve in water. In such case excess STMP was removed by filtering and washing with sufficient amount of water. Gui-Jie et al.¹²² also concluded, from their studies, that increasing the amount of sodium carbonate from 30% to 70% increased the DS from 0.02 to 0.024. This is because sodium carbonate was found to decrease the decomposition temperature of starch. While the reason for this is not clear, it is believed that sodium carbonate weakens the hydrogen bond between the starch molecules and make them swell which in turn makes the hydroxyl groups available for reaction.¹²² Starch phosphates were also prepared by dry heating starch with a phosphorylating agent including ortho, pyro or meta tripolyphosphate, phosphoric acid, phosphorus oxy-chloride, sodium and potassium orthophosphate, sodium and potassium tripolyphosphate and sodium and potassium trimetaphosphates.¹²² Muhammad et al.⁷² phosphorylated sago starch using 5% sodium

tripolyphosphate (STPP) as well as a mixture of 2% STMP and 5% STPP above a pH of 9 and noted uncontrolled crosslinking leading to thermosetting modification of starch.

Passaeur et al.^{102, 115, 124, 125} investigated the synthesis of novel starch phosphate hydrogels by monophosphorylation of potato, waxy maize and high amylose maize starches followed by crosslinking with different di- or tri-carboxylic acids such as succinic, adipic or citric acid.^{102, 115, 124, 125} Hydrogels are highly swellable polymer networks that can be used as an environment-friendly alternative to synthetic super absorbents composed of polyacrylates or polyacrylamides. Hydrophilicity of starches can be increased by modifying them with hydrophilic phosphate groups followed by crosslinking which converts these hydrophilic materials to water swellable hydrogels with higher mechanical stability and lower biodegradability than the native starches.^{102, 115, 124} To evaluate the effect of crosslinker concentration on the hydrogel properties, starch phosphate with a DS of 0.14 was crosslinked with citric acid.¹⁰² The experimental results pointed out that the optimum swelling capacity of 150 g H₂O/g polymer was obtained with a citric acid concentration of 0.071 mmol/g. It was further observed that both high and low concentrations of citric acid led to a decrease in the swelling capacity. It must be pointed out that gel formation requires a critical network or crosslink density for the sol-gel transition. At a lower concentration of crosslinking agent the gel was increasingly water soluble while excessive crosslinker hampered the swelling of the gel by restricting the diffusion of water into the network. Optimization of the phosphate and crosslinker concentration led to the formation of sponge like porous structures with fast water absorption and high swelling capabilities. The experiments also showed that the longer the chain of the carboxylic acid group, the lower was the swelling capacity of the resulting gel.¹⁰² Additional functional groups (citric acid with an extra hydroxyl group) and double bonds (maleic acid) also reduced the swelling capacity by making the polymer network more rigid.

Demigroz et al.¹²⁶ attempted to find adequate methods to reduce water sensitivity and degradation rate of corn starch by crosslinking starch blended with different polymers such as a) a copolymer of ethylene and vinyl alcohol, b) cellulose acetate or c) poly-epsilon-caprolactone.

The blended materials were crosslinked with STMP at pH 10-11 in aqueous conditions. The contact angle measurements carried out for the blended specimens indicated that corn starch blended with polycaprolactone exhibited the highest contact angle of 73.6 as compared to ethyl vinyl alcohol (65.1) or cellulose acetate (50.2). In cases of ethyl vinyl alcohol or cellulose acetate there is an increase in the polar component due to ionization of the phosphate crosslinked points. These blends showed 15% reduced water uptake as compared to native starch. In addition, these materials were stiffer and had lower degradation rates, making them useful in many applications.

Carboxymethylation of starches

Carboxymethylation of starch is another simple modification technique that leads to many useful properties. For example, introduction of bulky carboxymethyl groups has been shown to aid in crosslinking and such carboxymethylated crosslinked starch can increase the efficiency of drug delivery by 60%.¹²⁷⁻¹²⁹ This is because derivatization of starch with polar carboxymethyl groups allows easy manipulation of the swelling properties by controlling the pH, a property essential for drug delivery. Since starch can easily swell and dissolve in water, suitable surface modification of starch is required in order to make it water proof. Such materials are required for food packing applications for bottles, packages and films. Takahashi et al.¹³⁰ treated carboxymethylated starch (CMS) with water soluble carboimide in the presence of zein in 70% ethanol or 70% acetone and the resulting acid-amide crosslinkages resulted in increased hydrophobicity of the film. Zein is a family of alcohol soluble storage proteins of maize and is rich in glutamine, proline, leucine, alanine and phenylalanine residues. The structural features of zein are indicative of hydrophobicity of the molecular as well as the aggregate surfaces. The crosslinked starch films conjugated with zein showed remarkably low water vapor permeation ($0.041\text{g}/\text{sec}\cdot\text{m}^2$) as compared to the control crosslinked films ($0.057\text{g}/\text{sec}\cdot\text{m}^2$).¹³⁰ The solubility of the films were also examined and it was found that crosslinked starch films conjugated with zein were insoluble in water while the solubility of the CMS crosslinked films was 20% at 50°C. The insolubility of the zein-CMS films was attributed to the

hydrophobicity of the protein molecules on the surface of the crosslinked starch films.¹³⁰ Carboxymethylated starch can be used for a variety of applications including paper additives and thickening agents. Heinze et al.¹³¹⁻¹³³ prepared carboxymethylated starch by reacting it with sodium monochloroacetate in the presence of NaOH in methanol, ethanol and isopropyl alcohol medium respectively. DS and reaction efficiency (RE) were investigated and it was found that isopropyl alcohol led to maximum DS (1.4) and RE of about 82%. A one step synthesis was also carried out based on the microstructure and specimens with DS of 1.51 were achieved. Mechanical properties of the modified starch, however, were not studied.¹³²

Other crosslinking modifications

A new approach to increase hydrophobicity of starch films is the deposition of a thin layer of polymer on the surface with the help of sulphur hexafluoride plasma treatment. Bastos et al.¹³⁴ extensively crosslinked starch without any chemicals by plasma glow discharge technique with sulfur hexafluoride in which highly reactive species produced by the plasma induced chemical reaction in starch. The hydroxyl groups on the α -D glucose unit dehydrated causing a crosslinking. The energy for this reaction was provided by the collision of F* species which was adsorbed in the helical network of starch chains. The F* species also caused polarization of the O-H bonds of the hydroxyl groups which helped in speeding up the reaction.¹³⁴ It was evaluated that starch films which originally exhibited a contact angle of 45°C with water became hydrophobic with a contact angle of around 138°C after treatment with the plasma. The contact angle was found to be dependent on the treatment time.

Starch has also been modified by crosslinking with N, N-methylenebisacrylamide at 50°C in an alkaline medium.¹⁰⁶ The swelling behavior declined from 150 g H₂O/g polymer to 45 g H₂O/g polymer as the concentration of crosslinker increased from 5 to 15 mol%.¹⁰⁶ This was attributed to the increase in the crosslinking points and decrease in the size of mesh width within the gel.

Esterification

A wide variety of starch esterifications have been carried out.¹³⁵⁻¹³⁸ This type of modification has been shown to drastically change the properties of starches depending on the DS and the carbon chain lengths of the substituting groups.¹³⁵⁻¹⁴⁰ The DS is defined as the number of substituents per D-glucopyranosyl rings. There are three reactive hydroxyl groups present on each D-glucopyranose ring and hence the maximum possible DS is 3. Common esterification methods and their effect on modified starch properties are briefly described below.

Acetylation

Acetylation, one of the most common chemical modifications of starches, is obtained by reacting starch with acetic anhydride or vinyl acetate in the presence of an alkaline catalyst.^{136, 141} The extent of change in the physicochemical properties of acetylated starch is a function of the DS. It is important to measure this DS quantitatively to control the degree of acetylation in various processes as many properties are a function of the DS. A wide variety of methods including wet-chemistry titration, Raman spectroscopy, ¹H NMR spectroscopy have been employed to obtain accurate DS for the acetylated products.^{142, 143} Moorthy¹⁴⁴ investigated acetylation of cassava starch in perchloric acid and obtained a DS of 0.13. Acetylation is a relatively simple chemical modification that significantly increases the physicochemical and functional properties of starch even at a very low DS.¹⁴⁴ Acetylated starches with low DS (0.1-0.2) have been used in applications as film forming, adhesion¹⁴⁵, binding^{146, 147} and thickening agents.^{148, 149} However, acetylated starches with high DS have received considerable attention because of their properties including hydrophobicity, melt processability, tablet producing binders, hot melt adhesives, coating, cigarette filters, biodegradable packaging materials and pharmaceutical applications.^{150, 151, 152, 142, 153} The extent of reaction has been shown to depend on the reactant concentration, reaction time, pH and the presence of catalyst.^{141, 142, 145-147, 154-158} Singh et al.¹⁵⁹ studied the effect of acetylation on physicochemical, morphological, thermal and rheological properties of potato and corn starches. In their studies, DS of 0.1 and 0.15 were obtained for corn and potato starches, respectively. The swelling power, solubility and light

transmittance (%) of modified potato and corn starches differed significantly from native starches. Native potato starch showed lower swelling power (70.15 g H₂O/g polymer) and solubility (0.102%) than that for acetylated potato starch (70.58 g H₂O/g polymer, 0.112%). The swelling power for corn starch was reported to be lower than that of potato starch. Native corn starch showed a swelling power of 36.2 g H₂O/g polymer and solubility of 0.081% while acetylated corn starch showed higher values (38.20 g H₂O/g polymer, 0.095%). These differences in properties of corn and potato starches were attributed to the fact that the amylose content in potato starch varied between 25 and 30% while that for corn starch was lower at around 24%. The lower swelling power of corn starch can also be due to the presence of lipids that reduced the swelling of individual granules by forming complexes with amylose. The increase in swelling and solubility with acetylation has been explained by the increase in water retention by the starch granules with introduction of the acetyl groups.¹⁵⁹ The DS of corn starch as determined by hydrolysis was found to increase from 0.81 to 2.83 as the temperature increased from 50°C to 75°C.^{142, 160} Several researchers have studied the effect of acetylation on the structure and physicochemical properties of corn and potato starches.^{147, 159, 161, 162} Owing to decreased availability of corn starch in developing countries sweet potato (*Ipomoea Batata*) starch was acetylated using vinyl acetate and a DS of 0.034 was obtained.¹⁶³ Oat starch is another important starch variety but little information is available on the chemical modification of oat starch. Mirmoghtadaie et al.¹⁶⁴ examined the effect of acetylation on physicochemical and thermal properties of oat starch. It was found that swelling increased from 19.6% to 27.5% for 8% acetylated starch as compared to parent starch since the acetyl groups facilitated the access of water to amorphous areas due to steric effects and disruption of hydrogen bonds within the starch granules.¹⁶⁴ The effect of pH, time and reagent concentration on acetylation of *Canavalia* (Jack-beans) starch and physico-chemical and functional properties of the modified starches have also been evaluated.¹⁴⁵ A DS of 0.091 was obtained for acetylation with 5% w/w with respect to starch acetic anhydride at pH 8 for 30 min. The incorporation of acetyl groups induced an increase in the viscosity as the number of acetyl groups increased. The apparent viscosity

increased to 88 cP as compared to 64 cP for native starch. This is because the acetyl groups facilitate the capture and retention of water molecules. The gelatinization temperature was lower in acetylated derivatives (66-72°C) than the native starches (77-73°C). All these properties are of commercial advantage in manufacturing pastes with higher stability where the thickening agent gels at lower temperature reducing the energy costs. A comprehensive study on the rheological properties of rice starches with different DS has provided important information on the role of acetyl groups on improved functional properties.¹⁶⁵ The swelling power of rice starches increased from 24.3 for native starch to 37.9 for DS of 0.1 while their solubility increased from 8.11% to 9.55%. Apparent viscosity increased from 0.82 Pa.s to 1.53 Pa.s, which suggests that starch pastes have higher hydrodynamic volumes after acetylation than native starches. It was also shown that the solubility of starch acetates increased with increase in the DS. This is because the acetyl group which is more hydrophilic than the hydroxyl group due to polarity of the C=O bond, allows retention of water molecule due to their ability to form hydrogen bonding.^{165, 166}

Thermosetting (crosslinking) and thermoplastic (acetylation) modifications of starches give rise to different properties as can be expected. Crosslinked starches have been observed to maintain their granular state, which assists in resisting swelling in hot water, due to the bond between starch molecules that held them together.¹²² Acetylation, on the other hand, increased the swelling power of starch due to structural disorganization caused by steric hindrance of the acetyl groups leading to more absorption of water.¹⁶⁵ In addition, crosslinking was shown not to affect gelatinization temperature while acetylation decreased gelatinization temperature due to introduction of bulky groups on the starch backbone. While crosslinking was shown to lead to a tighter structure of the starch chains leading to an increased syneresis, acetylation of starch decreased syneresis due to presence of acetyl groups.

n-succinylation

Succinic anhydride has been shown to react with starch to form starch succinates.^{137, 167-171} Starch succinates offer a number of desirable properties such as high viscosity, low

temperature viscosity stability, high thickening power, low gelatinization temperature, clarity of cooked pastes and good film forming properties. Thus starch succinates are used as binders and thickening agents in food, in tablet pharmaceuticals to help disintegration and as surface sizing agents and coating binders in papers.^{172-174, 137} Rapid preparation of starch succinates with high DS using a reactive extrusion process was studied by Wang et al.¹⁷⁵ Using a twin screw extruder at high temperature and high reactant concentration starch succinates could be prepared in just 1 min as compared to several hrs required for typical batch reactions. Starch succinate with a DS of 0.46 was prepared using starch, succinic anhydride and sodium bicarbonate (catalyst) used at a molar ratio of 1/3:0/0:75 at 110°C. Higher temperature resulted in the loss of granular structure of starch and hence led to a higher DS. Water solubility and viscosity of starch succinate increased with increase in DS. Solubility increased from 10 to 50% while viscosity increased from 5 to 40 cPa as DS increased from 0.05 to 0.5. The increased solubility was because of the presence of anionic succinate groups that hindered self-association and crystallization of the starch chains.¹⁷⁵

Esterification of starch under aqueous conditions by avoiding the use of organic reagents both for the modification as well as isolation to provide an 'environment friendly' route was investigated by Jeon et al.¹⁷⁶ In place of octenyl succinic anhydride they used dodecyl succinic anhydride to increase the chain length of the alkenyl substituent. Modified starch with longer alkenyl chain provides a route to increasing the hydrophobic character even at low DS. The maximum DS achieved under optimal conditions (pH 8.5 -9.0, 25°C and 5% anhydride concentration) was 0.04 after 6 hr of reaction. The reaction efficiency decreased dramatically from 80% to 20% as the alkenyl chain length increased from 8 to 18 implying that methods to develop efficient reaction for longer chain lengths still need to be developed.¹⁷⁶

Starch alkyl succinates have surface active properties useful in stabilizing oil water emulsions by forming a strong film at the oil water interface. Octenyl succinic anhydride (OSA) treated starch has been used in particular to encapsulate flavor and fragrances in beverages and salad dressings. They are also useful in applications like processing aids, body powder and

lotion because of their water resistance.¹⁷⁷ A study by Shrogen et al.¹⁷⁸ suggested that in starches with DS between 0.03-0.11 the OSA groups were distributed in the interior, amorphous domains of the amylopectin molecules as well as on the outside of the granule.¹⁷⁸

Jyothi et al.¹⁷⁹ investigated the succinylation of cassava starch in aqueous conditions and analyzed the paste properties of the modified starches. Cassava is a commercially important food starch which finds limited industrial application in the native form due to low paste and gel properties. Effects of succinic anhydride concentration, reaction time and pH of the reaction medium on the physicochemical properties were examined and maximum DS of 0.022 was obtained by reacting starch with 3% succinic anhydride at pH of 9-9.5 for 1 hr.¹⁷⁹ In comparison to native cassava starch, the modified starch showed enhanced properties. The swelling volume increased from 28.5 ml H₂O/g polymer to 44 ml H₂O/g polymer, peak viscosity increased from 2904 mPa to 4750 mPa, paste clarity (% light transmittance) increased from 21.4 to 28.9 and solubility increased from 21.6 to 24.2% on modifying cassava starch. As mentioned earlier, microwave irradiation provides an ultrafast synthesis technique and has been used in analytical chemistry, inorganic and organic synthesis and pharmaceutical chemistry. DS of cassava starch increased to 0.051 on reacting starch with 4% succinic anhydride at 120°C for 7 minutes by the use of microwave heating.¹⁶⁹ The peak viscosity of the starch with higher DS increased to 4968 mPa due to opening up of the starch chain caused by the bulky succinate groups.¹⁶⁹

Bhandari et al.¹⁷² succinylated amaranth and corn starch pastes with DS varying between 0.05 and 0.2. The swelling power for native amaranth starch was 4 g H₂O/g polymer at 45°C while that of succinylated amaranth starch with DS of 0.2 was 7.5 g H₂O/g polymer. The increase in swelling power was due to easy hydration with the introduction of succinate groups that resulted in disorganization of the structure. Both corn and amaranth starches showed improved swelling power, paste clarity and freeze thaw stability owing to introduction of hydrophilic succinate groups.¹⁷² Corn starch surface esterified with dodecyl succinic anhydride showed an increase in tensile strength (9.7 MPa) and Young's modulus (15.3 GPa) by 2.44 and 8.37 times, respectively, that of control native starch at 75% relative humidity.¹⁸⁰ Waxy maize

starch was modified with octenyl succinic anhydride (OSA) by He et al.^{170, 181} OSA modified starch derivatives are hydrophobic and have industrial applications such as emulsifying agent and additives in a large variety of products.⁹⁷ Reaction conditions such as temperature, pH and time were shown to affect the extent of chemical modification of the thermoplastic waxy maize starch.¹⁷⁰ The DS increased from 0.0075 to 0.025 with increasing concentration of OSA from 0.5% to 3% based on the starch weight, as can be expected, since more OSA molecules were available in the vicinity of hydroxyl group in starch molecules.¹⁷⁰ Highest DS was obtained at a pH of 8. At lower pH values the anhydride groups were hydrolyzed while at higher pH values the hydroxyl groups were not active enough. DS decreased with increase in temperature at pH 8.5 indicating that hydrolysis of the OH group was more pronounced at the high temperature. Emulsification and oil absorption capacity, however, did not vary much with the concentration of OSA.

Other esterification

Gelatinized corn starch was modified by introduction of ester group from oxalic acid, a strong dicarbonic acid, in the presence of DMSO, by Zhang et al.¹⁸² Starch oxalate half-esters, a term used to describe ester formed by one of the two carboxylic acid groups of the oxalic acid with starch, with DS ranging from 0.08 to 0.87 were prepared by controlling the concentration of oxalic acid.¹⁸² The well defined polygonal shape of the starch granule was lost on gelatinization and esterification. Gelatinized starch granules were empty with caves formed inside. As a result of this erosion, oxalate ester granules exhibited a rough surface. The crystalline order was completely destroyed due to the disruption of hydrogen bonding owing to the substitution of hydroxyl groups with larger carboxyl groups. Thermal stability markedly decreased with increase in the DS of the oxalate half-ester due to the presence of free carboxylic acid group that could not react with starch. The temperature at 5% weight loss (in TGA) for native corn starch and gelatinized corn starch were 278°C and 277°C, respectively, while that for modified starch with DS 0.8 was 215°C. The loose carboxylic group also increased the hydrophilicity of the

starch molecules and water absorption increased as well. As the DS of starch oxalate half ester increased from 0.08 to 0.87 the moisture absorption increased from 33% to 42.5 %.¹⁸²

Jang et al.¹⁸³ synthesized maleated thermoplastic corn starch (MTPS) to improve compatibility and interfacial adhesion between polylactic acid (PLA) and starch. SEM images of maleic acid (MA) compatibilized PLA/starch blends showed good interfacial interaction without any edge, cavity or holes resulting from poor adhesion. The surface tension of starch and PLA was reduced by introduction of MA which allowed it to act as a plasticizer. Good adhesion was also due to the reaction between the hydroxyl groups on starch molecule and the anhydride group of MA which further reacted with PLA. Raquez et al.¹⁸⁴ maleated glycerol plasticized thermoplastic corn starch (TPS) by esterifying with MA using a reactive extrusion process to introduce functional groups on the starch backbone. It was observed, using XRD, that the residual crystalline structure of TPS was disrupted by plasticization. Consequently, a broad melting endotherm was observed in the DSC thermogram for TPS at around 140°C. Melting temperature of the maleated thermoplastic starch (MTPS) was observed to be 153°C, 10°C higher than TPS, and two sharp melting endothermic peaks were observed. This change in thermal behavior was due to chemical modification of TPS with maleic anhydride. Maleated thermoplastic corn starch has also been used for making composites by mixing with montmorillonite (layered silicate) using a twin screw extruder.¹⁸⁴⁻¹⁸⁶

Oxidation and acetylation also introduced disorder in the internal structure of the starch granules causing a decrease in temperature of gelatinization as compared to native starch. Oxidation also caused depolymerization of the starches particularly the amylopectin, leading to a decrease in the crystalline order.¹⁶⁶

Etherification

Chemical modification of native granular starch by etherification profoundly effects the gelatinization, pasting and retrogradation behavior. Some starch etherification methods and their effects on the properties are briefly discussed below.

Hydroxypropylation

Hydroxypropylation is a widely used chemical derivatization that facilitates starch gelatinization and increases cold stability of the starch pastes by reducing intermolecular hydrogen bonding. Structure for hydroxypropylated starch is presented in **Figure 18**.

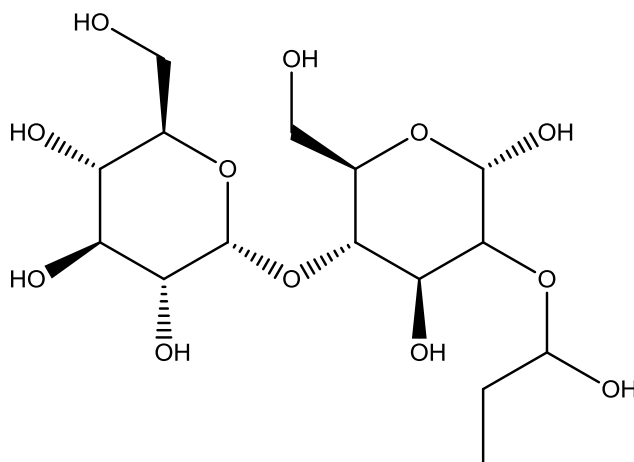


Figure 18. Structure for hydroxypropylated starch.

Hydroxypropylated starch has been produced by etherification of starch using propylene oxide or 3-chloro-2-hydroxy-N,N,N-trimethylpropylammoniumchloride under alkaline conditions.¹⁸⁷⁻¹⁸⁹ Hydroxypropylation is a thermoplastic modification that increases the number of side chains on the starch molecules that in turn increases the free volume in the starch granules.^{190, 191} This results in an increased flexibility of the modified thermoplastic starch. This process of grafting short side chains to the backbone of the molecule is commonly regarded as internal plasticization.¹⁹² Hydroxypropylated maize starches have been studied as a functional ingredient in sustained release application because of their improved functionality such as gel forming ability, biodegradability and biocompatibility over their native counterparts.¹⁹³

Wootton and Manatsathit¹⁹⁴ determined the water binding capacity of hydroxypropylated maize starches with molar substitution between 0 and 0.27 using differential scanning calorimetry (DSC). The water binding capacity was found to increase from 0.39 g H₂O/g dry unmodified starch to 0.45 g H₂O/g dry starch with molar substitution 0.27. Another study by

same authors showed that gelatinization temperature of hydroxypropylated maize starch decreased from 68°C to 50°C as the molar substitution increased from 0 (control) to 0.1.¹⁹⁵ Disruption of the granular structure of starch on modification with hydroxyl group led to increased swelling ability and enabled hydration of starch accompanied by an increase in the water binding capacity. The lowering of gelatinization temperature is also explained by the ease of gelatinization in substituted starches due to introduction of bulky groups in the starch chains and disruption of the structure as stated earlier. Research on hydroxypropylation of buffalo gourd and field pea starches was conducted to understand the effect of hydroxypropylation on the properties.¹⁹⁶ Buffalo gourd (*Cucurbita foetidissima*) is an arid climate perennial crop commonly grown in South-west USA with potential to be used as a source of starch once it is chemically stabilized against the effects of lower temperature and retrogradation. It has large fleshy roots consisting of 50% starch on an average.¹⁹⁶ Native buffalo gourd starch shows extensive retrogradation when subjected to freeze-thaw conditions. Hydroxypropylation has been shown to reduce the susceptibility towards retrogradation and syneresis in starches with a DS above 0.04 as a result of steric hindrance and hydrophilic groups within the starch chains that attract water.¹⁹⁶ Gelatinized starch consists of swollen or disrupted starch granules with entrapped water. Water separates from starch pastes through syneresis when subjected to freeze-thaw cycle contributing to undesirable textural changes to starch pastes. Retrogradation, caused by reformation of hydrogen bonds between the starch molecules, stored for a long time, causes starch pastes to lose texture and clarity. Pea starch is a legume starch produced during isolation of protein concentrates or protein isolates from the field peas using wet milling techniques.¹⁹⁷ The high amylose content in these starches leads to extensive retrogradation by association of the amylose molecule with outer branches of amylopectin. The high susceptibility to retrogradation and syneresis reduced with increase in molar substitution (MS). At 0.12 MS, water released by thawing was 76% lower than that obtained for native starch. Gelatinization temperature also reduced from 66°C for native pea starch to 56°C for hydroxypropylated starch with DS of 0.12. The hydroxypropyl groups introduced into the starch chains disrupt the inter and intra molecular

hydrogen bonding leading to an increase in accessibility of starch granules to water.¹⁹⁷ A DSC study conducted on rice starch by Seow and Thevamalar¹⁹² showed that gelatinization temperature decreased from 68.7°C for native starch to 62.9°C as the DS increased to 0.10. Another interesting observation was a broadening and shortening of the endotherm as the DS increased. This can be explained by the fact that introduction of hydroxypropyl groups in the starch chains, primarily in the amorphous region, increases the number of flexible short side chains and therefore free volume of the system. The increase in free volume, due to the internal plasticization process, facilitates absorption of water causing a decrease in gelatinization temperature. Effect of hydroxypropylation on high amylose, normal and waxy starches was evaluated by Liu et al.¹⁹⁸ It was observed that hydroxypropylation caused no observable changes in the waxy starch as a consequence of rapid hydration that obscured any changes. In all the starches swelling power and solubility increased, gelatinization temperature decreased with increase in DS of hydroxypropylation. Clarity of all the starches also increased with hydroxypropylation as a result of increase in amorphous content. Loss in paste clarity is associated with the retrogradation which is inhibited by hydroxypropylation.

The banana plants growing abundantly in humid regions of many developing countries can be also used as a potential source of starch production. Waliszewski et al.¹⁹¹ hydroxypropylated banana starch obtained from unripe banana fruit for better paste clarity, stability to retrogradation and freeze-thaw stability. The water binding capacity of the starch pastes increased from 8.9 for native starch to 11.5 for hydroxypropylated starch. Hydroxypropylated starch also showed improvement in paste clarity (2.0% transmittance after 24 hours) as compared to native starch paste (0.7% transmittance at the end of 24 hours).¹⁹¹ De Graaf and Janssen¹⁹⁹ showed that using a twin screw extruder complete conversion of propylene oxide is possible which is important because of the price and the toxic character of the material. Twin screw extruder was used as reactors for chemical modification of starch since this equipment is a good mixer for high viscous fluids, has enhanced heat transfer properties and good plug flow characteristics. Kaur et al.²⁰⁰ hydroxypropylated different cultivars of potato

starch and observed the morphological, rheological and retrogradation properties to be associated with amylose content and granule morphology. Their investigation showed that larger the size of the granule of the starting population higher was the extent of hydroxypropylation of starch. The higher the amylose content of the starch the higher was the MS. Kufri Jyothi, a potato variety studied with an amylose content of 26.9%, showed the highest MS (0.122) while Kufri Chandermukhi, another potato variety with amylose content of 19.4%, showed the least MS (0.098). Film forming properties of low substituted hydroxypropylated potato, wrinkled peas and amylo maize (high amylose) starches were investigated by Vorwerk et al.¹⁹⁰ to test their suitability for the development of flexible, highly cast transparent films.¹⁹⁰ It was concluded from the experiments that hydroxypropylated starch with high amylose content formed films with higher mechanical properties, flexibility and transparency.

The ease of casting flexible and transparent films with hydroxypropylated starch resulting due to the lower solubilization temperature is desirable for use as packaging materials. The influence of drying conditions and molecular weights on the structure and properties of hydroxypropylated starches were studied by Lafargue et al.²⁰¹ By controlling the molecular weight and casting temperature they found that modified starches with the desired structural properties can be obtained for applications such as aqueous coating in pharmaceutical industry. During the casting process it was observed that the hydroxypropylated samples of pea starch crystallized in B-type crystal structure. XRD studies demonstrated that films with molecular weight of 1.6×10^6 g/mol were amorphous while films with molecular weight of 4.7 g/mol were crystalline showing that molecular weight has profound effect on the crystalline structure of films. This behavior, common in synthetic polymers is the result of longer chains requiring more time to reorganize owing to chain entanglements and viscosity effects while shorter chains are very prone to crystallize. Casting temperature played a significant role in the crystallinity of the films in that for starch films with molecular weight of 15×10^4 crystallinity increased from 0 to 16% as casting temperature dropped from 65°C to 25°C. It was also observed that mechanical properties were not influenced by the crystallinity or molecular weight of modified starches in

the glassy region, but were affected in the rubbery region. At 25°C all the films with different molecular weight showed brittle behavior with Young's modulus values around 0.86 GPa, tensile stress at break around 34 MPa and strain at break of 9%. For example, at 25°C the flexural storage modulus was same for all specimens (1.7×10^9 Pa) but dropped dramatically to $\approx 10^7$ Pa at temperatures between 65°C and 85°C. It was also observed that in the rubbery regime (65-85°C) there was a decrease in the flexural storage modulus as the molecular weight decreased.

Maize starch has also been modified with methyl methacrylate via etherification and it was observed that factors such as NaOH concentration, reaction time, temperature affected the DS.²⁰² The reaction was carried out in several organic solvents using 1:1::water:organic solvent ratio. The extent of etherification followed the order: isopropanol > n-propanol > acetone > DMSO > ethanol.

Temperature responsive polymers were obtained by modifying starch with quaternary dimethyl alkyl ammonium groups and mechanism behind phase and gelation behavior of these modified starches were studied using turbidity and rheological measurements.²⁰³ The modified starches were both amphiphilic and amphoteric and the phase and gelation behaviors were a function of the starch concentration. Turbidity of the modified starch solution increased as the temperature decreased and at a given temperature precipitation occurred at low concentration and was reversible at higher concentration. Turbidity for 4.7% (w/w) starch solution in water decreased from 3 cm^{-1} to 1 cm^{-1} as the temperature increased from 20°C to 80°C. The phase separation and gel formation were a result of interaction between hydrophobic starch groups.²⁰³

Dual modifications

A dual modification is a combined chemical modification technique that takes advantage of the two properties obtained from both the modifications. Dually modified starches have been used in food industries as thickener, binders and emulsifiers and in non-food industries as absorbents for heavy metals. Insoluble starch xanthates were prepared by crosslinking starch with epichlorohydrin followed by xanthation.²⁰⁴ Zamudio-Flores et al.²⁰⁵ prepared films from dually modified banana starch (acetylation and oxidation) that was blended with chitosan to

evaluate their mechanical and barrier properties. In general, starch oxidation increased the tensile strength of the films (17.5 MPa) as compared to native starch (7.5 MPa) but incorporating a second modification showed no noticeable change in the mechanical properties. Blending with chitosan, however, resulted in higher tensile strength of dually modified films to 30 MPa owing to better interaction between the carboxyl and carbonyl groups of oxidized starch with the amine groups of the chitosan.²⁰⁵ Das et al.¹⁶⁶ compared properties of acetylated starch with dually modified (acetylated and hydroxypropylated) starch. Acetyl content increased during acetylation by vinyl acetate in acetylated starch but decreased in starch that was dually modified with propylene oxide followed by adipic acid anhydride.¹⁶⁶ The acetyl content in acetylated potato starch ranged between 0.47% and 1.55% (w/w). In the case of dually modified starch the acetyl content ranged between 0.52% and 0.89% (w/w). Acetylation occurred primarily in the amorphous region of the starch and in the outer lamellae of the crystalline region. The water binding capacity was lower in native starch (77%) due to hydrogen and covalent bonds formed by hydroxyl group within the starch chains and increased with modification (up to 91%). In the modified starch water binding was primarily found in the regions where amylose and amylopectin were loosely bound. Oil binding capacity of starch also increased with increase in substitution in modified starch but decreased at higher level of substitution due to reduction of amorphous regions in starch granules which reduces the available binding sites for oil in starch granules. Oil binding capacity for native starch was about 66% and varied from 77.7% (DS = 0.058) to 82.7% (DS = 0.018) for acetylated starches. Paste clarity also increased in the case of modified starch specimens (7.8% as compared to 6.0% for native starches) although the increase was much lower for dually modified starch (7.5%) than in acetylated starch (7.8%). Paste clarity is a result of retention of amorphous nature of starch as the substituted groups prevent association of starch chains. Dual modification of starch also increased the gel-strength during low temperature storage. The gel elasticity of dually modified starch was lower than that of acetylated starch and thus the rupture strength increased with increase in the acetyl content but decreased with dual modification. Acetyl groups in starch prevent interaction between starch

molecules and as a result, prevent sedimentation whereas crosslinks reduce swelling of starch molecules thus decreasing sedimentation volume. Swelling power and solubility of acetylated starch (swelling power varied from 15.5% to 18.6% and solubility varied from 4.9% to 7.3%) samples were much higher than those of native starch (13.4% and 4.7%, respectively) and the swelling power and solubility of dually modified starch was much lower (swelling power varies from 10% to 13.3% and solubility varies from 5.1% to 7.5%) than that of native starch. This is because hydroxypropylation weakens the bonding between the starch molecules and increases the chances of crosslinking.¹⁶⁶

Waxy starches are notorious for bad paste textures. Crosslinking helps in stabilizing starch pastes by getting rid of the stringiness. A second modification is generally required to improve the paste clarity, consistency and cold temperature stability. Wu and Seib²⁰⁶ crosslinked waxy barley (WB) starch with phosphoryl chloride and the resulting distarch phosphates were then acetylated and hydroxypropylated and their properties studied.²⁰⁶ Modified WB starch showed extraordinary freeze thaw stability owing to their short chain amylopectin. The dually modified WB starches also displayed clarity, i.e., high amorphous content, and good pasting properties as expected from a modified starch.²⁰⁶

Raina et al.²⁰⁷ modified broken rice kernels by hydroxypropylation with propylene oxide followed by crosslinking with adipic acid anhydride or vinyl acetate. Rice starch has unique properties like ability to form soft gel and a creamy texture due to their small granule size. The solubility of native rice starches was 8.3%, for acetylated starches it was 14.5%, for hydroxypropylated crosslinked starches it was 6.8% while for acetylated and hydroxypropylated crosslinked starches it was 10.3%. Acetylation of hydroxypropylated crosslinked starch decreased chain interaction between the hydroxyl groups of starch resulting in increased paste clarity in aqueous suspensions. The decreased interaction between the starch molecules also increased the swelling power and solubility of starch granules. Crosslinking rendered the starch more resistant towards acidic medium, heat and shearing and, as expected, decreased the solubility of crosslinked starch. Crosslinking also inhibited swelling due to strengthening of the

granules.²⁰⁷ Further, it decreased the solubility of the starch granules by reinforcing the starch granule. Acetylation, on the other hand, increased the solubility of starch by introducing intergranular disorder and facilitating the access of water to the amorphous areas. The gel strength measurement was done by the probe (cylindrical plunger; diameter 5 mm) which penetrated into the gel at a speed of 2.0 mm/s to a depth of 15 mm. During this penetration the force is shown to drop at the point where the gel breaks. A gel strength measurement is taken at the initial stage of penetration, (in this case 3 mm) where little gel deformation has occurred. The extent of increase in gel strength was lower in crosslinked starch (24.6) than in acetylated starch (31.7). Similarly, gel strength was higher in dually modified starch (34.8) than in crosslinking or acetylation alone. This is because crosslinking strengthens the starch granule thereby increasing the temperature of hydration and decreasing solubility and prevent proper gel formation. Acetylation on the other hand caused starch to remain more hydrated by opening up the polymer structure due to substitution by an acetyl group.²⁰⁷

Other factors affecting properties of chemically modified starch resins and films

It is clear that the property of modified starch resin is related to the microstructure of starches and the size and architecture of amylose and amylopectin chains, the constitutive elements. Starches rich in amylopectin such as waxy maize starch are much weaker and less stiff since amylopectin molecules do not have significant interaction with each other.²⁰⁸ Amylose chains, on the other hand, interact with each other through hydrogen bonding and hence the films formed by starches with high amylose content are much stiffer and stronger than those of amylopectin starch. It was noted that retrogradation was absent in starches that were modified with hydroxypropyl group. Retrogradation properties are indirectly influenced by the structure of the starch molecules in the amorphous and crystalline regions of the ungelatinized starch granules. Hydroxypropyl groups provide steric hindrance and thus prevent aggregation of amylopectin reducing the retrogradation behavior.²⁰⁸ Modified starches also showed improved freeze thaw stability which is influenced by the interaction between the amylose and amylopectin in the hydroxypropylated starch gels. Between acetylated, acetylated and crosslinked,

hydroxypropylated and crosslinked and acid modified corn starches, the acetylated starches with concentration of 4% and 6% in water showed the best film forming properties. The films were transparent, i.e., fully amorphous, and could be easily removed from the cast plate. Acetylated starch films formed good films because the chains showed higher degree of substitution.²⁰⁸

Several authors have already reported the formulations of composites and films from chemically modified starches.²⁰⁹⁻²¹¹ Controlling the composition, microstructural and functional properties of films allowed tailoring their properties for various applications. Plasticizers are often added to aid processing and to modify properties, particularly to reduce the brittleness, of the final products. In case of starches, plasticizers such as different polyols and lipids have been widely used to overcome film brittleness and improve extensibility and flexibility.^{212, 213} In addition, modified starches such as starch esters have also been mixed with biopolymers including gelatin and κ -carrageenan to prepare biodegradable laminate films. It was found that unplasticized films had pores and cracks; addition of plasticizer reduced the rigidity or brittleness of the network producing less ordered structures and thus improving the film quality. Plasticizing modified starch with 1.5 g glycerol/100 g of modified starch suspension reduced the water vapor permeability by 87% and increased flexibility of acetylated film by 34%.²⁰⁸

Teixeira et al.²¹⁴ studied the influence of plasticizers such as glucose, sucrose and fructose on thermoplastic cassava starch and compared it to the native starch. It was observed that presence of just 2% concentration of these sugars in the starch-glycerol system reduced the glass transition temperature and the storage modulus as a result of further plasticization and inhibited formation of crystal structure in thermoplastic starch.²¹⁴ The water uptake reduced by 60% when no glycerol was used but increased when sucrose was used as a plasticizer along with glucose. The glass transition temperature for starch with and without glycerol as plasticizer was 35°C while addition of sucrose reduced the T_g to 0°C. The loss modulus at 25°C for samples without glycerol was 0.68 MPa while that for samples plasticized with glycerol was 0.42 MPa. This is because there were two opposing effects that influenced the modulus, the presence of

crystallites and the plasticization. The final properties of the starch were modified by the additive effect of the sugars even at a very low concentration of 2 wt%.²¹⁴

Hydrophobicity of starch plasticized with glycerol increased when treated with phenyl isocyanate, toluene diisocyanate, styrene-co-glycidyl methacrylate, and stearoyl chloride due to introduction of hydrophobic and bulky functional groups. The contact angles for starch treated with phenyl isocyanate, styrene-co-glycidyl methacrylate and stearoyl chloride were 107, 84 and 99, respectively, as compared to 63 for starch films in the presence of glycerol.²¹⁵

Sorbitol is commonly used as a plasticizer to improve the mechanical properties, particularly the extensibility, of the starch films. A disadvantage with sorbitol is its tendency to crystallize over time reducing its plasticizing efficiency and thus resulting in lower film flexibility. Use of non-crystalline sorbitol (which is different from sorbitol), produced by partial hydrolysis of corn, wheat or potato starches followed by hydrogenation under high pressure has been shown to solve this problem.²¹⁶ It was observed that the elongation for sorbitol plasticized films decreased from 144% to 80% and 44% on storing for one or two months, respectively, due to retrogradation. The films, however, became stiffer and modulus changed significantly from 40 MPa to 150 MPa as a result of crystallization of starch. Also, sorbitol has lower plasticization efficiency than glycerol. The fracture strain for non-crystalline sorbitol plasticized films did not change significantly upon storage for a month.²¹⁶

Paterson et al.²¹⁷ studied the effect of adding different lipids such as acetic acid ester of monoglyceride (acetam) on starch-lipid film cast from starch solution in water at different drying temperatures (25°C – 50°C). Water vapor permeability (WVP) of the films cast at high temperature (50°C) with acetam reduced by 50%. This was because a compact structure with less free volume was created by increasing the cohesive interaction between the starch molecules at a higher temperature which dominated over the effect of adding acetam. Adding a small amount of acetum at low temperature increased the WVP by hindering chain-chain interaction. Adding 5% acetam decreased the Young's modulus (from 2.5 GPa to 2.3 GPa), tensile stress (46.2 MPa to 39.5 MPa) and strain at break (from 10.3 to 3.4). On adding more than 10%

acetam the lipid phase separated and aggregated to form droplets which appeared as bright spots under the microscope in a continuous starch film.²¹⁷

Starch type and aging time and interaction between the two factors have significant influence on the properties like Young's modulus, maximum stress and strain-at-break and moisture absorption by starch films.^{149, 218} Films made of waxy maize starch with high amylopectin content had high stiffness (Young's modulus). This is because of the structure of amylopectin molecule, which is branched, has reduced crystalline order and is more entangled in the films formed by casting. The entanglement decreases the mobility of the molecules increasing the stiffness and results in a higher glass transition temperature. The Young's modulus for films made with starches containing higher amylose content was lower than that obtained for starches with higher amylopectin content. This indicates that the entanglement had a stronger effect on the branched amylopectin structure than the H-bonding in the amylose chains. Modified starches with high amylose content also showed very low Young's modulus values.²¹⁹⁻²²⁴

The retrogradation of starch films was monitored by refractive index measurements which varied with logarithm of time.²²¹ There was a rapid rise in storage modulus of amylose gel to around 40 KPa for the first 10 hours at 25°C after which slower rise was seen. The rapid increase in modulus was due to the establishment of a 3D network structure through interchain associations while the subsequent slow rise was due to rearrangement of the crosslinked chains. Thin films, in general, aged faster than thick films as can be expected owing to the ease of diffusion of free volume to the surface of the film.²²¹

Potato starch films of varying crystallinity were produced by controlling the film formation conditions like drying temperature and humidity.^{225, 226} The starch films were all dried for 3 days at 23°C and conditioned for 2 days at 20%, 50%, 70% and 90% relative humidity. The films formed at low air humidity were amorphous while increasing the air humidity which allowed slower drying increased the crystallinity of the films with a B-type crystal structure.²²⁵ The crystallinity of the films formed from the gel depends on the ability of the chains to form

crystals as well as mobility of the chains during the process of crystallization. For the samples with a higher relative humidity (90%) the starch chains were in contact with the water molecules for a longer time which gave them greater chain mobility to rearrange into a crystal structure.

It has been shown that films formed from high amylose corn starch (55% amylose) developed B-type crystal structure below the drying temperature of 60°C and developed A-type crystal structure at or above the drying temperature of 80°C and RH of 25%.²²⁶ This transition from B-type to A-type crystal structure takes place at high temperature and high moisture content as the energetically higher double helical conformation of B-type crystal structure rearranges to a energetically more favorable A-type crystal structure. Mechanical and water resistance properties of chemically modified corn starch with lipid additives such as stearic acid, glycerol monoester of stearic acid and lecithin were studied by Leeman et al.²²⁷ Extruded strands of high amylose corn starch showed lower die swelling and greater water resistance than normal corn starch. Die swelling refers to the phenomena of increased diameter of the viscoelastic fluid as it exits the die mouth or the spinneret and occurs if the tension on the extruded filament is not sufficient and the molecules are allowed to relax. Lipid additives such as stearic acid formed complexes with high amylose starches as well as chemically modified starches which resulted in better mechanical properties and elongation than native or hydroxypropylated starch.²²⁷

Starch films blended with polyvinyl alcohol (PVOH) also showed reduced biodegradability than films made of native starch. An activated sludge which was acclimatized to synthetic waste water was used for testing the biodegradation of the blended films. It was observed that starch-PVOH films in an activated sludge did not degrade even after three months under optimized conditions. However, with the addition of PVOH degrading enzyme the film fragmented into small pieces within 10 days. This was argued to be because the degradation of the PVOH fraction in the film is a prerequisite for the complete decomposition and degradation of the starch-PVOH blended plastic films.²²⁸ Waxy maize starch acetates internally plasticized by treating with n-alkyl-succinic anhydride showed excellent film forming properties with high mechanical strength and considerable flexibility.^{183, 184} The effective plasticization by n-alkyl-

succinic anhydride was a result of the hydrocarbon chain of with accessible carbonyl groups.^{229,}

230

Native sago starch blended with PVOH was reacted with maleic acid in aqueous condition to esterify the hydroxyl groups of starch and PVOH.²³¹ The weight loss due to thermal degradation of the starch sample occurred within the temperature range of 210 to 180°C, whereas for the starch-maleate ester the weight loss occurred between 220 and 300°C and for the starch-PVOH-maleate ester it occurred between 250 and 400°C showing a significant improvement in thermal degradation behavior. This was due to the extensive crosslinking and ease of esterification of maleic acid with PVOH compared to starch which has a more complex molecular structure than PVOH. The swelling behavior could be controlled by monitoring the feeding precursor compositions, pH and temperature of swelling medium.²³¹

Chemically modified (acetylated and oxidized) banana starch blended with polyethylene formed smooth films.^{186,187} The tensile strength and elongation at break decreased when the starch concentration in the blend increased indicating that starch acted as non-reinforcing filler. The tensile strength for native starch decreased from 8.4 MPa to 7.8 MPa while the elongation at break decreased from 46.7% to 12.7%.^{232, 233} Starch acetates blended with PVOH were found to destroy crystallinity of the starches forming completely amorphous regions thus reducing their mechanical properties.²³⁴

Rheological properties of films from a nongelling modified starch such as hydroxypropylated pea starch (HPPS) was improved by mixing with K^+ (κ)-carrageenan.²³⁵ The film forming ability of starch and gel formation by κ -carrageenan helped monitor the macromolecular behavior of the mixtures in solution and the final rheological properties of the film.²³⁵ The rheological properties of these binary mixtures arise from excluded volume effects (κ -carrageenan excluded from volume occupied by HPPS). The 3-D network formed by κ -carrageenan in the mixture formed a continuous phase filled by the highly concentrated HPPS.²³⁵

Starches have also been made soluble by reacting with acid anhydrides in hot water and then blended with canola oil.²³⁶ This soluble starch was then used as dry film lubricants after

cooking in co-jet mixture of starch and lipophilic materials (oil) under high steam conditions.²³⁶⁻

²³⁸ Coefficient of friction (CoF) of dry film lubricant starches modified with anhydrides of different acids was shown to decrease in the presence of canola oil. CoF of starch with 0.02% soybean oil was 0.697 while that of starch with 31.7% oil was 0.033. Such dry film lubricants formed by starch-lipid composites were applied to steel plates as a thick coating to protect surface quality of the metal sheets, optimize CoF and reduce tool wear.²³⁶

A chemically modified thermoplastic starch (CMTPS) such as starch formate with reactive carboxyl group on the starch backbone was blended with polycaprolactone which is a biodegradable plastic to overcome the hydrophilicity and low mechanical properties of starch.²³⁹⁻

²⁴¹ Starch has also been crosslinked with trisodiumtrimetaphosphate to make it compatible with the hydrophobic polycaprolactone. The flow behavior of the blends was controlled by the polymer forming the continuous phase. Blends with lower content of CMTPS showed Newtonian type flow behavior while blends with higher content of CMTPS showed pseudoplastic behavior. Tensile strength and elongation decreased with increase in CMTPS which did not possess desirable mechanical properties to be used as bioplastic on its own.²³⁹⁻²⁴¹

Reinforced polymers with enhanced mechanical properties have been obtained by blending starch modified with resorcinol-formaldehyde (RF) and N-bis(aminoethyl)- γ -aminopropyl trimethoxy silane as fillers in rubber matrix.²⁴² In this case starch was modified with RF and silane to make it hydrophobic and compatible with styrene-butadiene rubber. Tensile strength increased with RF modification, tensile strength was 2.7 MPa for starch with no modification and 11.1 MPa for RF modified starch. The silane modified starch had a tensile strength of 4.6 MPa. The condensed crosslinked oligomer was found to bind the starch particles and rubber molecules together.²⁴²

Starch acetates have been used for their hydrophobic properties and also as blends with other compatible polymers, e.g., poly (tetramethyleneadipate-co-terephthalate) (PTMAT).²⁴³ The foams with a small amount of PTMAT were found to have homogeneous morphology with high radial expansion ratio (26.9), spring index (0.897), low density (0.5 g/cm³) and compressibility

(1.42 MPa).²⁴³ Foams from synthetic polymers like polyurethane foam from precursor liquid with density 240 kg/m³ was found to have a compressive modulus of 133.6 MPa.²⁴⁴

Conclusions

Starch is a biodegradable and yearly renewable polysaccharide that is produced in all parts of the world in large quantities. As a result, it has the significant potential to be used on an industrial scale as ‘green’ resin or film forming material. However, the inherent hydrophilicity and retrogradation properties of starch limit its application as an industrial commodity. Starches have been both chemically and physically modified using a variety of techniques as discussed in this chapter to improve their properties and making them useful as resins and films. Chemically modified starches have indeed demonstrated to have better thermal and mechanical properties whereas physical modifications like blending or heat-moisture treatment can change the rheological properties of starches. Various analyses of the structure of native starch granules obtained from different sources and their properties have been discussed in this paper. Several different modifications and their influence on film and resin forming properties are also discussed. Applying green techniques to chemically modify starch is an ecofriendly way to achieve the targeted properties. Physical and chemical modifications performed using inexpensive, naturally obtained green chemicals, harmless solvents and mild reaction conditions represent a new and pioneering field of research that is expected to expand in the future. Further modification of starches using nanoparticles and fibers can provide even better properties and can form the basis for future research.

CHAPTER 4

'GREEN' CROSSLINKING OF NATIVE STARCHES WITH MALONIC ACID AND THEIR PROPERTIES

Abstract

Starch is a highly hydrophilic biomaterial with weak mechanical properties rendering it useless for commercial applications. A fully 'green' water based process is presented to crosslink corn (cereal) and potato (tuber) starch to enhance mechanical properties as well as lower hydrophilicity. In addition, malonic acid, a green, plant based water soluble and relatively inexpensive polycarboxylic acid, was used as the crosslinker. The reactivity of potato starch towards esterification and crosslinking was found to be higher than that of corn starch owing to the inherent differences in the granule morphology and internal structure of the two starches. It was observed that potato starch granules had a higher degree of substitution (DS) of 0.19 than corn starch granules (DS = 0.1) under similar reaction conditions. Chemical, thermal and mechanical test results confirmed the crosslinking as well as reduced moisture sensitivity.

Published as:

T. Ghosh Dastidar and A. Netravali, *Carbohydr Polym*, 2012, **90**, 1620-1628

Introduction

Starches, proteins and cellulose together form an important and a large part of the available biomass and have received considerable attention because of their low cost, biodegradability, annually renewal and abundant supply throughout the world.^{245, 246} These biomaterials can be used as suitable substitutes for petroleum based products, particularly if their properties can be matched with those of petroleum based polymers. Starch is composed of two polymers of D-glucofuranose; amylose and amylopectin. Amylose is formed by glucose units joined by 1, 4 glycosidic linkages and amylopectin is formed by glucose units joined by 1, 4- as well as 1, 6- glycosidic linkages. While amylose is a low molecular weight polymer consisting of 1000- 10,000 glucose units and is linear, amylopectin is a larger branched macromolecule with degree of polymerization (DP) sometimes exceeding one million.⁷⁰ Starch based materials and composites have been used in highly sophisticated applications including biomaterials for tissue engineering.²⁴⁷⁻²⁵¹

Native starches have been crosslinked using polycarboxylic acids such as citric acid, polyphosphates such as sodium trimetaphosphate, sodium tripolyphosphate as well as epichlorohydrin, phosphorus oxychloride and 1, 2, 3, 4-diepoxybutane.^{16, 17, 99-102} Carboxymethylated starch with a DS of 0.45 has been further crosslinked using malic, tartaric, citric, malonic, succinic, glutaric and adipic acid to synthesize crosslinked hydrogels.²⁵² Crosslinking is a thermosetting modification that interconnects the starch molecules by covalent bonding, thus it not only increases the molecular weight but also enhances the mechanical properties. Water stability of starches is improved by crosslinking while at the same time the swelling is reduced.¹⁶ Further, crosslinked films also show higher thermal stability and resistance to degradation than non-crosslinked films.¹⁶

The present paper describes esterification and crosslinking of native corn starch (CS) and potato starch (PS) using malonic acid (MA) and the effects of chemical modification on their thermal, mechanical properties and swelling abilities under aqueous conditions. Corn, a cereal starch containing 27% amylose, and potato, a tuber starch containing 24% amylose, show many

differences in functional properties under similar processing conditions owing to their different origins.⁷³ The degree of amylose content influences the reactivity of corn and potato starches. Among other constituents lipid contents of the two starches are different; 0.32% in PS and 1.22% in CS.⁷³ Lipids form complex with the amylose in CS which leads to more rigid structure and high turbidity. PS also has higher content of phosphate ester groups bound to the native starch, which has been claimed to cause lower pasting temperature, higher viscosity and improved clarity.⁷³ PS granules are also fragile in nature and have a different crystal structure (B-type) as compared to CS (A-type crystal structure).⁷³

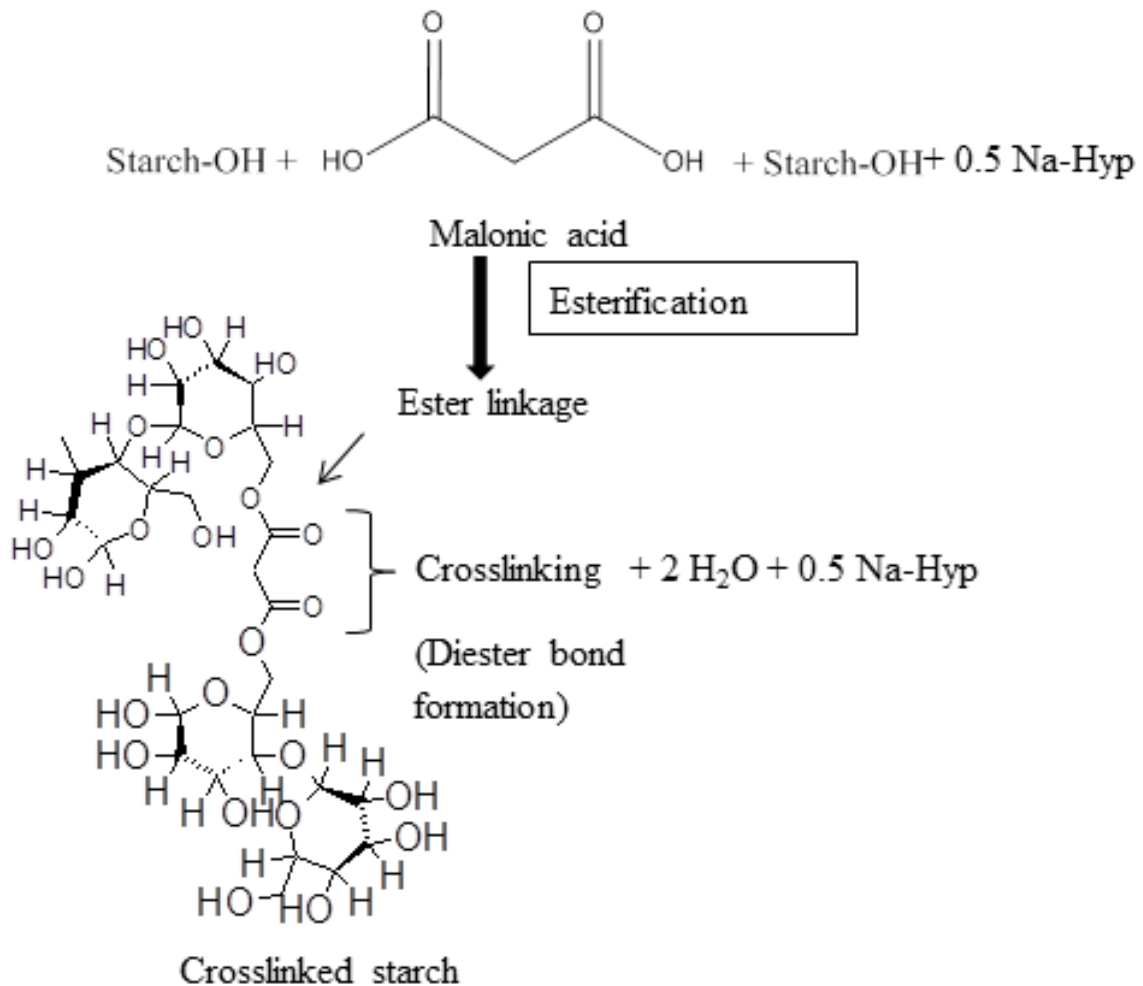


Figure 19. Proposed scheme for crosslinking starch with MA.

MA is a plant derived green dicarboxylic acid with a molecular weight of 104 g/mol that can react with the hydroxyl groups on the D-glucopyranose ring present in starch by forming ester bonds. MA is soluble in water at room temperature and was chosen as a crosslinker for starch since it is nontoxic and relatively inexpensive. In general, esterification reactions are carried out in organic solvents, require the use of toxic reagents and repeated washing of the end product by water and alcohol to remove excess organic solvents. An example is the acetylation of starch carried out by Garg and Jana²⁵³ in the presence of acetic anhydride and pyridine. The esterification of starch with MA, shown in **Figure 19**, carried out in aqueous and non-toxic conditions, using simple lab based techniques, is a benign, economical and facile way of crosslinked starch-ester synthesis.

Experimental Procedure

Materials

Native CS (73% amylopectin and 27% amylose) and PS (76% amylopectin and 24% amylose) powders were obtained from Sigma Aldrich (Saint Louis, MO). Analytical grade MA and sodium hypophosphite monohydrate (Nahyp) were also purchased from Sigma Aldrich.

Preparation of Precured and Cured Starch Films

To process CS and PS into a crosslinked resin, starch was at first gelatinized by adding 20 g starch to 500 ml water and heating at 90°C for 45 minutes with constant stirring. Theoretical calculations based on stoichiometry showed that $\approx 31.5\%$ MA is required for complete crosslinking of starch with MA. For the precuring of starch resins 3, 5, 7.5 and 10 g MA (or 15%, 25%, 37.5% and 50% MA based on the initial dry weight of starch) were added, separately, to the gelatinized starch followed by addition of sodium hypophosphite (50% by weight of MA) as catalyst. Nahyp is proven to accelerate the process of esterification with polycarboxylic acids by increasing the speed of the formation of the cyclic anhydride intermediate.²⁵⁴

The mixture was stirred continuously for 60 min at 90°C with a magnetic stirrer. After cooling the precured starch was cast to form thin films of approximately 0.3 mm thickness on a

Teflon[®] coated glass plate and dried in an oven for 48 hours at 40°C. The dried films were peeled off from the Teflon[®] coated plates and stored in sealed polythene packets. The precured PS and CS films were further heated in Carver Hydraulic hot press (model 3891-4PROA00) for complete crosslinking (curing) at 120°C under 0.1 MPa pressure for 20 min. Precured PS films (precured with 37.5% MA at 90°C for 60 min) were also cured at 100°C and 140°C at 0.1 MPa pressure for 20 min to understand the effect of temperature on crosslinking. The cured CS and PS films were then thoroughly washed in water to remove excess MA and Nahyp. The starch films were completely soaked in DI water for 8-10 hours, the water was changed a couple of times, and it was expected that the unreacted MA and Nahyp molecules which were highly soluble in water leached out into the water (also confirmed by FTIR of the washed water containing traces of MA). The washed films were either air-dried in an oven at 70°C for 2 days or conditioned at 21°C and 65% relative humidity for 4.5 days for further characterization.

Determination of Degree of Substitution (DS)

The DS of precured PS and CS films (as a function of concentration of MA) and cured PS films (as a function of temperature) were calculated using the titration method.²⁵⁵ Precured or cured starch specimens, 0.5 g, were accurately weighed into a 100 ml vial and 50 ml deionized (DI) water was added. The sealed vial with water and starch was agitated in a shaker bath at 200 rpm for 4.5 days. The excess unreacted MA that leached out into the water was carefully neutralized with standard sodium hydroxide solution using phenolphthalein indicator. Excess standard NaOH (1 N, 10 ml) was added and shaken on a shaker bath for 1 hr at 200 rpm to achieve homogeneous mixing. The entire set up was stored at 50°C for 3 days with occasional shaking for complete hydrolysis. At the end of 3 days the excess alkali was back-titrated with standard HCl (0.4 M) solution. A blank (control) was simultaneously titrated with native starch instead of precured or cured starch. Degree of substitution was calculated using following formulae.⁹⁶

$$\% \text{ malonate} = \frac{([\text{ml (blank)}] - \text{ml (sample)}) \times \text{normality of acid} \times 0.104 \times 100}{\text{sample weight in grams (dry basis)}}$$

$$\text{degree of substitution (DS)} = \frac{162 \times \% \text{ malonate}}{104 \times 1000 - (103 \times \% \text{ malonate})}$$

Attenuated Total Reflectance-Fourier Transform Infrared (ATR-FTIR) Spectroscopy

ATR-FTIR spectra were collected using a Nicolet Magna 560 FTIR spectrometer with a split pea accessory for ATR. Each scan was an average of 150 scans recorded from 4000 cm^{-1} to 550 cm^{-1} wavenumbers obtained at a resolution of 4 cm^{-1} . The spectra of pure starches, pure MA and precured and cured starches were obtained and compared.

In order to construct a calibration curve from the ATR-FTIR spectra, the absorption peak at 1725 cm^{-1} due to the ester carbonyl (C=O) stretching vibrations was chosen as the analyte peak. It monitored the concentration of ester, which is related to the concentration of MA in the specimen. Since the absorption due to aliphatic -C-H stretching vibration, at 2929 cm^{-1} , remains unchanged after the crosslinking reactions, it was chosen as the reference peak for the internal standard. The ratio of absorbance by the analyte peak and the reference peak was plotted against concentration of MA. This method was similar to the calibration method used by Coma et al.²⁵⁶, to assess the degree of crosslinking of cellulose with citric acid.

Thermogravimetric Analysis (TGA)

Native and crosslinked starch specimens (both PS and CS) were scanned from 25°C to 600°C using a thermogravimetric analyzer (TGA-2050, TA Instruments, Inc., New Castle, DE) at a rate of 10°C/min in nitrogen atmosphere to characterize their thermal stability and degradation behavior. Malonic acid was scanned from 25°C to 400°C at 10°C/min.

Differential Scanning Calorimetry (DSC)

In order to test the specimen in DSC the precured and cured specimen were conditioned for 3 days at 21°C and 65% relative humidity. Specimens weighing about 12 mg (MA, native PS as well as precured and cured PS) were accurately weighed and scanned on the DSC (model-2920, TA Instruments, Inc., New Castle, DE) from 25°C to 400°C at a ramp rate of 25°C/min to obtain thermograms¹⁶. The DSC was calibrated using ASTM 968-99 and E967-97 procedures.

The melting, decomposition and crystallization temperatures were obtained using ASTM 794-98 procedure.

Wide Angle X-ray Diffraction Study (WXR)

Scintag θ - θ powder wide angle diffractometer (PADX, Scintag, Inc., Cupertino, CA) with a solid-state intrinsic germanium detector was used at 40 kV and 40 mA to study the X-ray diffraction (WXR) patterns in MA, native and crosslinked (cured) PS and CS specimens. The specimens were scanned from 5°C to 40°C at the speed of 1°C/min using the Cu K α X-ray radiation (1.5405Å) at 45 kV and 40 mA. The crosslinked resin specimens were used in the form of films.⁷⁸

Swelling Power and Gel Fraction of Films

The swelling power of crosslinked PS (cured at 120°C and 0.1 MPa for 20 mins) films with 15%, 25% and 37.5% initial concentration of MA, were determined according to the method given by Yun and Yoon²⁵⁷. Accurately weighed dry crosslinked (cured) PS films (0.5 g) were immersed in distilled water at room temperature (25°C) for 3 days. At the end of soaking period the films were taken out, the moisture on the surface was removed and the weight of the films was measured.

The swelling power was calculated as follows:

$$\text{Swelling power} = \frac{W_e - W_o}{W_o}$$

where W_o is the dry weight of the starch films and W_e is the weight of the film after being immersed in water for 3 days.

The swelling power of starch in DMSO was found by using the modification of a method demonstrated by Zhou et. al.²⁵⁸ The crosslinked starch films were conditioned in 21°C and 65% relative humidity for 2 days prior to soaking in 20 mL DMSO at room temperature for 24 hr. The films were accurately weighed (m_d) before immersing in DMSO. The swollen films were filtered, washed with water and ethanol, wiped lightly and weighed (m_s).

The swelling power was calculated as follows:

$$\text{swelling power} = \frac{m_s - m_d}{m_d}$$

To calculate the gel fraction the insoluble part of the film was washed thoroughly with water and ethanol and vacuum dried at 80°C. The films were conditioned at 21°C at 65% relative humidity and weighed (m_g)

The gel fraction was calculated as follows:

$$\text{Gel Fraction} = \frac{m_g}{m_d} \times 100\%$$

Mechanical Properties

The resin films were cut into rectangular pieces of 50 mm × 10 mm dimensions to test their tensile properties. The film thickness was approximately 0.30 mm. The films were thoroughly washed with water, conditioned for 4.5 days at 65% relative humidity and at a temperature of 21°C prior to testing. The tensile properties of gelatinized and crosslinked films were characterized using Instron, model 5566 (Instron Co., Canton, MA), according to ASTM D882-02. A gauge length of 30 mm and a strain rate of 0.6 were used for all specimens. At least 5 specimens were tested to obtain the average values.

Results and discussions

Infrared Spectroscopy

The ATR-FTIR spectra of gelatinized PS, MA, blend of native PS and MA and PS crosslinked (cured at 120°C at 2000 lb for 20 min) with 37.5% MA are presented in **Figure 20(A)**. From the ATR-FTIR spectra it can be observed that gelatinized starch has three C-O stretching absorption peaks (C-O-C and C-O-H) between 923 and 1162 cm^{-1} , the fingerprint region¹⁵⁰. The peaks at 1083 and 1023 cm^{-1} are attributed to the glucopyranose ring O-C stretching vibrations. The peak at 1640 cm^{-1} is assigned to the water adsorbed by starch molecules. The hydrogen bonded hydroxyl group appears as a very broad peak at 3403 cm^{-1} while the aliphatic C-H stretch is observed as a sharp peak at 2629 cm^{-1} .¹⁵⁰ ATR-FTIR spectrum of MA shows a sharp peak at 1695 cm^{-1} for the carbonyl stretching. The broad peak at 2890 cm^{-1} is attributed to the stretching of hydrogen bonded hydroxyl groups. Hydroxyl, O-H, deformations and C-O stretching modes show peaks at 1433 cm^{-1} and 1293 cm^{-1} , respectively. On comparing the spectra of gelatinized PS, MA and PS esterified with MA shown in **Figure 20**

(A), the presence of ester bond can be confirmed by the presence of carbonyl (C=O) peak in cured (crosslinked) PS that is observed at 1725 cm^{-1} . A similar peak at 1725 cm^{-1} was also observed for CS esterified with MA. The ATR-FTIR spectra obtained for CS and PS esterified with MA were identical and hence the spectrum for CS is not presented. It was further noted that the carbonyl stretching peak for MA appeared at 1695 cm^{-1} and that for the mixture of PS and MA appeared at 1682 cm^{-1} . These results are similar to those observed by Sauperl and Stana-Kleinschek²⁵⁴ in which the carbonyl peak for unreacted 1, 2, 3, 4 -butanetetracarboxylic acid appeared at 1701 cm^{-1} and shifted to 1725 cm^{-1} after ester formation.^{254, 259} Mathew and Abraham⁹⁶ reported the esterification of native PS with ferulic acid which showed the presence of carbonyl peak in the FTIR spectrum at around 1726 cm^{-1} which was distinct from the carbonyl peak obtained for ferulic acid at 1692 cm^{-1} .

Figure 20 (B) shows the extent of esterification of PS and CS as a function of initial MA content, using the internal calibration curve. A gradual increase in the A_{1725}/A_{2929} ratio was observed as the concentration of MA increased which leveled off as the concentration of MA reached 50%. This implies that with the increase in MA concentration there was an increase in the number of ester bonds formed.²⁵⁶ The absorbance of the standard peak (A_{2929}) did not vary with crosslinking. The absorbance at 1725 cm^{-1} becomes saturated at a higher concentration of MA (50%) which may indicate a possible saturation in terms of crosslinking percentage or saturation of the infrared signals.²⁵⁶ On comparing the internal calibration curves for precured PS and CS it was evident that at any concentration of MA, PS had a higher extent of esterification. This can be related to the more flexible granular microstructure of PS. This observation was also confirmed by the DS values of precured PS and CS determined by titration method as discussed later. It was also found that the ester carbonyl peak absorbance increased with the decrease in pH the highest being at pH of 1.5.

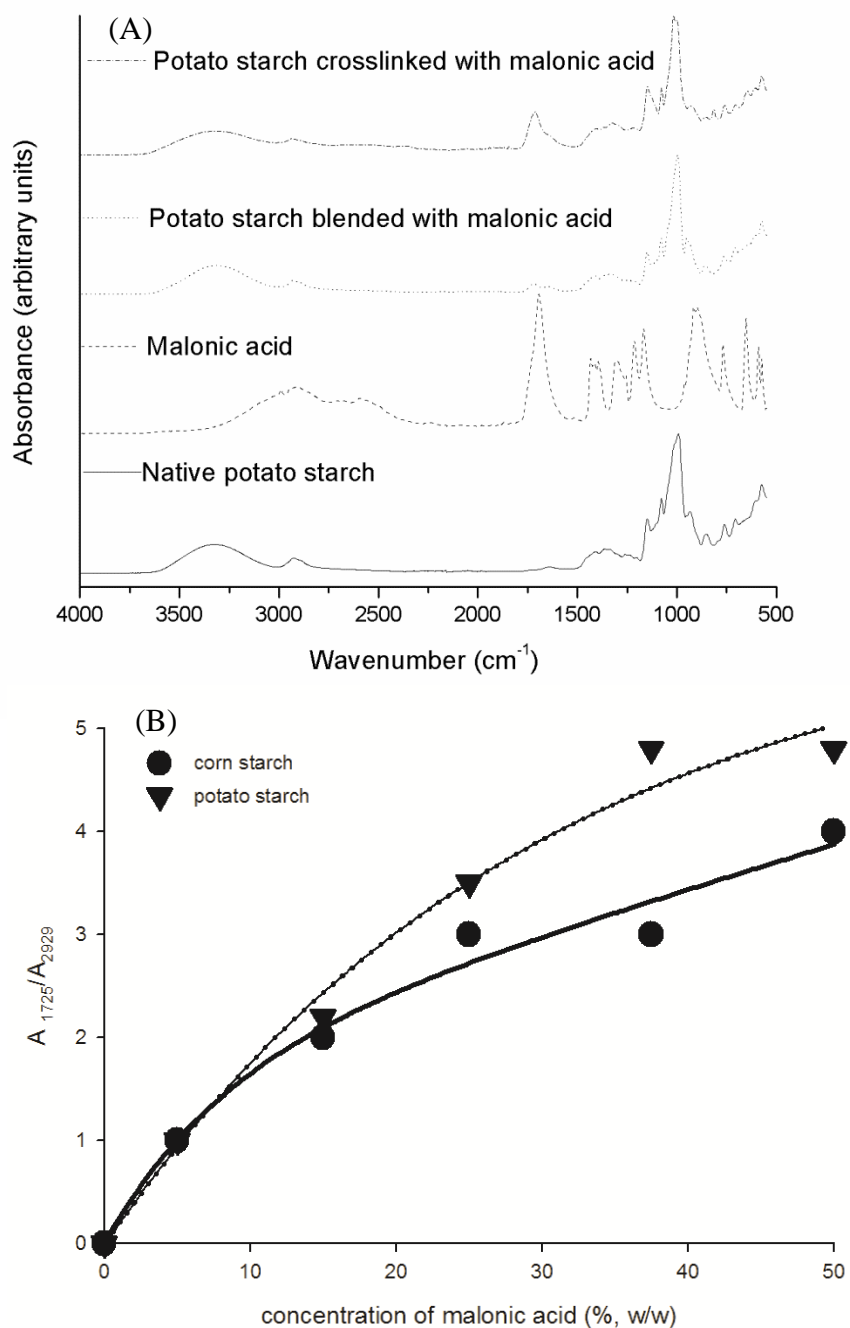


Figure 20. (A) The ATR-FTIR spectra of gelatinized PS, MA, blend of native PS and MA and PS crosslinked (cured at 120°C at 2000 lb for 20 min) with 37.5% MA (B) Extent of esterification of PS and CS as a function of initial MA content, using the internal calibration curve.

Degree of Substitution by Titration

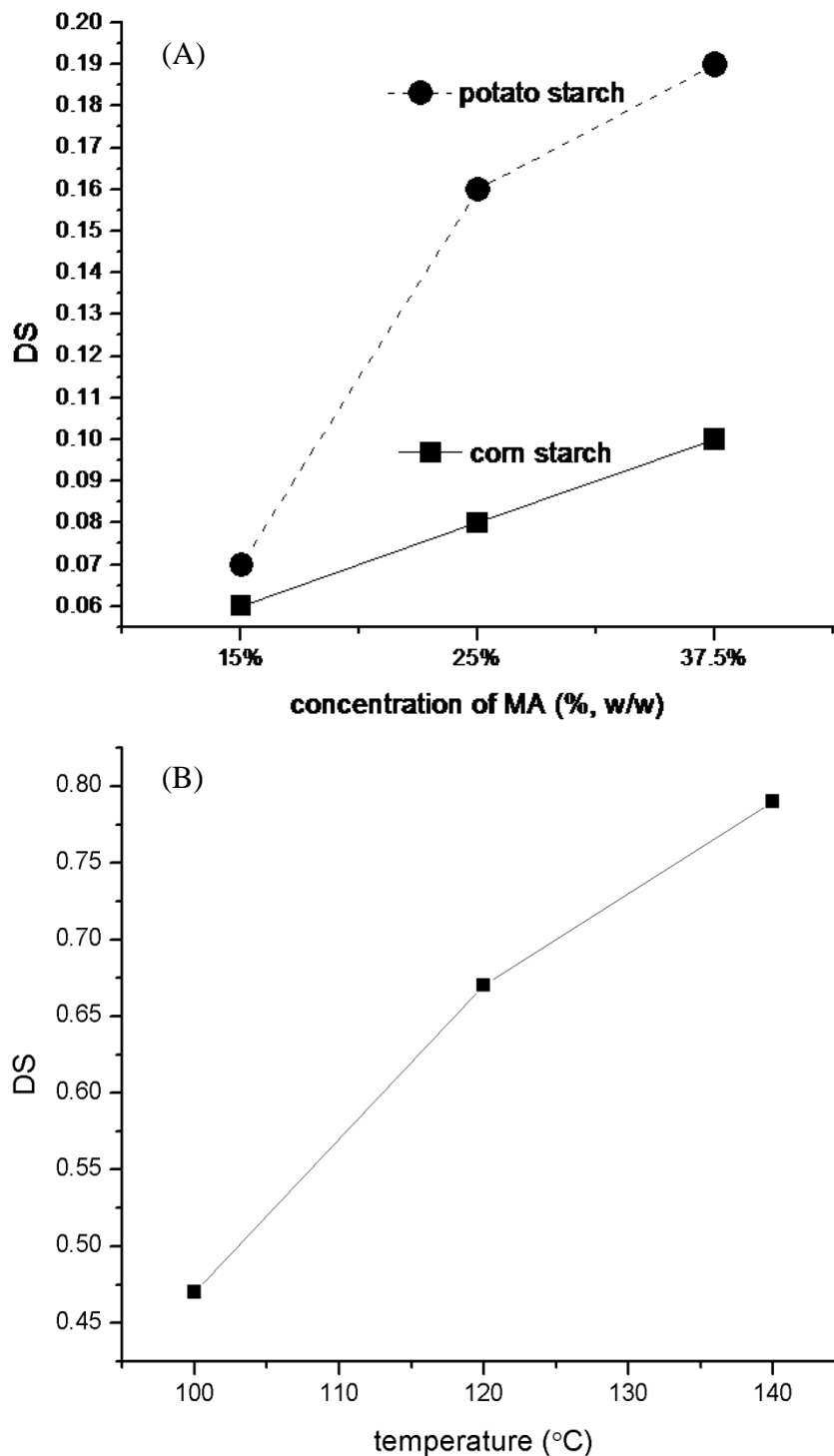


Figure 21. DS of (A) precured PS and CS as a function of MA concentration (B) PS (precured with 37.5% MA at 90°C for 60 min) as a function of curing temperature.

The DS of a starch derivative is defined as the number of hydroxyl groups substituted per D-glucopyranosyl ring.⁹⁶ Since each ring possesses three hydroxyl groups, the maximum DS possible is 3. However, the primary hydroxyl group (C-6) is much more reactive than the two secondary hydroxyl groups (C-2 and C-3) due to steric hindrance.⁹⁶ DS is affected by various factors like source of starch, amylose and amylopectin content, reactant concentration, reaction time and temperature.^{96, 158, 234}

Figure 21 (A) shows DS of precured PS and CS as a function of MA concentration while **Figure 21** (B) shows the DS of PS (precured with 37.5% MA at 90°C for 60 min) as a function of curing temperature. The DS values were calculated by the titration method. It is clear that the DS values increased with increase in the MA concentration (**Figure 21A**). This is because high MA concentration results in greater availability of MA in the vicinity of the OH groups on the starch molecules.¹⁵⁸ The DS values were 0.07, 0.16 and 0.19 for PS precured with 15%, 25% and 37.5% MA for 60 min, respectively; the corresponding DS values for CS were 0.06, 0.08 and 0.1 (**Figure 21A**). Since the internal calibration curve **Figure 21B** already showed that crosslinking reached a saturation at higher concentrations of MA, DS was not calculated for MA concentrations above 37.5%. The data in **Figure 21** A indicate that the DS for CS at any concentration was lower than that of PS. This is expected since PS has been shown to be more reactive than CS.¹⁵⁹ This is further attributed to the more compact structure and presence of lipids in CS granules. Lipids form complex with the amylose and leads to the formation of a rigid structure which inhibits penetration of external reactants and prevents substitution. PS on the other hand has a more flexible structure and the hydroxyl groups are more exposed for reaction.^{73, 159} The DS values obtained by the titration method (**Figure 21** A) confirm the earlier discussed results of the extent of esterification reaction obtained by the internal calibration curves (**Figure 20 B**) that higher esterification is obtained with increase in the concentration of MA. This trend is consistent with the results of crosslinking cellulose with a polycarboxylic acid like citric acid reported by Coma et al.²⁵⁶ As mentioned earlier, the DS values obtained for PS were higher than those of CS at any concentration of MA. Since the DS of the precured PS

specimen, with 37.5% MA, was the highest, this specimen was chosen for curing in a hot press. The DS of cured specimens were significantly higher than DS of precured specimens as could be expected. DS values for the crosslinked PS specimens (with 37.5% MA) cured at 100, 120 and 140°C were found to be 0.47, 0.67 and 0.79, respectively, as shown in **Figure 21(B)**. It was also observed that films of PS precured with 37.5% MA for 60 min, showed a significant reduction in the ester carbonyl peak absorbance in ATR-FTIR after soaking in deionized water (pH = 7) for 2 days and drying thereafter. This was possibly due to hydrolysis of the ester bond in presence of water as well as washing away of unreacted malonic acid. However in the case of PS specimens precured with 37.5% MA for 60 min followed by curing for 120 min at 0.1 MPa and 20 min, the ester carbonyl peak was much more stable and soaking in water for 1 day to 4 days did not produce any significant reduction in the ATR- FTIR absorbance of the ester carbonyl peak. From these experiments it was concluded that after curing, the number of ester bonds formed was significantly higher and the number of ester bonds hydrolyzed, after soaking in water, was negligible compared to the total number of ester bonds formed. This confirms that high temperature (120°C) curing increases the extent of esterification. Also, there was much less unreacted MA in the system after curing which is indicative of higher crosslinking that leads to higher ester peak intensity both before and after the soaking in DI water (pH = 7). These results combined with the increase in DS values with increase in curing temperature led us to conclude that the DS of starch specimens increased with increase in curing temperature due to higher extent of esterification at higher temperature. While in the hot press MA and starch also react at a higher temperature in the absence of water that leads to higher esterification and crosslinking than precuring the specimens in aqueous conditions. Carrying out esterification reaction in the presence of minimum water is crucial due to reversibility and hydrolysis of the esterification reaction, as explained earlier. The DS of the starch ester prepared with malonic acid in aqueous conditions were higher than the DS values reported (maximum DS of 0.02) for starch (waxy maize and amaranth) ester formation in aqueous conditions with n-octenyl succinic anhydride.²⁶⁰

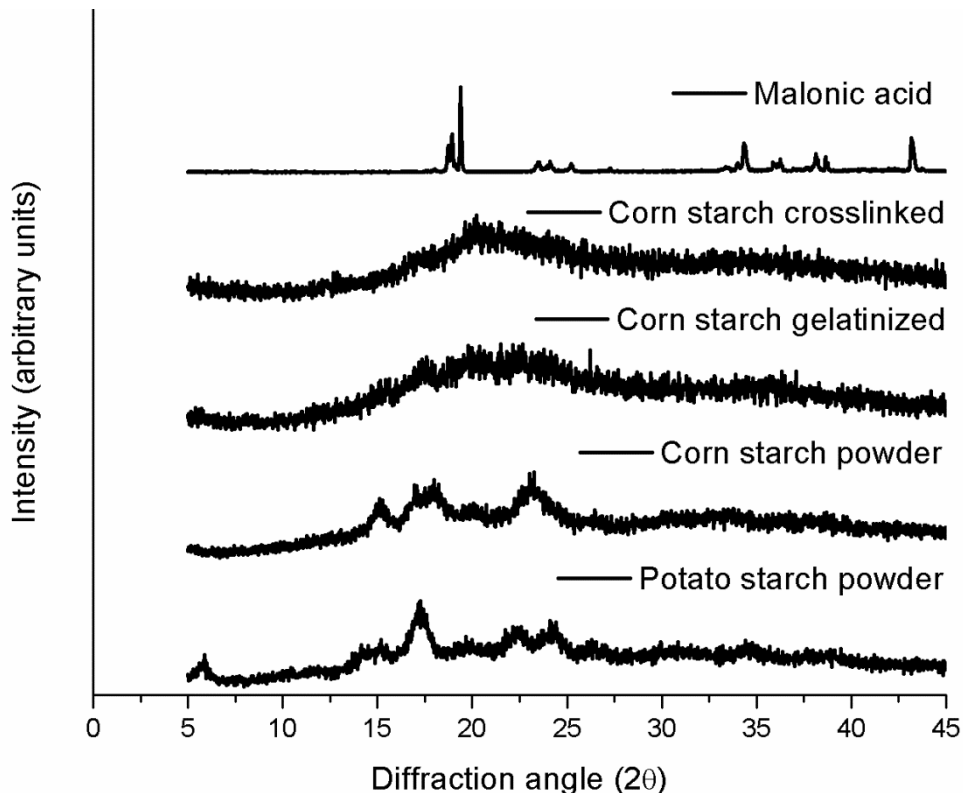


Figure 22. WXR patterns of native PS and CS powders, MA and gelatinized and crosslinked CS.

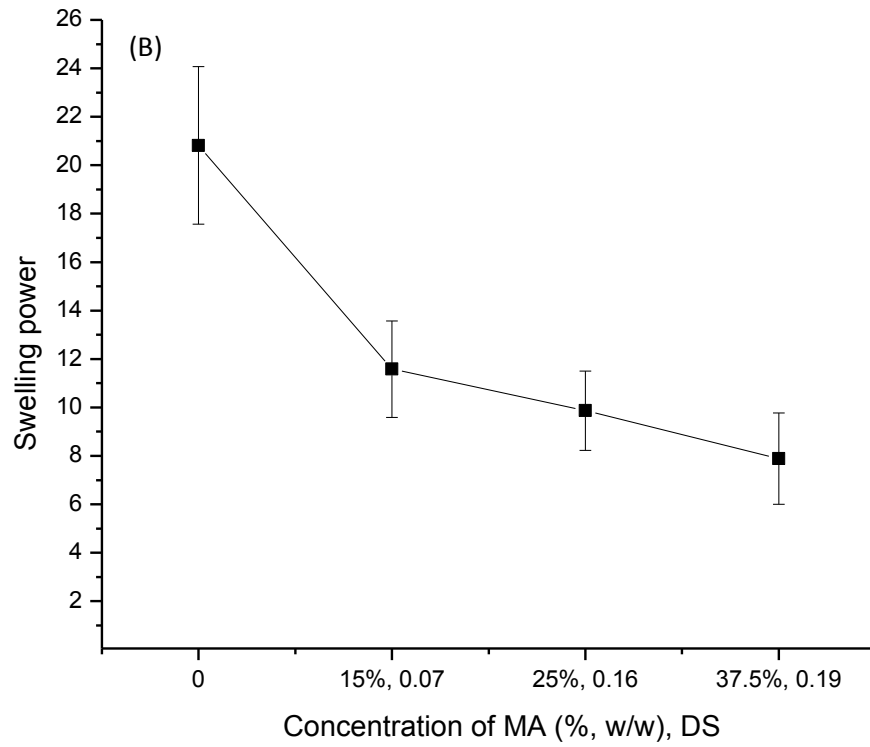
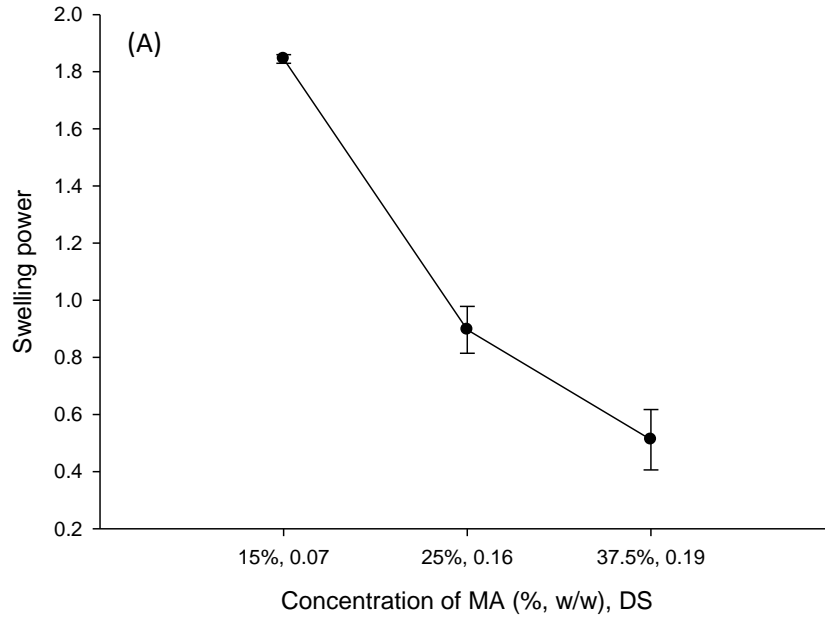
Figure 22 shows WXR patterns for native PS and CS powders, MA and gelatinized and crosslinked CS. Native CS shows A-type crystal structure typical for cereal starches whereas native PS shows B-type crystal structure typical for root or tuber starch.²⁶¹ It was observed that native CS powder showed crystal peaks at 2θ of 15° , 17° , 18° and 23° and native PS powder showed crystal peaks at 2θ of 5.6° , 15° , 17° and 22° which is consistent with previously reported values.²⁶¹ The WXR patterns for gelatinized and crosslinked PS were identical to those of crosslinked CS, and therefore, not shown. WXR patterns in Figure 4 indicate that the crystal structures of CS and PS as well as MA were completely destroyed after gelatinization and crosslinking. The destruction of crystallization due to gelatinization helped in exposing the hydroxyl groups of the starch molecules which ensured better reaction with MA molecules. In addition, the substitution of the hydroxyl groups on the starch molecules with the ester groups

prohibited the inter- and intra-molecular hydrogen bonding, completely disrupting the crystal structures. This is in agreement with the DSC results which confirmed that the MA crosslinked starch showed no crystal melting endotherm and are discussed in details later. It is also expected that as the crosslinked molecules cannot reorganize in 3-D crystal structures this prevented the recrystallization of the starch molecules after crosslinking.

Swelling power and gel fraction studies

Figure 23 shows (A) the swelling power of crosslinked PS (cured at 120°C and 0.1 MPa for 20 min) with 15%, 25% and 37.5% initial MA concentration, in water (B) the swelling power of crosslinked PS (cured at 120°C and 0.1 MPa for 20 min) with 15%, 25% and 37.5% initial MA concentration, in DMSO and (C) the gel fraction of crosslinked PS (cured at 120°C and 0.1 MPa for 20 min) with 15%, 25% and 37.5% initial MA concentration, in DMSO. The swelling power of starch depends on the nature of the polymer network like presence of hydrophilic groups, crosslink density, elasticity of polymer network, pH and the swelling medium and its temperature.²³¹

The inherent property of starch to absorb a lot of moisture affects the mechanical properties of starch and any improvement in reducing the moisture sensitivity is important for industrial application of starch. It has been shown in **Figure 23** (A) the swelling power decreases as the initial concentration of MA increases. As the concentration of MA initially used to crosslink starch increases, there is an increase in the degree of substitution as shown in **Figure 21** (A). The decrease in the swelling power with the increase in initial MA concentration was clearly due to the increase in the crosslinking density which hindered the penetration of water into the starch molecular network. The destruction of crystallization due to gelatinization helped in exposing the hydroxyl groups of the starch molecules which ensured better reaction with MA molecules. This led to higher degree of substitution as well as crosslinking. The formation of a network structure with crosslinking prevents absorption of water.



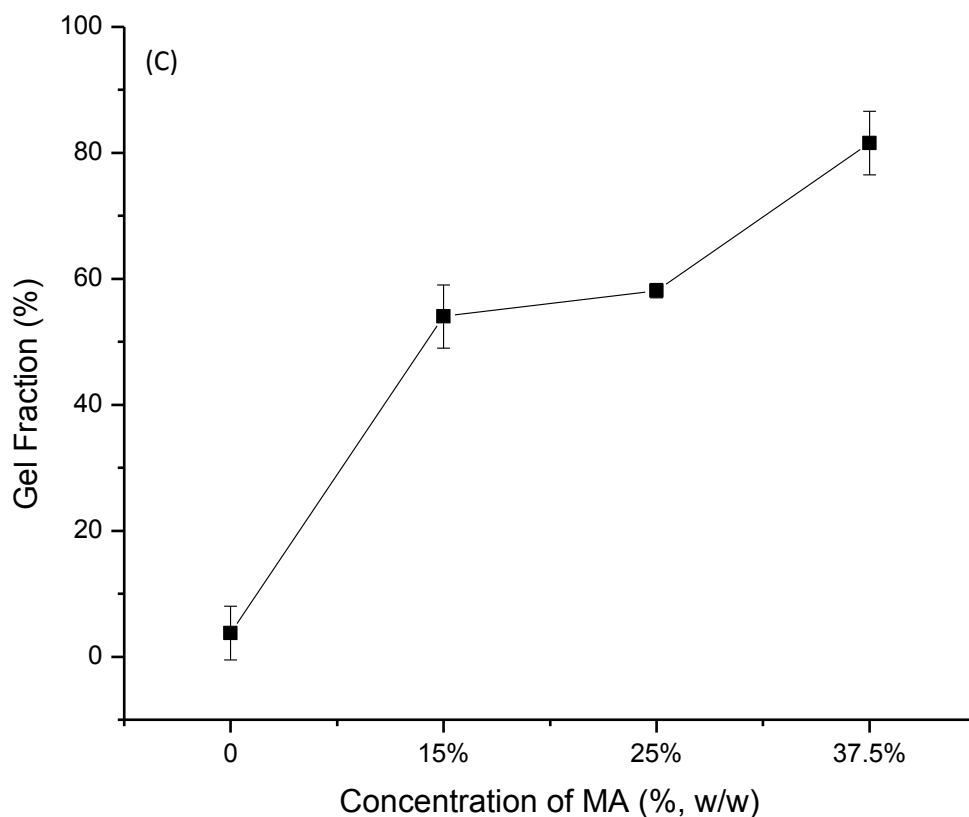


Figure 23. (A) the swelling power of crosslinked PS (cured at 120°C and 0.1 MPa for 20 min) with 15%, 25% and 37.5% initial MA concentration, in water (B) the swelling power of crosslinked PS (cured at 120°C and 0.1 MPa for 20 min) with 15%, 25% and 37.5% initial MA concentration, in DMSO and (C) the gel fraction of crosslinked PS (cured at 120°C and 0.1 MPa for 20 min) with 15%, 25% and 37.5% initial MA concentration, DMSO.

The wet and swollen crosslinked (cured) PS specimens curled up and folded but remained intact in water and the water was completely transparent indicating that the specimens did not disintegrate. The gelatinized PS (without MA) specimen on the other hand disintegrated in water. Swelling powers of CS for different concentrations of MA were not calculated because of the difficulty in handling the swollen CS films which led to inconsistent values. The swelling power of 1.15 obtained for crosslinked (cured) CS with 37.5% MA after swelling for 3 days was, higher than that of PS (0.6), under similar conditions, because of the lower reactivity resulting in

lower crosslinking density of the CS films. As explained earlier, crosslinking strengthens the polymer network reducing the absorption of water and does not allow it to swell.

DSC and TGA Studies

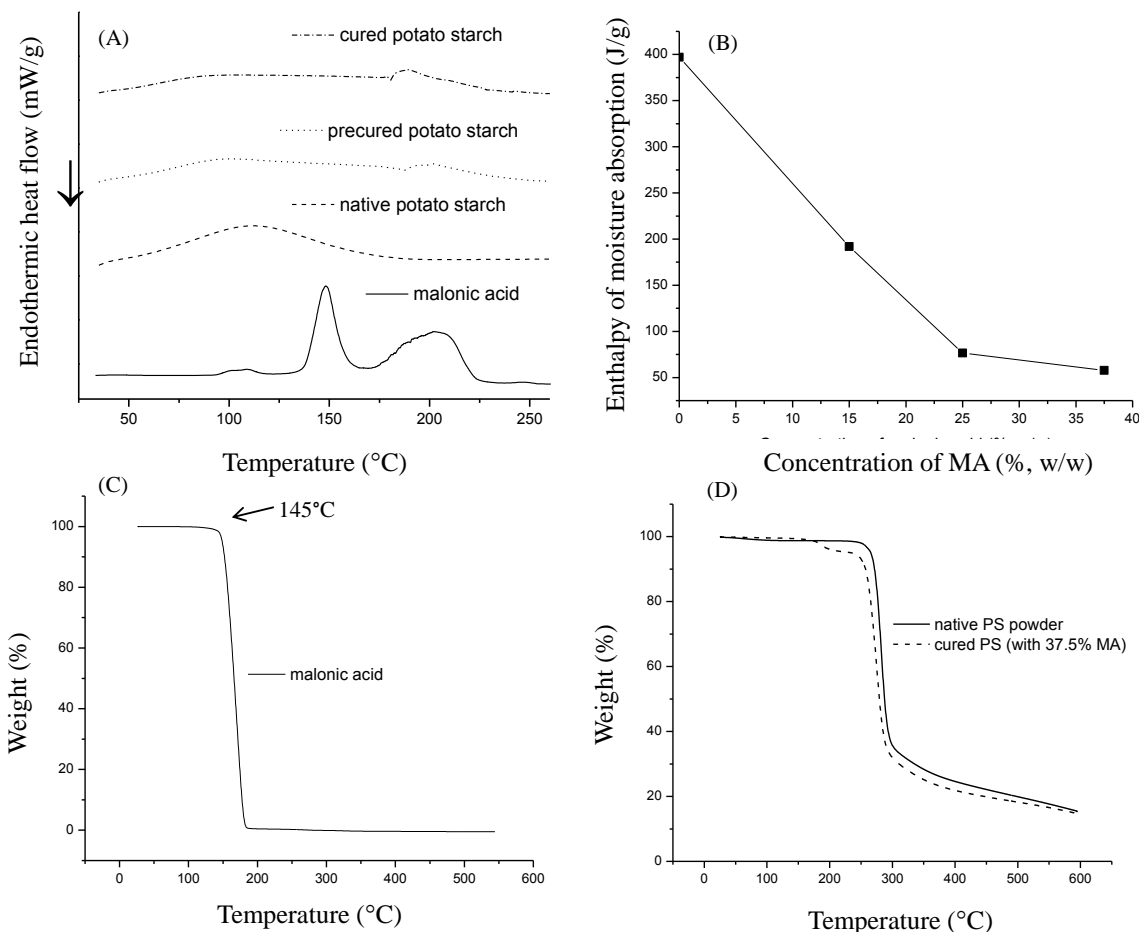


Figure 24. (A) DSC thermograms of MA and native, precured and cured PS heated from 25°C to 260°C at 25°C/min (B) DSC enthalpy values for moisture absorption for PS specimens precured with different MA concentrations (C) Thermal degradation behavior of MA and (D) TGA of PS powder and cured PS (with 37.5% MA).

DSC thermograms of MA and native, precured and cured PS specimens heated from 25°C to 260°C at 25°C/min are shown in **Figure 24(A)**. A broad endothermic peak was observed for native, precured and cured PS specimens at 100°C corresponding to the evaporation of the absorbed moisture. The DSC thermogram for native, precured and cured specimens indicated no

glass transition or crystal melting peak before 260°C.¹⁸² After 260°C the starch decomposes, as was indicated by TGA studies that are discussed later. After crosslinking, the remaining dispersed MA remains completely amorphous as indicated by the absence of crystal melting peak in the DSC thermograms and was confirmed by WXR D results discussed earlier.

Figure 24 (B) indicates the DSC enthalpy values of moisture absorption for PS specimens precured with different MA concentrations. The data indicate that as the concentration of MA increased the enthalpy for moisture absorption of precured PS specimens decreased. This is expected since higher concentration of MA leads to higher crosslinking lowering the moisture content in the crosslinked starch. This trend is similar to the decrease in swelling power for PS with increase in concentration of MA, as explained before. The plot also shows that DSC enthalpy value for moisture absorption for cured PS specimen (with 37.5% MA) is lower than the precured specimen with the same initial concentration of MA due to higher extent of crosslinking with curing.

Figure 24(C) shows the TGA thermogram of MA while **Figure 24** (D) shows the thermogram of PS powder and cured PS (with 37.5% MA). These thermograms show that MA starts to degrade at 145°C (**Figure 24C**) while native PS and CS powder as well as gelatinized PS and CS powder start to degrade at 260°C (**Figure 24D**). It was observed that after crosslinking there was no change in the thermal properties of PS and CS. In the studies done by Zhang et al.¹⁸² it was observed that the initial thermal degradation temperature was 278°C for gelatinized CS which decreased to 204°C for starch oxalate ester (DS = 0.87, obtained by titration). This was believed to be due the presence of half reacted carboxylic acid groups (starch oxalate half ester formation) which resulted in lower thermal stability of the starch resin. Since reaction of starch with malonic acid did not lead to lowering of the thermal degradation temperature it can be expected that both the carboxylic groups of MA reacted with starch to form a complete ester.

Tensile Properties

The tensile properties such as Young's modulus, tensile stress at maximum load and strain (%) at maximum load of gelatinized CS and PS, precured and cured PS films are summarized in **Table 1**. The tensile stress-strain curves for gelatinized PS (without MA) presented in **Figure 25 (A)** show classic yielding prior to fracturing.

Sample	Modulus (MPa)	Tensile stress at maximum load (MPa)	Tensile strain at maximum load (%)	Tensile strain at break (%)
Gelatinized PS	923 (12.54)	33.45 (17.67)	5.85 (32.5)	7.6 (45.72)
Precured PS	1359.8 (22.68)	35.5 (2.14)	4.68 (15.8)	6.3 (17.76)
Cured PS	2701 (18.79)	23.17 (27.74)	1.58 (34.48)	2.08 (46.19)

Table 1. The tensile properties such as Young's modulus, tensile stress at maximum load and strain (%) at maximum load of gelatinized CS and PS, precured and cured PS films.

The stress-strain curves of gelatinized, precured and cured PS are presented in **Figure 25(B)**. The Young's modulus for gelatinized PS was 923 MPa. After precuring and curing the Young's modulus increased significantly to 1359.8 and 2701 MPa, respectively (**Figure 25 B**). This increase in modulus is attributed to higher crosslinking of the PS after curing as compared to precured starch and gelatinized starch. Crosslinking forms a rigid network structure and thus increases the Young's modulus.

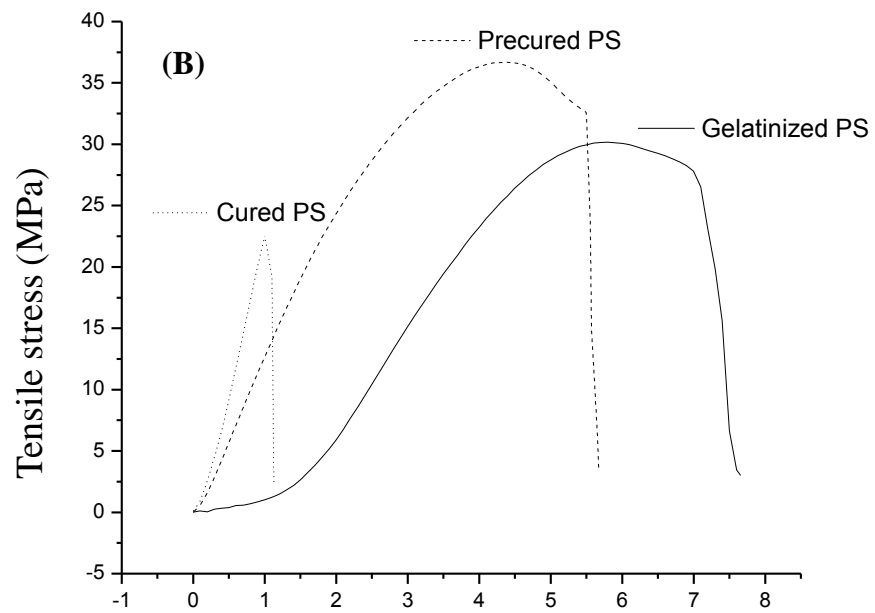
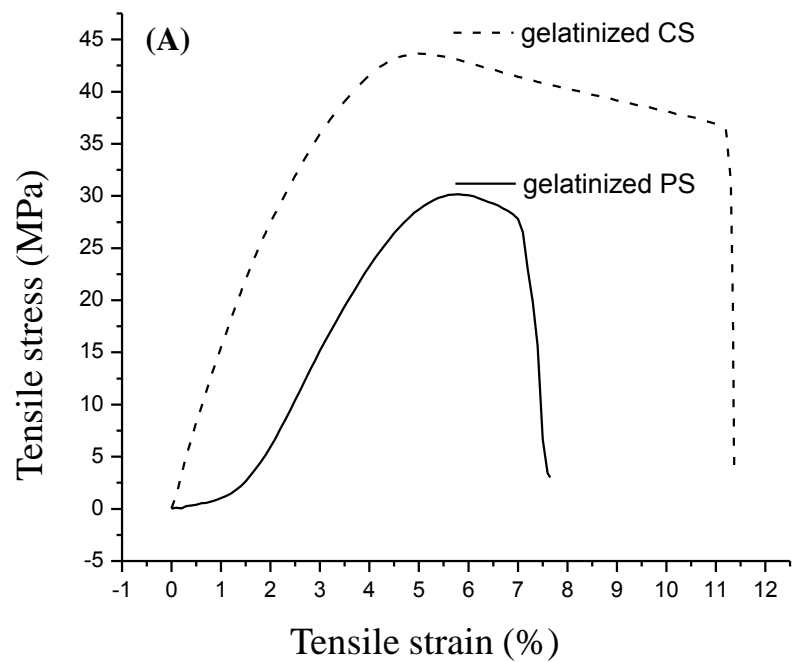


Figure 25. Tensile stress-strain curves of (A) gelatinized CS and PS, (B) gelatinized, precured and cured PS.

However, part of the increased Young's modulus is also due to the lower moisture absorption after crosslinking. The tensile stress at maximum load decreased from 35.5 MPa for precured PS and to 23.17 MPa for cured PS and strain at break (%) at maximum load decreased from 4.68% to 1.58% for precured and cured starches, respectively. The lower value of strain at break (%) at maximum load is attributed to the brittle nature of the cured PS compared to the precured PS and native PS both of which show yielding prior to fracture. The decrease in stress at maximum load for the cured PS is primarily due to its significantly lower fracture strain. It was also evident from **Figure 25 (B)** that there was a significant increase in strain at break as compared to the strain at maximum load for both gelatinized and precured starch indicating yielding. The strain at break (2.08%) in case of cured PS was not much higher than strain at maximum load (1.58%) indicating a brittle fracture; there was no yielding prior to fracture. The typical stress-strain curve for a highly crosslinked specimen as in the case of cured PS **Figure 25 (B)**) in absence of a plasticizer show brittle fracture, the specimen attains the highest load and then fails catastrophically. This is attributed to the decrease in molecular mobility as a result of crosslinking and formation of a thermosetting polymer.²⁶²

Conclusions

A completely green, easy to scale-up water based process was developed for crosslinking of starches using malonic acid, a plant based, non-toxic, sustainable crosslinker. Malonic acid esterification of corn starch and potato starch indicated that potato starch is more reactive compared to corn starch owing to the inherent structural differences in these two starches. The differences in reactivity in the starches was evident from the degree of substitution, calculated using a chemical titration method, which showed that PS has higher degree of substitution than CS. The same results were confirmed from the internal calibration curve plotted using the ATR-FTIR spectra. Curing was found to increase the degree of substitution and hence crosslinking. The extent of esterification and crosslinking also increased with increase in concentration of malonic acid. Crosslinking potato starch with malonic acid also made the starch films brittle but led to an increase in Young's modulus. The hydrophilicity of crosslinked potato starch also

decreased as a result of crosslinking which may have contributed to the higher Young's modulus. These increases in Young's modulus and hydrophobicity are advantageous for industrial application of starch as films and resins for developing green composites.

CHAPTER 5

CROSSLINKED WAXY MAIZE STARCH BASED 'GREEN' NANOCOMPOSITES

Abstract

In this research, 'green' composites were fabricated by blending waxy maize starch (WMS) with micro/nano fibrillated cellulose (MFC). Further, an environment friendly, sustainable and water soluble crosslinker, 1, 2, 3, 4-Butane Tetracarboxylic Acid (BTCA), was used to crosslink WMS to fabricate crosslinked starch based composites. The method described here provides a benign and convenient way to produce crosslinked starch based composite films ($\approx 300 \mu\text{m}$ in thickness), comparable to commercially available plastic sheets. The process can be easily scaled up for commercial production. Industrially pregelatinized WMS was used to obtain smooth, transparent and defect-free films. Crosslinking helped in reducing the moisture absorption as well as made the films and composites insoluble in water. MFC (15% MFC)-crosslinked WMS composite films exhibited excellent tensile properties with a Young's modulus of over 2.3 GPa, fracture strain of 3.1% and fracture stress of 39 MPa, as a result of MFC incorporation. The toughness of these composites was also significantly higher, even without the use of plasticizers such as sorbitol. These materials can be good candidates for replacing petroleum based plastics as well as epoxy based composites.

Submitted to:

T. Ghosh Dastidar and A. Netravali, Carbohydr Polym, 2012.

Introduction

Majority of the conventional plastics and composites used today are derived from petroleum, a non-sustainable resource. They may also utilize manufacturing processes that are harmful to the nature.⁶¹ Since most of them cannot be easily collected, recycled and/or reused, more than 60 billion pounds of the plastics that are discarded every year in the United States of America, at the end of their life, end up in the landfills.⁶¹ Plant based natural polymers offer a sustainable, yearly renewable and environment friendly solution to the current problem of plastic waste.²⁶³ Natural polymers such as native starch are chemically and physically modified to form thermoplastic or crosslinked resins with enhanced film forming properties.^{264, 265} Starch is a polysaccharide composed of two polymers of glucopyranose - linear amylose molecule with (1-4) glycosidic linkage and branched amylopectin molecule with (1-6) glycosidic linkages. While amylose is a low molecular weight polymer consisting of 1000-10,000 glucose units and is linear, amylopectin is a larger branched macromolecule with degree of polymerization (DP) sometimes exceeding one million.⁷⁰

To synergize the effect of starch and cellulose, in this research a convenient, easy to scale up and water based process for fabricating sustainable, environment friendly composite films was developed. Cellulose in the form of micro and nano fibrillated cellulose (MFC) was used as the reinforcing element. Blending starch and cellulose provided a synergistic effect resulting in much higher mechanical properties. Further, WMS was crosslinked using 1, 2, 3, 4-Butane Tetracarboxylic Acid (BTCA), a nontoxic water based crosslinker, to prepare the resins. In this paper, the focus was obtaining completely environment friendly films in large quantities that had Young's modulus comparable to epoxy based plastic²⁶⁶ and composites as well as higher toughness and higher water resistance compared to native starch. The main thrust of this work was engineering composite films that were not only green but involved an easy water based fabrication as well as developing a process that could be easily scaled up. Each film was approximately 18 cm X 30 cm X 0.003 cm and could be produced in larger quantities without compromising the properties.

WMS is a genetically modified maize starch with more than 99% amylopectin which aids in the formation of amorphous, smooth, homogeneous, transparent and defect-free films.²⁶⁷⁻
²⁶⁹ The study by Myllarinen et al.²⁶⁷ revealed that pure amylopectin film was generally amorphous. Regular native starches also involve substantial amount of time in gelatinization and precuring that result in semisolid viscous resin difficult to fabricate into homogeneous.²⁶⁵ Commercially available pregelatinized and instantenized food grade WMS, used in this project, was crosslinked with BTCA for use as 'green' resin. The advantage of using industrially pregelatinized starch instead of native starch was the complete and easy gelatinization of starch ensuring maximum reaction, formation of a smooth film as well as a shorter blending time as compared to native starch. Complete gelatinization (and associated loss of crystallinity) of the amylopectin before casting the film was identified by Lopez-Rubio et al.²⁶⁸ as an important step in the formation of high quality amylopectin films.

It is well known that due to the highly hydrophilic nature of the thermoplastic starch resulting from the presence of hydroxyl groups, it is susceptible to changes in the atmospheric humidity which affects the stability and mechanical properties of thermoplastic starch films. Crosslinking of starch with bi- or poly-functional reagents interconnects the starch molecules by covalent bonding, thus increasing the molecular weight and consequently the modulus (stiffness) tensile strength, as well as water resistance.¹⁶ Polymers with hydroxyl functional groups including cellulose and polyvinyl alcohol²⁷⁰, have been commonly crosslinked with dialdehydes²⁷¹, epichlorohydrin^{110, 111}, dimethyloldihydroxyethyleneurea (DMDHEU)²⁵⁹ or polycarboxylic acids.²⁵⁶ BTCA, used in this research, is relatively inexpensive, nontoxic and is commercially available at a lower cost²⁵⁹ as compared to the more commonly used crosslinkers mentioned above. Many researchers also claim that BTCA is a more effective crosslinker than any other polycarboxylic acid, including the extensively used polymaleic acid (PMA).^{272, 273} It is postulated that the high reactivity and effectiveness of BTCA as a crosslinker, among other polycarboxylic acids such as polymaleic acid^{272, 273}, citric acid²⁵⁸ and malonic acid²⁶⁵, results from its ability to create highly reactive cyclic anhydrides under thermally increased

conditions.²⁷⁴ BTCA which was previously been used as an effective crosslinker for cellulose for making wrinkle resistant fabric^{254, 275}, was shown to successfully crosslink WMS in this study. The reaction conditions between WMS and BTCA were studied and optimized in this research. In the present study sodium hypophosphite (NaPO_2H_2 , Nahyp) was used as an effective catalyst for the crosslinking reaction. It is believed that Nahyp accelerates the process of esterification by increasing the speed of the formation of the cyclic anhydride intermediate.²⁷² Both BTCA and Nahyp are water soluble which enabled the reaction to be carried out in an environment friendly aqueous condition, rather than using organic solvents.

Previous studies have shown that crosslinking increases the Young's modulus of starch but makes the film extremely brittle and difficult to use.²⁶⁵ Incorporation of MFC which contains micro- and nano-fibrils with high aspect ratio was found to be a convenient and easy way to create uniform and defect-free composite films. The toughness of the composite films increased without compromising the Young's modulus as discussed later. Plasticizers such as glycerol and sorbitol (polyols) are commonly used with starch to create thermoplastic starches²⁶⁸ with improved flexibility (fracture strain) and toughness. However, plasticizers, while increasing the fracture strain of starch based resin, decrease the Young's modulus owing to increase in the free volume in the polymer²⁷⁶ as discussed later in the paper. The incorporation of MFC improved the toughness of the composites even without the use of plasticizers.

MFC used in this project was obtained by the mechanical shearing of cellulose fibers or paper pulp.^{8, 277} Fibrils in the MFC have a high aspect ratio and many have diameters in the range of a few nanometers. They have been used for fabrication of composites with high mechanical strength owing to their high tensile strength and stiffness (Young's modulus).^{8, 277, 278} While crosslinking of starch ensured a decrease in moisture absorption and increase in stability of starch against disintegration in water, a small amount of MFC (15% with respect to starches) was effectively used to create a composite film with high toughness and tensile strength. Thus a convenient, completely green, nontoxic and water based technique has been developed for

engineering composite films with potential commercial applications such as packaging and coating in this research.

Experimental Procedures

Materials.

Instantenized and water soluble, pharmaceutical grade waxy maize starch (WMS) powder was obtained from Nutra Bio (Middlesex, NJ). Analytical grade BTCA and Nahyp were purchased from Sigma Aldrich (Saint Louis, MO). MFC in water (KY-100G) was obtained in the form of paste from Dical Chemical Industries, Japan, containing 10% MFC and 90% water.

Fabrication of films.

Fabrication of crosslinked WMS based films:

In order to obtain crosslinked WMS resin, starch powder (20 g) was added to 500 ml water with magnetic stirring. The powder was easily soluble in water and resulted in a low viscosity, homogeneous and transparent solution. To ensure maximum possible gelatinization the mixture was heated at 90°C for 30 minutes with constant stirring. Predetermined BTCA weights (5%, 10%, 15% and 25% based on the weight of starch) were added, separately, to the gelatinized starch followed by addition of Nahyp (50% by weight of BTCA) as catalyst. The mixture was prepared by stirring continuously for 60 min at 90°C with a magnetic stirrer. Both BTCA and Nahyp are completely soluble in water, the heating and stirring ensured homogeneous mixing of these materials making the functional groups easily accessible for further reaction. After cooling, the prepared starch was cast to form thin films on Teflon[®] coated glass plates and dried in an oven for 48 hours at 40°C. The prepared solution had low viscosity, flowed easily and could be conveniently cast into relatively defect-free, transparent films. The dried films were peeled off from the Teflon[®] coated plates (18 cm X 30 cm) and stored in sealed polyethylene bags. The prepared films were further heated in Carver Hydraulic hot press (model 3891-4PROA00, Wabash, Ind.) for complete crosslinking (curing) at 120°C under a pressure of 0.1 MPa for 20 min. The films were easily washed by soaking in water, followed by ultrasonication for 1 hour to get rid of all the excess unreacted chemicals. The films were further

washed by soaking overnight for complete washing. After which, the films were taken out of water, dried completely and characterized. It was important to thoroughly wash off the unreacted BTCA and Nahyp as they are hygroscopic (absorb water) and can act as plasticizer if they remain trapped in the specimen. Presence of unreacted chemicals can potentially distort the mechanical property data of the films.

Fabrication of crosslinked WMS resin based composite films.

To obtain crosslinked WMS resin based composite films a dispersion of MFC in gelatinized starch was prepared by adding predetermined weights of WMS, MFC paste and sorbitol to 500 mL water and stirring with a high speed mechanical stirrer at 90°C for 1 hr. The stirring speed had to be increased from 600 rpm to 1100 rpm at higher loadings of MFC to prevent fibril clustering. This was followed by addition of 5 g BTCA and 2.5 g Nahyp and the entire mixture was precured at 90°C for 1 hr while stirring it at high speed. The mixture was cast on Teflon[®] coated glass plates to form films. The films were dried as described earlier followed by curing at 120°C for 20 min leading to the formation of the MFC- crosslinked WMS composite films. The composite films were washed following the same procedure as the crosslinked films.

Fabrication of MFC-BTCA films.

In order to investigate the interaction of BTCA with MFC a film was fabricated with MFC and BTCA. To prepare the film, MFC paste (15 g) was dispersed in water using high speed mechanical stirring. BTCA (25% by weight of MFC) was added. The mixture was precured at 90°C for one hour to ensure complete dispersion. The film was cast on Teflon coated glass plates, cured at 120°C for 20 minutes and washed following the same procedure described above.

Attenuated total reflectance–Fourier transform infrared (ATR-FTIR) analysis.

ATR-FTIR spectra were collected using a Nicolet Magna 560 FTIR spectrometer with a split pea accessory for ATR. Each scan was an average of 150 scans recorded from 4000 cm⁻¹ to 550 cm⁻¹ wavenumbers obtained at a resolution of 4 cm⁻¹.

In order to construct a calibration curve from the ATR-FTIR spectra, the absorption peak at 1725 cm^{-1} resulting from ester carbonyl (C=O) stretching vibration was chosen as the analyte peak which monitored the concentration of ester. Since the absorption due to aliphatic -C-H stretching vibration, at 2929 cm^{-1} , remains unchanged after the crosslinking reactions, it was chosen as the reference peak for the internal standard. The ratio of absorbance to the analyte peak and the reference peak was plotted against concentration of BTCA. This method is similar to the calibration method used by Coma et al.²⁵⁶ to assess the degree of crosslinking of cellulose with citric acid.

Scanning electron microscopy (SEM).

WMS starch powder, MFC, BTCA-MFC film, fracture surface of crosslinked WMS resin and the surface topographies of MFC-WMS (crosslinked) composites fractured in tensile mode, were characterized using LEO 1550 field emission SEM. The specimens were placed on standard aluminum specimen mounts (pin type) with double-sided adhesive electrically conductive carbon tape (SPI Supplies, West Chester, PA). The specimens were coated with carbon using Denton vacuum coater, (model BTT IV, Denton Vacuum, Moorestown, NJ). The coated specimens were then observed on the SEM using an accelerating voltage of 5 kV to observe the surface topography and characterize their fracture behavior.

Determination of swelling power.

The swelling power of crosslinked starch specimens in DMSO was obtained by using the modification of a method demonstrated by Zhou et al.²⁵⁸ The crosslinked starch films were conditioned in 21°C and 65% relative humidity for 2 days prior to soaking in 10 mL DMSO at room temperature for 24 hr. The films were accurately weighed (m_d) before immersing in DMSO. The swollen films were filtered out from the solvent, washed with water and ethanol, wiped lightly and weighed (m_s). The swelling power values for crosslinked WMS in DMSO were calculated as follows:

$$\text{Swelling Power} = \frac{m_s - m_d}{m_d}$$

Equation 1

Swelling power of crosslinked WMS in water was also determined using a modification of the method described above for DMSO. The crosslinked starch films were conditioned in 21°C and 65% relative humidity for 2 days prior to soaking in 50 mL water, films were accurately weighed (m_d) before immersing in water. The films were soaked for 3 days in water instead of 1 day (to reach equilibrium) keeping all the other experimental conditions exactly the same. The swollen films were wiped lightly using Kimwipes[®] and weighed (m_s). The swelling power of the crosslinked films in water was calculated using the same equation given for DMSO. *Thermogravimetric analysis (TGA).*

Native and crosslinked WMS as well as composite specimens were scanned from 25°C to 600°C using a thermogravimetric analyzer (TGA-2050, TA Instruments, Inc., New Castle, DE) at a rate of 10°C/min in nitrogen atmosphere to characterize their thermal stability and degradation behavior.

Tensile testing.

The WMS and composite films were cut into rectangular pieces of dimensions to characterize their tensile properties. To confirm that the tensile properties were isotropic, the rectangular films for tensile testing were cut randomly in different directions from the original film (18 cm X 30 cm). The film thickness (approximately 0.3 mm) varied with the specimen and was measured accurately before testing. The composite films with higher loading of MFC were thicker. The films were conditioned for 3 days at ASTM standard conditions of 65% relative humidity 21°C temperature prior to testing. The tensile properties of resin and composite films were characterized using Instron, model 5566 (Instron Co., Canton, MA), according to ASTM D882-02. A gauge length of 30 mm and a strain rate of 0.6 min⁻¹ were used for all specimens. At least 5 specimens were tested to obtain the average values.

Results and Discussion

Attenuated total reflectance – Fourier transform infrared (ATR-FTIR) analysis.

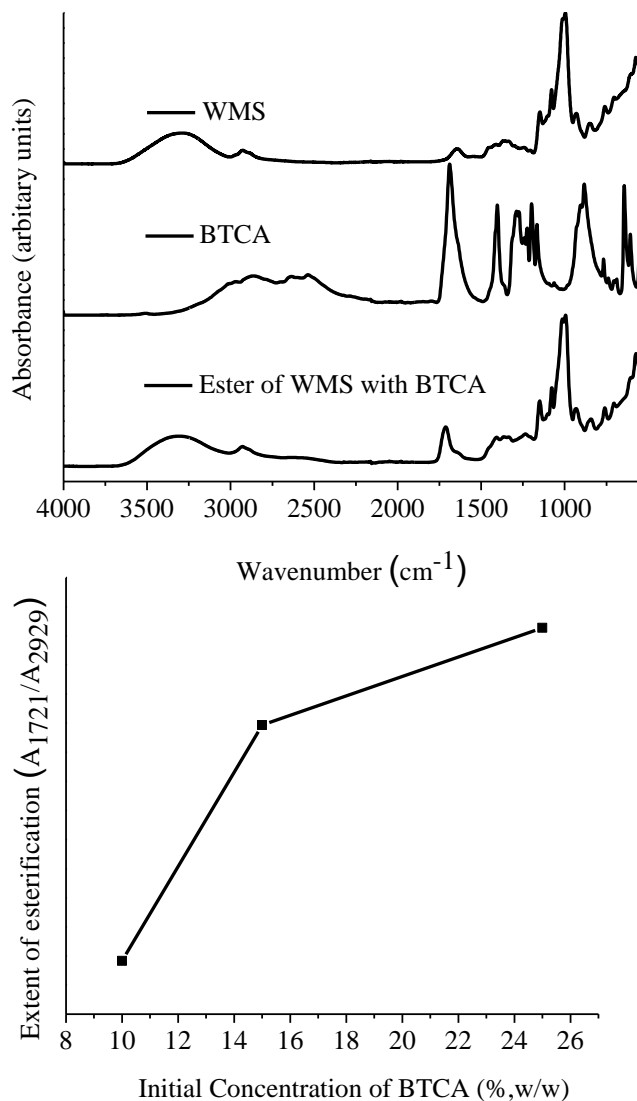


Figure 26. A) FTIR of WMS, BTCA and ester of WMS formed with BTCA; (B) Extent of esterification of WMS as a function of initial BTCA content, using the internal calibration curve.

To confirm the esterification reaction between WMS and BTCA ATR-FTIR spectra comparing WMS, BTCA and ester of WMS formed with BTCA were collected and are presented in **Figure 26 A**. The ATR-FTIR spectrum of BTCA presented in **Figure 26 A** shows a sharp peak at 1689 cm⁻¹ assigned to the carboxyl carbonyl stretching. Native WMS does not

show any carbonyl peak while, WMS reacted with BTCA shows the ester carbonyl peak at 1725 cm^{-1} . The crosslinking proceeds through esterification via formation of a cyclic anhydride intermediate, aided by the catalyst Nahyp, the reaction mechanism being similar to cellulose crosslinking with BTCA shown by Yang.²⁷⁹ Starch esterified with carboxylic acids typically show ester carbonyl peak at around 1725 cm^{-1} . FTIR of corn starch crosslinked with citric acid showed an ester peak at 1724 cm^{-1} ¹⁶ while potato starch esterified with ferulic acid showed as ester peak at 1726 cm^{-1} .⁹⁶

Figure 26 B illustrates the extent of esterification of WMS as a function of initial BTCA content, using an internal calibration curve. The internal calibration curve (**Figure 26 B**) was constructed by the method shown previously by Ghosh Dastidar and Netravali²⁶⁵ for crosslinking of native starches with malonic acid. A gradual increase in the A_{1725} (absorbance of the ester carbonyl stretch)/ A_{2929} (absorbance of aliphatic stretching) ratio, implied an increase in the extent of esterification reaction with increase in the initial BTCA concentration. Recent studies by Coma et al.²⁵⁶ have shown that A_{1725}/A_{2929} ratio is linearly related to the percentage of crosslinking of cellulose with citric acid, calculated by a chemical titration method. An increase in the internal calibration curve indirectly indicates an increase in the degree of substitution (and crosslinking) with BTCA, similar to research results reported by Ghosh Dastidar and Netravali²⁶⁵ and Coma et al.²⁵⁶

The film prepared with just BTCA and MFC did not show any ester carbonyl peak (FTIR in supporting information) after curing proving that at 120°C not enough for crosslinking of BTCA with MFC. Some papers have shown that higher temperature and longer time are needed for reaction of MFC with BTCA.^{103, 254} Since it was desired to specifically understand the effect of starch crosslinking, the MFC was not crosslinked with BTCA.

Swelling power of resin.

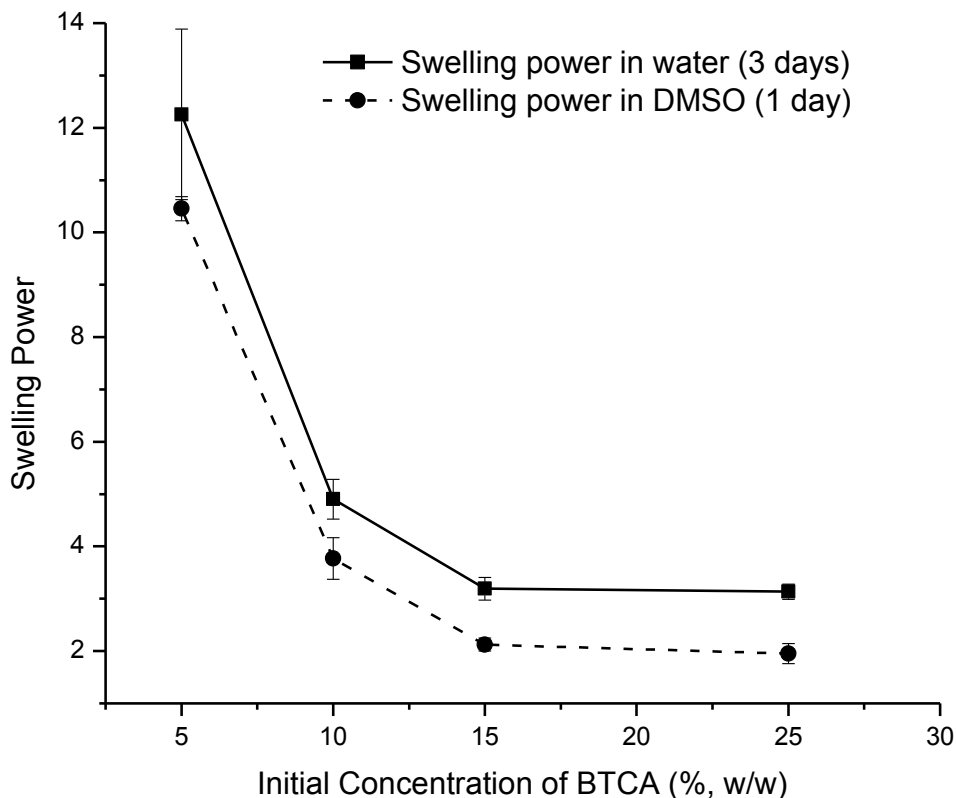


Figure 27. Swelling power of WMS crosslinked with BTCA in water and DMSO as a function of BTCA concentration.

The swelling power of WMS crosslinked with BTCA in water and DMSO as a function of the initial concentration of BTCA is shown in **Figure 27**. The swelling power of crosslinked WMS in water and DMSO, as shown in **Figure 27**, decreased as the initial concentration of BTCA (percentage of crosslinking) increased. The insolubility of WMS (esterified with BTCA) in these solvents also indirectly suggests strengthening polymer network by crosslinking. Crosslinking leads to formation of a rigid network of gel reducing the absorption of water which does not allow it to swell. Crosslinking of starch helps in reducing the moisture sensitivity which would be important for industrial application of starch.²⁶⁴ As mentioned earlier, starch is inherently hydrophilic because of the hydroxyl groups and the absorbed moisture affects its mechanical properties as a result of plasticization.

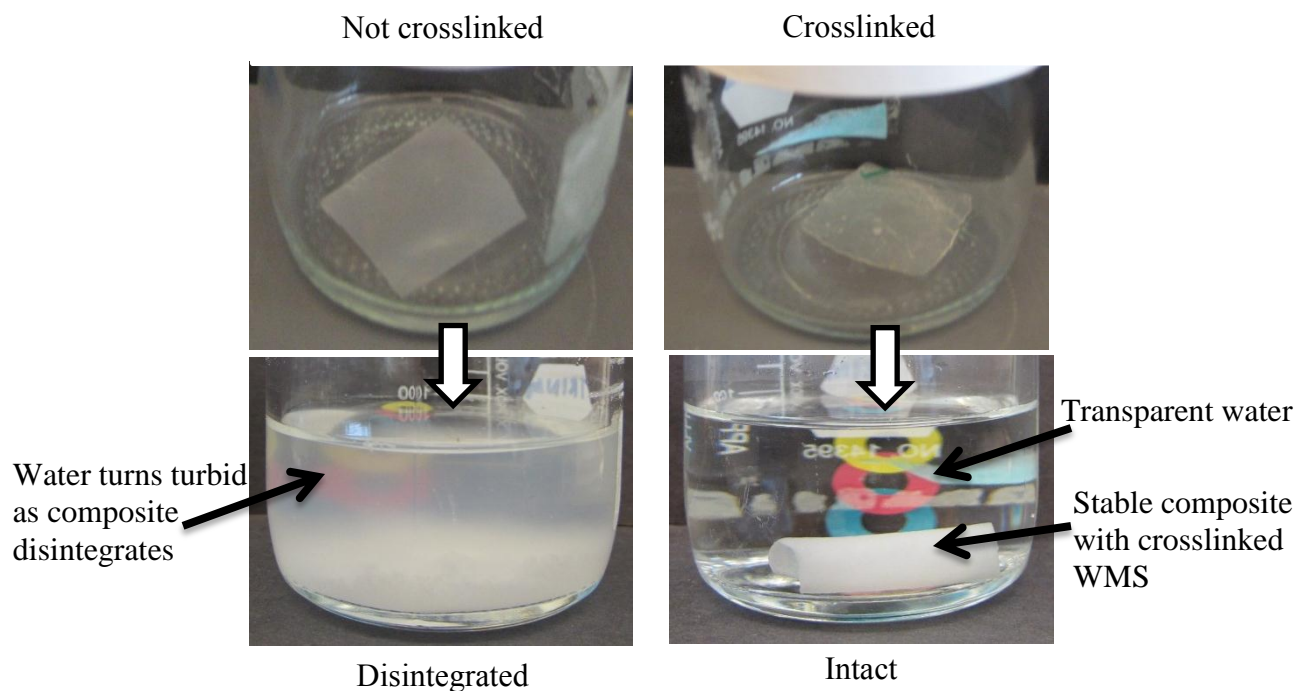


Figure 28. Stability of crosslinked composite in water.

The stability of starch in water is also increased by crosslinking, which makes it potentially more useful for commercial applications. **Figure 28** shows the stability of WMS resin and composite in water. It was observed that the MFC-WMS (gelatinized but not crosslinked) composites rapidly disintegrated in water while the MFC-crosslinked WMS composites only swelled in water but remained stable and retained their original shape even after continuously shaking for several months as can be seen from **Figure 28**. It can be concluded that crosslinking increases the stability of the resin (and subsequent composite) in water due to formation of network structure.

MFC-WMS (crosslinked) nanocomposite films.

Mechanical properties.

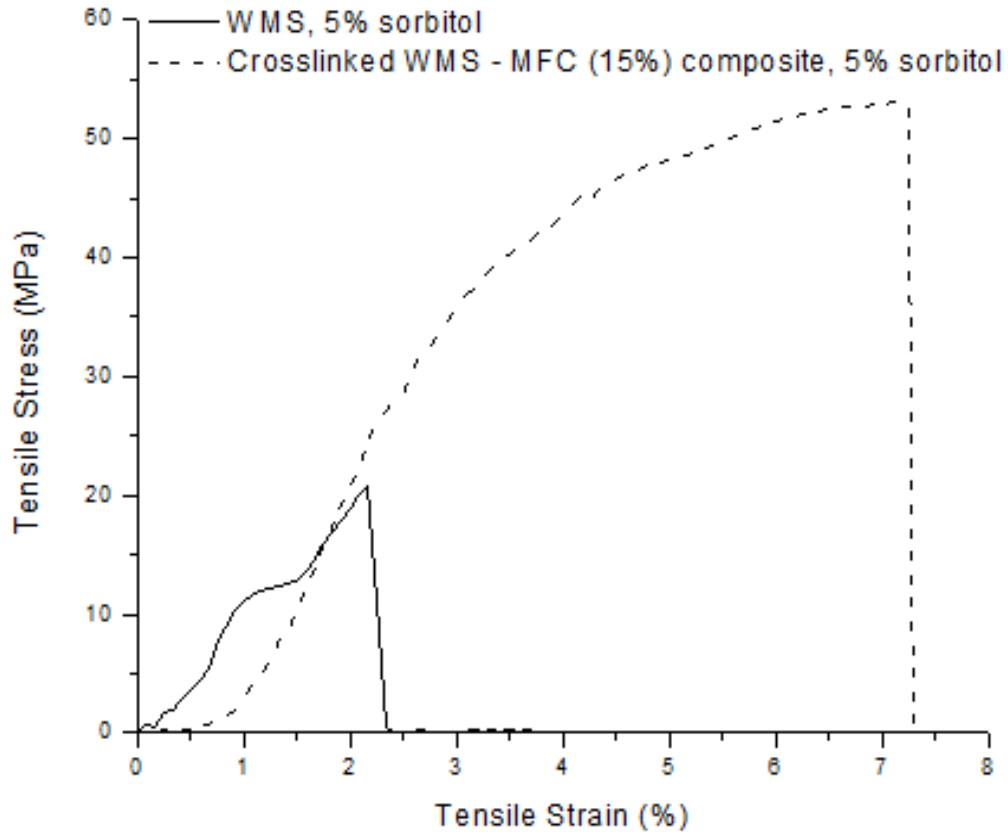


Figure 29. Tensile properties of WMS resin and composite.

Table 2. Mechanical properties of WMS and MFC-WMS (crosslinked) composites as a function of sorbitol (%).

MFC (%)	Sorbitol (%)	Modulus (MPa)	Fracture Stress (MPa)	Fracture Strain (%)	Toughness (MPa)
0	5	1354 (50)	17.6(65)	3.1(37)	0.4 (90)
15	0	2341 (32)	39 (20)	3.1 (29)	0.7 (47)
15	2.5	1679 (6)	45 (25)	10 (43)	3.3 (74)
15	5	1686 (40)	44 (33)	7.8 (32)	2.3 (44)

Table 3. Mechanical properties of MFC-crosslinked WMS composites as a function of MFC loading.

MFC (%)	Sorbitol (%)	Modulus (MPa)	Fracture Stress (MPa)	Fracture Strain (%)	Toughness (MPa)
15	2.5	1679 (6)	45 (35)	10 (43)	3.3 (74)
25	2.5	1737 (8)	56.5 (21)	6 (35)	2.3 (58)
35	2.5	2207 (16)	58 (16)	7 (33)	2.9 (51)
50	2.5	2566 (12)	63 (15)	7.6 (38)	3.5 (52)

A strong interfacial adhesion is expected between WMS and MFC resulting from the chemical match between the two and strong hydrogen bonding resulting from the hydroxyl groups. A good H-bonding interaction is also expected between MFC and BTCA (crosslinker) due to the presence of four carboxylic acid groups which make BTCA hydrophilic. In addition, as shown by Huang and Netravali²⁷⁸, MFC has a broad size distribution in terms of the fibril diameter and the small diameters of the nanofibrils. Along with its high aspect ratio MFC provides a significantly large area for the interfacial interaction. This strong interfacial interaction increases the load transfer efficiency from broken to intact fibers in the composites, reduces the critical length required for effective load transfer and, thus, increases the mechanical properties.^{278, 280} The native WMS films and crosslinked WMS films (both without MFC) were too brittle and hence could not be tensile tested. The crosslinked films also revealed numerous defects after curing. A reason for defect formation in this method could be that internal stresses are caused during the curing process. Other influences are the existence of cracks or uneven geometries of the sample. These influences, however, were easily mitigated by incorporation of MFC in the sample manufacturing. The resulting composite films were relatively defect-free and were easily cured without developing cracks and wrinkles. MFC (15% MFC)-crosslinked WMS composite films exhibited excellent mechanical properties with high stiffness and toughness (Young's modulus of 2341 MPa, fracture strain of 3.1% and fracture stress of 39 MPa), even without the use of any plasticizer. The hydrophilicity of the MFC fiber network makes the film sufficiently ductile to be tensile tested without the use of any plasticizer. However, it should be noted that even though MFC is hydrophilic it is highly crystalline in nature and hence does not allow it to absorb a significant amount of moisture.²⁷⁸ Due to the similarities of the chemical structure of starch and cellulose, incorporation of MFC is an environment friendly and facile way for

fabrication of smooth, defect-free, flexible films that are easier to handle and do not need any plasticizers. The strengthening of network structure and reduction in moisture absorption (as observed from the swelling power data) due to crosslinking of the WMS resin with BTCA also contributed to the higher modulus of the composites. **Figure 29** shows typical stress vs. strain plots for WMS resin (not crosslinked, no MFC) and MFC (15%)-WMS (crosslinked) composite, both containing 5% sorbitol as plasticizer. Clearly the MFC reinforced composite showed a higher toughness than WMS resin, as was expected. Plasticizers such as glycerol and sorbitol (polyols) absorb moisture which increases the free volume within the polymer and reduce their glass transition temperature. This, in turn, results in lower Young's modulus and higher fracture strain values as well as reduction in brittleness and increase in toughness.²⁶⁸ It should be emphasized, that incorporation of MFC, instead of polyol based plasticizers, increased the fracture strain without compromising the Young's modulus. Thus, MFC is a potential environment friendly substitute for glycerol and sorbitol in fabricating crosslinked starch based films. The fracture stress, fracture strain and toughness data are presented in **Table 2** and show significant improvement with crosslinking and subsequent incorporation of MFC. However, the Young's modulus decreased from 2341 MPa to 1686 MPa with the addition of 5% sorbitol to the crosslinked MFC (15%)-WMS composite film. The reduction in Young's modulus with plasticizer was expected. As mentioned earlier, it was not possible to conduct tensile tests on crosslinked WMS resin films (without MFC) even after adding 5% sorbitol owing to the brittleness of the films as well as experimental difficulty in fabricating defect-free films. Hence, no data could be collected for pure crosslinked WMS resin films.

Table 3 provides mechanical properties for MFC-WMS (crosslinked) composites as a function of MFC content. It is evident from data presented in Table 3 that Young's modulus increases with

increase in MFC content from 15% to 50% (2.5% sorbitol). As mentioned earlier, this is because the cellulose fibrils are known to possess very high Young's modulus of up to 140 GPa owing to their high degree of molecular orientation and highly crystalline nature.^{8, 271} In addition, MFC also forms strong hydrogen bonding with the starch resin leading to higher interfacial adhesion which also contributes to the higher Young's modulus and fracture stress.²⁸⁰ The tensile properties of the MFC reinforced composites were also completely isotropic which can be attributed to the network structure of the MFC fibrils as revealed in the SEM images (discussed later).

The properties of MFC-crosslinked starch based composites were comparable or in some cases higher than petroleum based polymers such as nylon-6 (Young's modulus: 1800 MPa; fracture stress: 70 MPa).

Microscopic analysis.

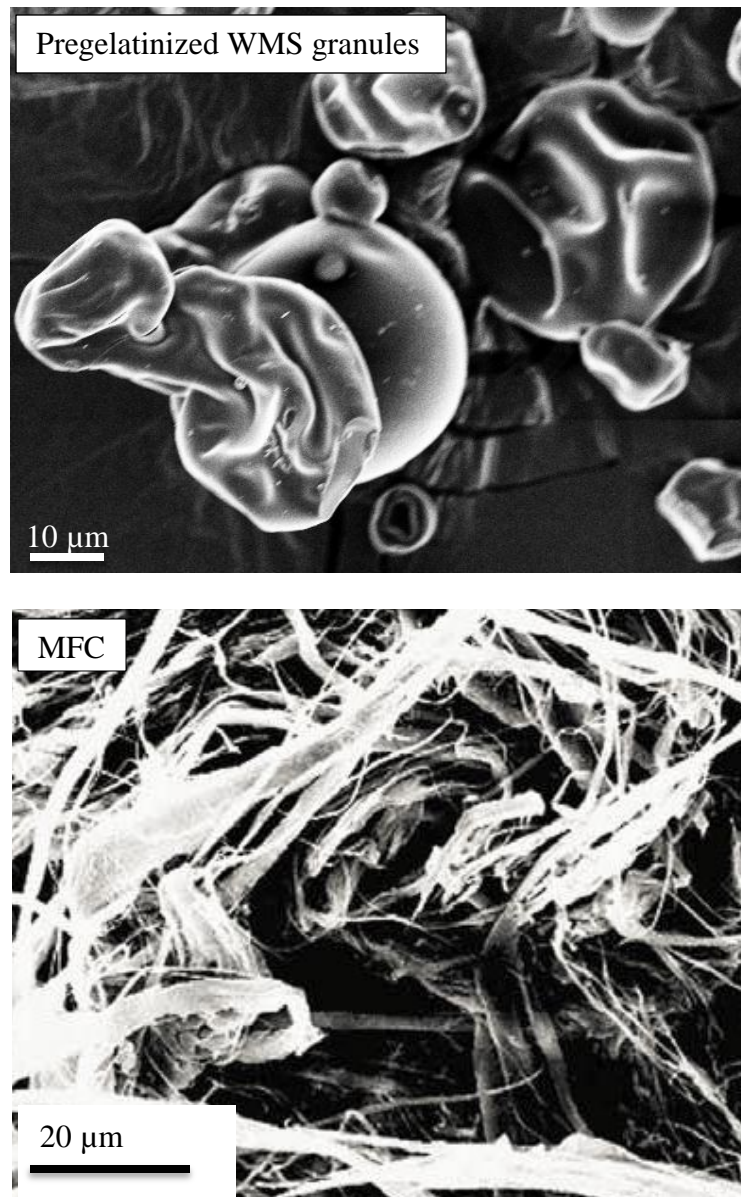


Figure 30. SEM images of A. Pregelatinized WMS granules B. MFC fibers.⁸

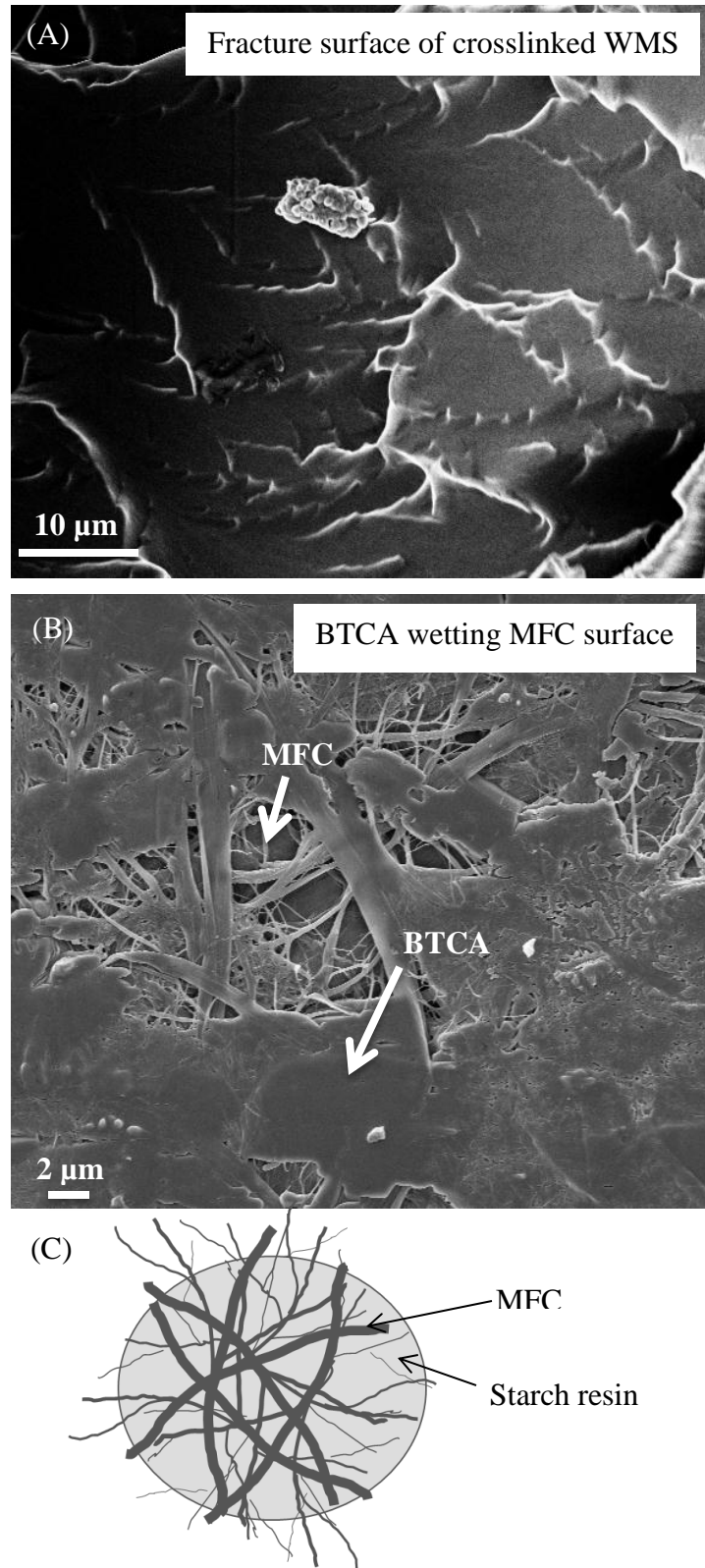


Figure 31. SEM images (A). Fracture surface of crosslinked WMS, (B). BTCA wetting MFC network and (C). Schematic of MFC-WMS composite showing the network structure of MFC incorporated in starch based resin.

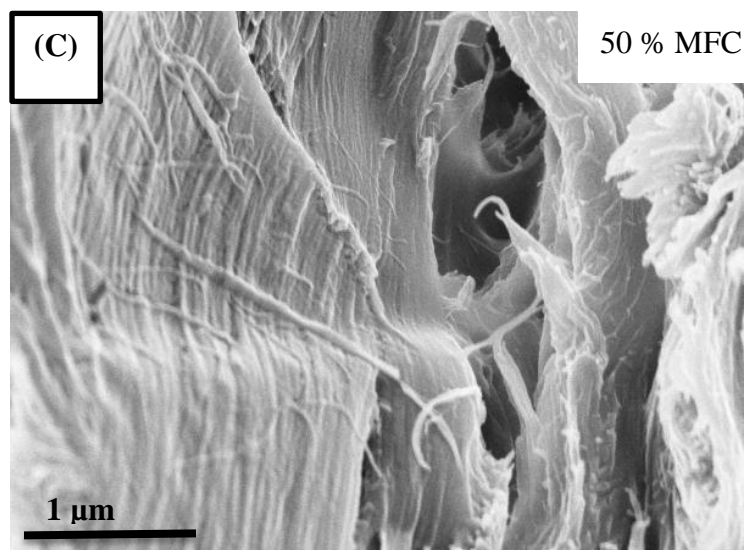
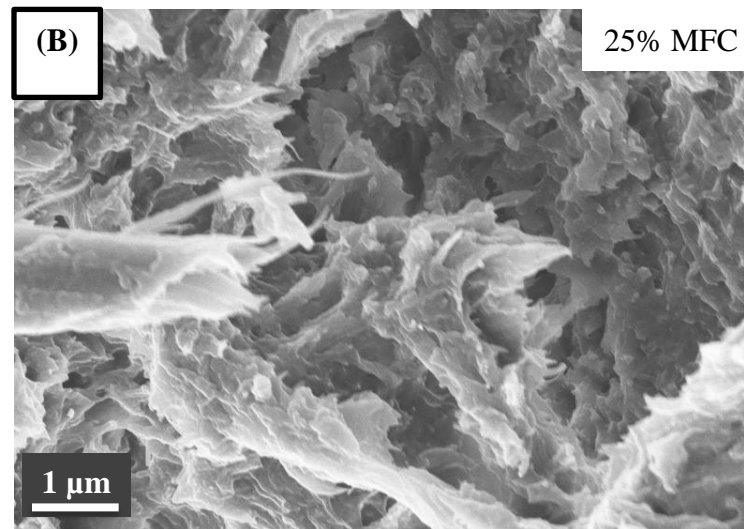
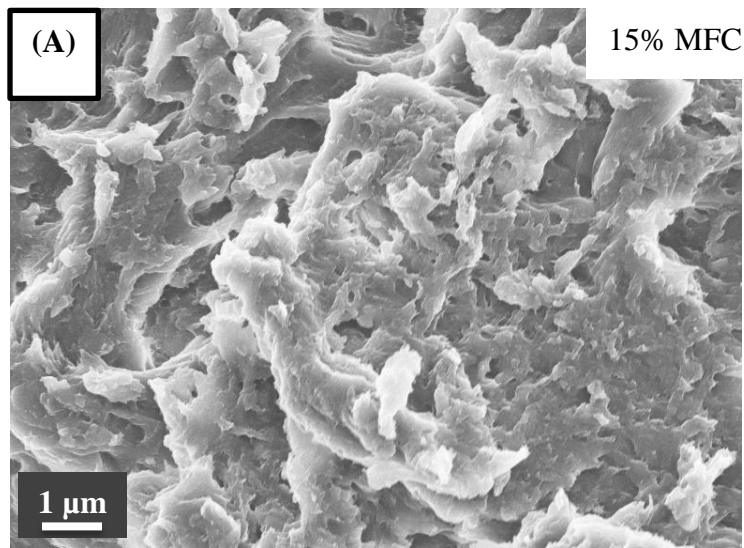


Figure 32. SEM images of MFC-WMS crosslinked composites.

Figure 30A shows SEM images of pregelatinized WMS granules as is obtained from the vendor. The collapsed granules of industrially pregelatinized and instantenized WMS, used in the present study, dissolved easily in water at 90°C and formed a homogeneous transparent solution. It was possible to uniformly disperse MFC in the solubilized WMS by mechanically stirring at high shear rate to ensure that no aggregates were formed. Lopez-Rubio et al.²⁶⁸ have reported that the formation of high quality amylopectin films is dependent on the full gelatinization (and associated loss of crystallinity) of the amylopectin before casting the film. **Figure 30 B** shows SEM image of MFC fibers.⁸ From the SEM image, it is clear, that the MFC is a mixture of fibrils with broad range of distribution of the diameters, including both micro sized and nano sized fibrils.⁸

Figure 31 A shows the SEM image of the fracture surface of crosslinked WMS resin. The SEM image of crosslinked WMS, not reinforced with MFC, showed a smooth fracture surface, as expected for a brittle fracture for resins such as epoxies.²⁸¹

Figure 31 B shows the SEM image of the film prepared by curing BTCA with MFC. The image clearly shows that BTCA spreads on the surface of the network structure of MFC. This may be attributed to the strong H-bonding interaction between the hydroxyl groups in MFC and the four carboxylic acid groups in BTCA. It is expected that the strong interaction between the reinforcing filler and the crosslinker also contributes to the higher tensile properties of the composites. As explained earlier, no crosslinking reaction was observed between BTCA and MFC at 120°C. The random network and branched structure of MFC in **Figure 31 C** also accounts for the isotropic properties of the composites.

Figure 32 shows the SEM images of typical fracture surfaces of MFC-WMS crosslinked composites, failed in tension. The fracture surfaces of MFC-WMS crosslinked composites,

showed surface roughness due to incorporation of MFC, rather than a smooth fracture surface of the brittle resin. The images show a close association between the fiber and the resin. Owing to similar chemical compositions of starch and cellulose, significant hydrogen bonding is expected between the two. The fiber (MFC)-resin (crosslinked WMS) interaction plays a significant role in improving the mechanical properties of the composites.^{281, 282} The SEM images showed that the MFC fibrils were embedded into the starch resin to a large extent. The surface topography of composite with 50% MFC is distinctly different from the composites incorporated with 15% and 25% MFC. It is assumed, that as the loading of MFC increased to 50%, MFC became one of the dominant phases rather than reinforcing filler, with the crosslinked WMS resin occupying the voids within the porous MFC network. It was difficult to draw any definite conclusion about the dispersion of the fibers from the SEM images.

Thermal properties.

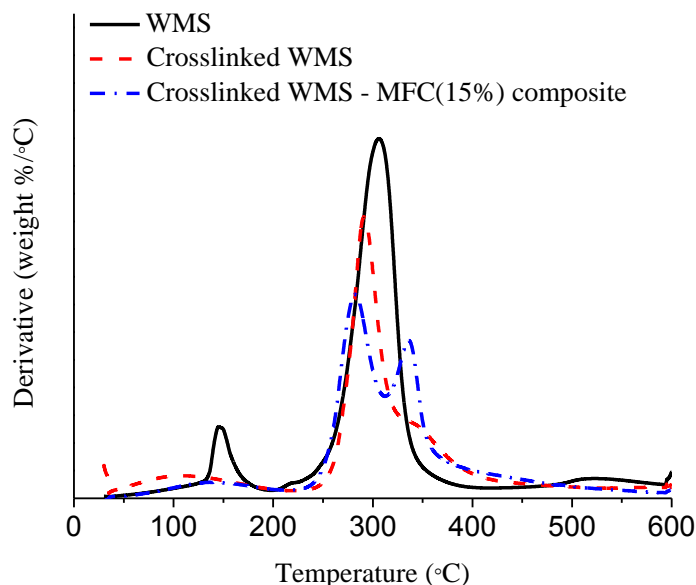


Figure 33. DTGA of WMS. Crosslinked WMS, MFC (15%)-crosslinked WMS composite.

The DTGA plots in **Figure 33** show that gelatinized WMS and crosslinked WMS resins as well the composite start to degrade at about the same temperature ($\approx 270^\circ\text{C}$). There was around 90% weight loss at 600°C in the case of gelatinized WMS (not crosslinked) resin compared to 70% weight loss observed for the crosslinked WMS resin. WMS already had a high initial thermal degradation temperature which did not change on crosslinking. The DTGA plot for MFC (15%)-crosslinked WMS composite showed a two stage thermal degradation for the composite. This is confirmed by the two sharp peaks observed in the DTGA curve at around 270°C and 300°C . The peak observed around 270°C for the crosslinked MFC-WMS composites is same as that observed for the WMS resin and represents the onset of resin degradation. The peak (at $\approx 300^\circ\text{C}$) corresponds to the degradation of MFC, which is thermally more stable than crosslinked WMS.^{8, 278} These results suggest that there was only slight enhancement in thermal degradation properties on incorporation of MFC as the fibrils stay as a separate phase in the composites.

CHAPTER 6

STUDY ON STARCH BASED ADHESIVE FOR WOOD

Abstract

Formaldehyde based resins like phenol-formaldehyde and urea-formaldehyde based resins are routinely used as popular adhesives for wood and paper. However, owing to current environmental concerns there is a growing need to develop more biobased alternatives for these toxic formaldehyde based adhesives. Starch is one of the most abundantly available biomaterials and is successfully fabricated into resin by various physical and chemical modification techniques. In the present research different starch varieties were characterized for their adhesive property with wood. In addition, waxy maize starch (WMS) was crosslinked using butane tetra carboxylic acid (BTCA) and its adhesive property with wood has been characterized. Effect of different factors including sources of starch origin, application of weight and crosslinking on the adhesive properties of starch are presented in this paper.

Introduction

Formaldehyde based resins such as phenol-formaldehyde and urea-formaldehyde are popular commercial choices as adhesives for wood composites.²⁸³ These adhesives are fast curing, durable, have good adhesion to wood and are not very expensive. However, formaldehyde based resins are not environment friendly and the world health organization recently declared formaldehyde as a carcinogen.²⁸³ With increased awareness on the environmental effects of these toxic materials, research on alternative 'green' materials and processes has intensified.²⁸³ Protein generated by mussels to attach themselves to stones is an excellent example of a natural, renewable adhesive. The adhesive mainly consists of a protein decapeptide (Ala-Lys-Pro-Ser-(Tyr/DOPA)-Hyp-Hyp-Thr-DOPA-Lys) which contains hydroxyl groups that chelate with the metal ions and form strong hydrogen bonding.²⁸³ They also undergo oxidation and various crosslinking reactions to form water insoluble three dimensional mussel adhesion proteins.²⁸³ Soy protein based adhesives have also been used as a green source of adhesive.²⁸³ Soy products such as soy protein isolate (SPI), soy protein concentrate (SPC) and defatted soy flour (SF) have also been used as biobased adhesives for wood.²⁸³ For using as an adhesive SPI was crosslinked with maleic anhydride via amide and ester linkages.²⁸⁴ The SPI modified with polyethyleneimine has shown high strength and water resistance due to the formation of highly crosslinked polymer network.²⁸⁴ SPC has also been combined with gelatin which increases the shear strength of SPC by increasing the amount of hydrogen bond formation with the wood surface as well as by reducing the viscosity of the resin which helps in easy penetration of the resin in the wood.⁵ Such soy protein based resins, because of their good adhesive property, have been used to fabricate composites by adding fibers as reinforcing elements.⁵ Starch is one of the most abundantly available plant based materials and has been successfully fabricated into resin by various physical and chemical modification techniques.²⁸⁵ Since starch is

obtained from many cereals and roots/tubers, it is available in a wide range of varieties. The properties of starches vary depending upon their source of origin which controls the amount of amylose and amylopectin contents.²⁸⁵ The source of origin also controls the crystallinity of the starch.²⁸⁵ While both amylose and amylopectin are made up of glucose as the monomer, amylose is a linear polymer with (1-4) glycosidic linkage with a degree of polymerization (DP) between 1000 and 10,000.²⁸⁵ Amylopectin, on the other hand, is a much larger molecule with a DP that may exceed one million.²⁸⁵ Also, unlike amylose, amylopectin is branched with both 1,4 and 1,6 glycosidic linkages and exist in the form of double helices. The adhesion properties of starches depend upon their source of origin, i.e., amylose/amylopectin ratio, and granular microstructure as explained later.⁷³ Stein-Hall type starch based adhesives are partially gelatinized starches (wheat, corn and tapioca) which form lyophilic colloidal emulsions in water and have been used as adhesives for manufacture of corrugated boards. The adhesive properties can be controlled by tuning the degree of gelatinization of the starch granules.²⁸⁶ These adhesives consist of two phases, the first one is the gelatinized starch which forms the carrier phase and the second one (not gelatinized or partially gelatinized starch) is the latent adhesive phase. The potential of these adhesives is not fully developed until they are applied on corrugated boards and cured at high temperature and pressure.²⁸⁷⁻²⁸⁹ Starch gelatinized in the presence of sodium hydroxide, diacetone acrylamide-formaldehyde and water forms a thixotropic adhesive gel and has been used as adhesive to make corrugated paper and card boards as well.²⁹⁰ In another invention an adhesive gel consisting of polyvinyl acetate and partially hydrolyzed polyvinyl alcohol that provide the required wet tack, glyoxal which provides water resistance, wood flour which helps in enhancing the water resistance and xanthan gum as a viscosity and rheology modifier was used to bond wood.²⁹¹

Figure 34 shows the surface wetting and contact angle and (b) wetting of the wood substrate surface by starch. The adhesive strength depends on the strong attachment of the adhesive on the surface of the substrate.^{5, 283, 284} The surface chemistry between the adhesive and the substrate plays an important role and the adhesive strength is higher if the adhesive can spread or has zero contact angle **Figure 34 (A)** with the surface of the substrate. Since wood specimens usually have surface roughness associated with them, an adhesive that spreads well on the surface of the substrate also penetrates deeper into the rough crevices of the surface (**Figure 34 (B)**). Wood is composed of cellulose, hemicellulose and lignin. Starch, a polysaccharide made up of glucose molecules (similar to cellulose), has surface hydroxyl groups resulting in a compatible chemistry between starch and cellulose. Thus, starch on its own can be expected to act as an adhesive for wood and paper.

In this research various starches were crosslinked with butane tetra carboxylic acid (BTCA) and its performance was characterized as an adhesive for wood.

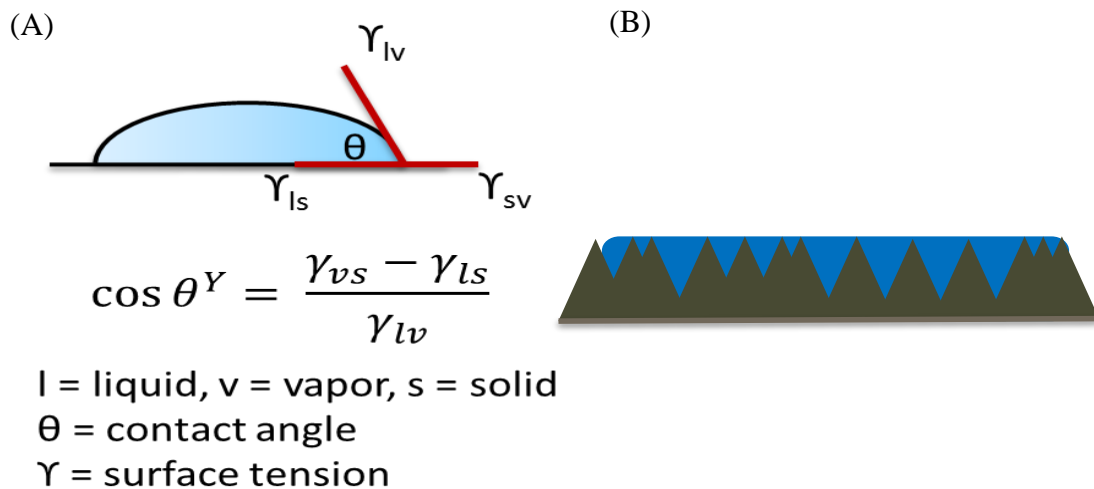


Figure 34. (A) Surface wetting and Contact angle (B) Wetting of starch on the surface of wood substrate

Materials and experimental methods.

Materials.

Analytical grade rice starch, corn starch and potato starch were obtained from Sigma Aldrich (Saint Louis, MO). Instantenized and water soluble, pharmaceutical grade waxy maize starch (WMS) powder was purchased from Nutra Bio (Middlesex, NJ). Analytical grade 1, 2, 3, 4- Butane tetra carboxylic acid (BTCA) was purchased from Sigma Aldrich (Saint Louis, MO). Titebond-II (TB-II) wood glue (Franklin International, Columbus, OH) was purchased from Home Depot and used as benchmark to compare the adhesion properties of the starch based adhesives prepared in this study. Tongue shaped wood applicator blades (wood strips) were obtained from Puritan to be used as wood sticks for testing the adhesives. It is a smooth, splinter-free tongue blade, made from northern white birch with a length of 15.2cm and width 1.75 cm.

Preparation of starch based adhesives (starch pastes).

To obtain gelatinized starch, 20 g starch was added to 100 ml water and allowed to mix with a magnetic stirring at 90°C for 60 min. To obtain crosslinked WMS resin, WMS was first gelatinized by adding 20 g starch to 500 ml water and heating at 90°C for 30 min with constant stirring. BTCA (10% based on the weight of starch) was added to the gelatinized WMS. The mixture was precured by stirring continuously for 60 min at 90°C with a magnetic stirrer.

Preparation of wood specimen.

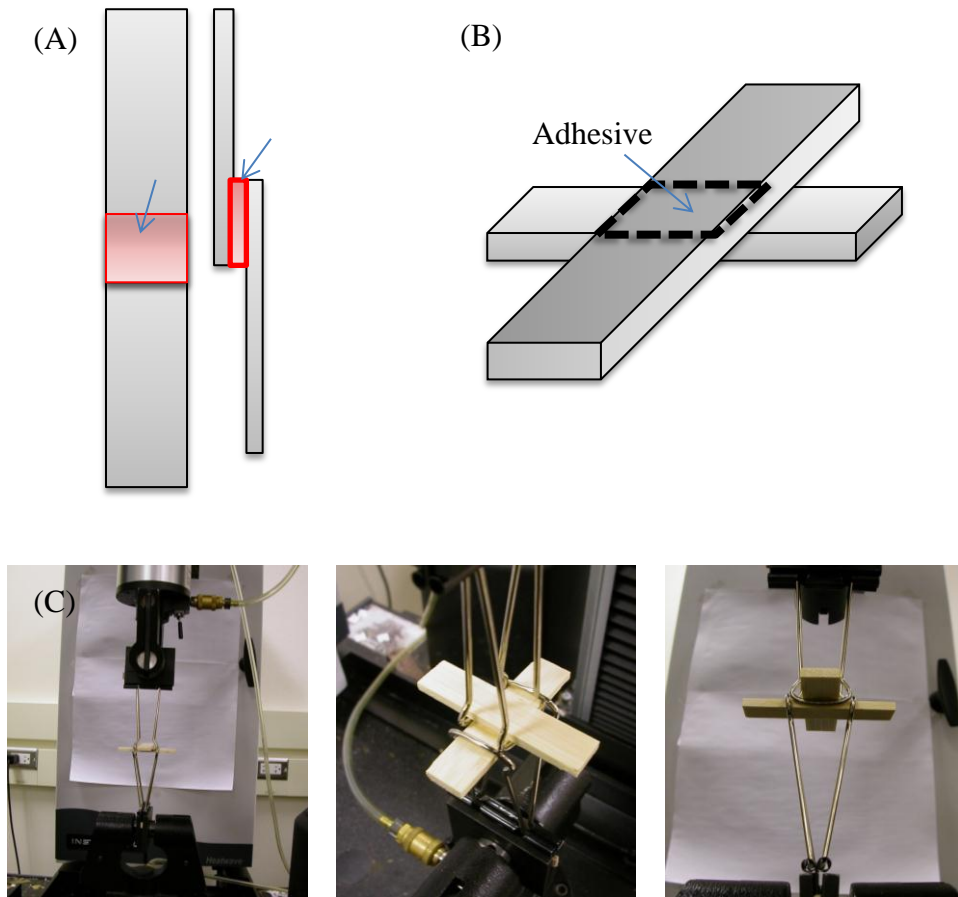


Figure 35. The adhesive (A) shear and (B) tensile strength test specimens (C) Picture of modified clip binder as a holder for Instron.⁵

The specimens for adhesive shear strength (shear strength) and adhesive tensile strength (tensile strength) were prepared as shown in **Figure 35**. To prepare specimens for shear strength test, two wood strips were placed in parallel direction and the adhesive was applied to the area to be bonded as shown in **Figure 35(A)**. Two pieces of the same wood strip were attached to the ends of the specimen for ease of handling to avoid the torsion in the grip during the shear test. To prepare specimens for tensile strength test, the top wood strip was placed in a perpendicular direction on top of the bottom wood strip as shown in Figure 35 (B). The adhesive was applied at the interface in between top and bottom wood strips. For curing the chemically modified

(crosslinked with BTCA) starch based adhesives, the bonded wood strips were cured in a convection oven at different temperatures for 2 hours.

Investigation of adhesive strength properties (in shear and tensile modes) to wood.

All specimens were conditioned at American Society for Testing and Materials (ASTM) conditions of 21°C and 65% relative humidity (RH) for 72 hr prior to testing their adhesion strength in shear and tensile modes.

Shear strength: Shear strength of the adhesive-bonded wood specimens was characterized using an Instron (model 5566, Instron Co., Canton, MA) according to ASTM D1002-10. The crosshead speed was maintained at 1 mm/min. The maximum load at break was recorded and the adhesive shear strength was calculated by the following equation:

$$\tau = \frac{P_M}{L \times W} \quad \text{Equation 2}$$

where P_M is the maximum load, L is the joint overlap length and W is the joint overlap width. At least 7 specimens were tested to obtain the average values.

Adhesive tensile strength: In this study a simple small scale test method developed by Kim and Netravali⁵ for tensile strength of adhesive-bonded wood strips was used.⁵ For this the commercially available binder clips were modified to perform as specimen holder.⁵ The specimen could be easily mounted using two of such holders, one for the top and one for the bottom, as shown in **Figure 35 (C)**. Tensile strength of the adhesive-bonded wood strips was characterized using the same Instron (model 5566). The crosshead speed was maintained at 1 mm/min and at least 10 specimens were tested to obtain the average adhesive tensile strength.

Results and Discussions

Effect of starch variety on adhesive properties.

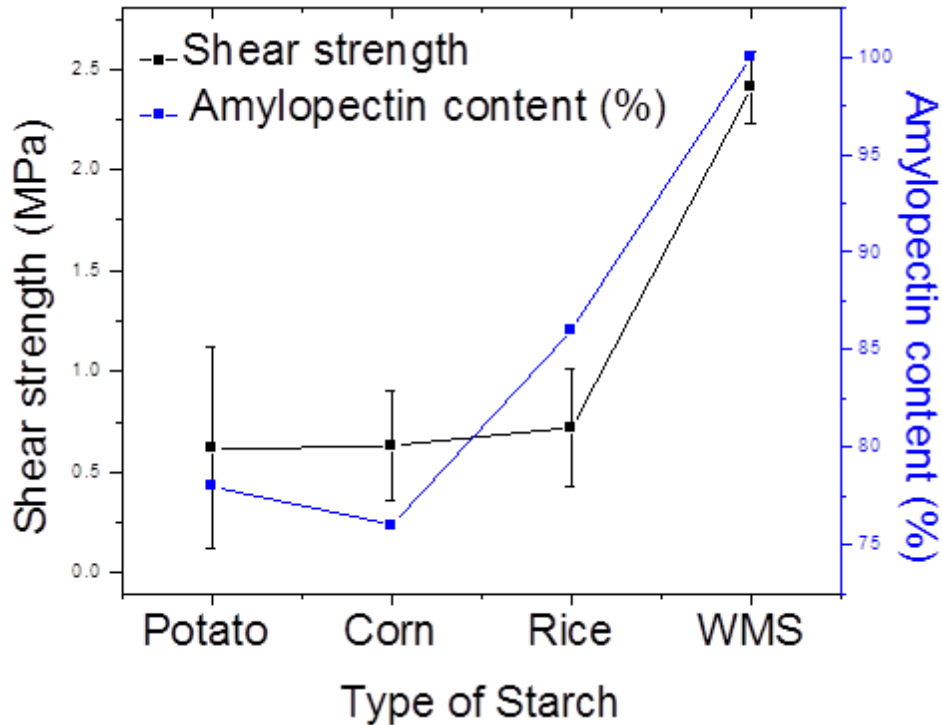


Figure 36. Effect of starch variety on the adhesion strength in shear

Both shear and tensile strength of the bonded wood specimens were characterized. **Figure 36** shows the effect of starch variety on the adhesion strength in shear. The adhesive properties (including shear strength) of gelatinized starch pastes prepared in water depend upon their source of origin of the starch which affects the microstructure of the starch granules and consequently the pasting properties. Cereal starches such as rice, corn and wheat contain a high amount of lipids that form complexes with the amylose molecule.⁷³ This makes it difficult for the starch to gelatinize by absorbing moisture and reduces their ability to form a thick paste.⁷³ These granules mostly remain insoluble in water and, as a result of the inclusion of these inert amylose-lipid complexes, the cereal starch films are opaque or cloudy. On the other hand tuber starches such as potato and tapioca absorb moisture, swell and become highly viscous on

gelatinization.⁷³ Potato starch also has 0.6-1.0% phosphate monoester group covalently bonded to the amylopectin chains.⁷³ The repulsive interaction between the negative charges of the phosphate groups help in uncoiling and extension of the starch molecules. This contributes to the increase in viscosity during gelatinization of potato starch as well as its ability to form a thick paste.

The microstructure of the starch granules which depends on their source of origin also affects the gelatinization and the adhesive properties of starches. It has been shown in earlier studies that cereal starches have A-type crystal structure while tuber starches have a B-type crystal structure.⁷³ The microstructural arrangement of B-type cereal starch is more flexible than A-type tuber starch structure.⁷³ Hence it is easier to gelatinize and react tuber starches with other chemicals including crosslinkers, compared to cereal starches.

Waxy maize starch (WMS), on the other hand, is a genetically modified cereal starch with very high amylopectin content (more than 99%) which gives it unique properties. It is easy to gelatinize and solubilize WMS and the resulting resin is optically transparent compared to other starch varieties. It was concluded that among all the different starch varieties, WMS was the best adhesive, in terms of adhesive shear strength as well as ease of application on the wood strips.

Effect of application of weight on adhesion of wood with starch based resin.

Figure 37 shows (A) Schematic of how application of weight helps in penetration and spreading of adhesive (B) Effect of application of weight on the strength of the gelatinized WMS based adhesive. When weight is applied the pressure pushes the resin to penetrate every possible valley and crevice available in the wood specimen. This provides more bonding surface and promotes lock-and-key type mechanical bonding.³ As a result, application of weight helps in increasing the adhesive shear strength. Plasticization also helps the resin penetration by lowering its viscosity. It is clear that hand pressing, on the other hand, does not produce sufficient pressure for the resin to penetrate.

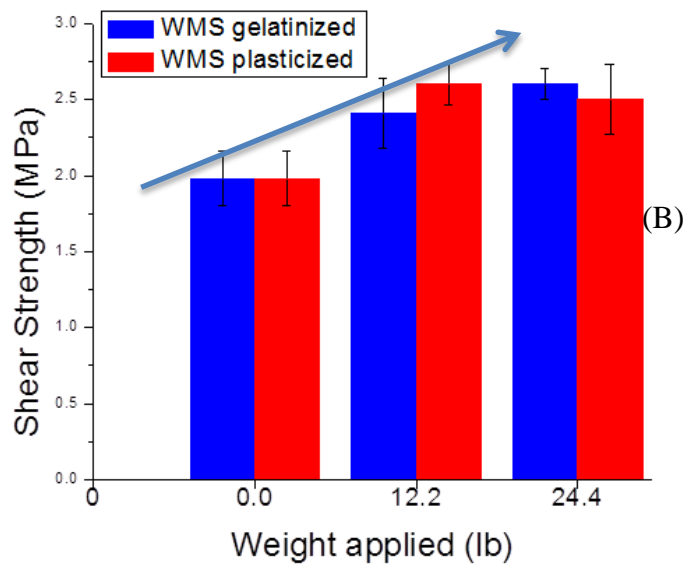
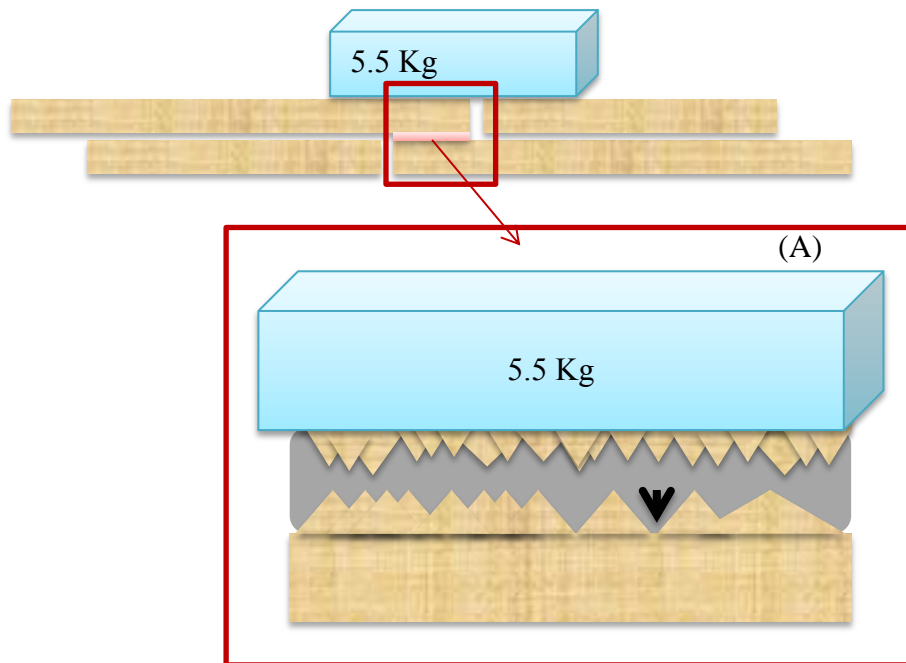


Figure 37. (A) Diagram showing how application of weight helps in penetration and spreading of adhesive (B) Effect of application of weight on the strength of the gelatinized WMS based adhesive.

Effect of crosslinking

Figure 38 shows increase in shear strength with increase in curing temperature. As described earlier WMS was crosslinked with BTCA, a polycarboxylic acid. Among other polycarboxylic acids, BTCA is a relatively inexpensive and a less toxic crosslinking agent compared to traditional crosslinkers such as dimethyloldihydroxyethyleneurea (DMDHEU) and has been used successfully for crosslinking cellulose for wrinkle-free fabrics.^{103, 259, 273-275, 279} It is also more effective than other polycarboxylic acids such as polymaleic acid (PMA). It has been postulated that BTCA creates highly reactive cyclic anhydrides under increased thermal conditions which results in its high crosslinking ability.^{103, 279} Ghosh Dastidar and Netravali²⁹² have been successful in crosslinking WMS with BTCA when sodium hypophosphite was used as a catalyst. In the current research the crosslinking was done at a higher temperature and for longer time instead of using the catalyst. The catalyst sodium hypophosphite was not used for making crosslinked adhesives due to problem faced in removing the catalyst after crosslinking. The unreacted crosslinker (BTCA) and the excess catalyst absorb moisture from the atmosphere, if not removed fully after the reaction.¹¹ The additional absorbed moisture leads to reduction in the shear strength of the materials. In the present study the curing reaction was carried out for 2 hours, without the catalyst instead of 20 minutes with the catalyst, to ensure maximum crosslinking and associated increase in shear strength due to formation of water resistant three dimensional crosslinked networks. The shear strength increased from 1.5 MPa to 2.3 MPa on increasing the curing temperature from 120°C to 140°C. There was not much change in the adhesive shear strength on increasing the reaction time from 2 hours to 4 or 6 hours (data not shown here). **Table 4** presents the tensile strength of gelatinized and crosslinked WMS based adhesives. Tensile strength of commercially available wood adhesive Tite Bond II is also shown for comparison. Tite Bond II is a commercially available polyurethane wood glue with adhesive shear strength of 7 MPa and adhesive tensile strength of 0.5 MPa measured using similar conditions as the starch based adhesives. The strength of the adhesives were still not close to

Tite Bond II. This may be because starch based adhesives absorb moisture during conditioning (3 days) which reduces their strength. More work needs to be done on improving the hydrophobicity and adhesive strength of the starch based adhesives to match them with commercial wood adhesives such as Tite Bond II. This research provides a general understanding of how microstructural changes in starch affects their adhesive properties.

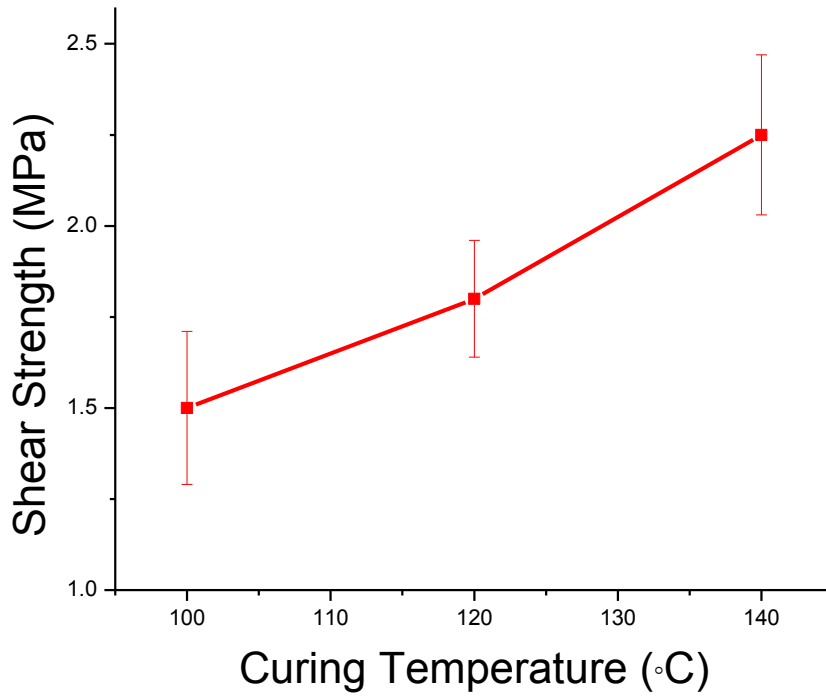


Figure 38. Increase in shear strength with increase in curing temperature.

Adhesive	Tensile strength (MPa)
WMS gelatinized	0.13 (38)*
WMS crosslinked	0.17 (20)
Tite Bond 2	0.5

Table 4. Tensile strength of gelatinized and crosslinked WMS based adhesives.

Conclusions

From the results it can be concluded that the adhesive property of starch for wood based materials depends on the granular microstructure and the source of origin of the starch granules. The gelatinization of granules affects the adhesive properties and starches (such as potato or waxy maize) which are completely gelatinized and have higher adhesive shear strength. A starch variety with lower viscosity can flow into the crevices of the rough surface of wood and provide higher penetration of the adhesive and thus result in higher mechanical bonding. The waxy maize starch which can be easily gelatinized and has lower viscosity shows superior adhesive strength compared to other starches which are more difficult to gelatinize (corn and rice) or have higher viscosity after complete gelatinization (potato). Application of weight (pressure) helps the penetration of starch based adhesive and hence increases the shear strength of the adhesives. The starch was crosslinked using BTCA alone. The adhesive strength of starch based resins and the shear strength was found to increase with the increase in crosslinking as the curing temperature increased.

CHAPTER 7

NOVEL THERMOSETTING RESIN FROM SOY FLOUR CROSSLINKED USING GREEN TECHNOLOGY

Abstract

In the current research a novel, clean and green reaction scheme was developed to crosslink the soy proteins present in soy flour, without using any external crosslinker. Soy flour (SF), which contains about 55% protein and 32% carbohydrate and is the least expensive commercially available soy protein variety, was used for this research. In this work sugars and protein from the SF were separated using a simple lab based filtration technique. Sugars were then oxidized using H₂O₂, a benign oxidizing agent to obtain aldehydes and carboxyl groups. The oxidized sugars containing those groups were then used to crosslink the reactive groups present the protein from SF, mainly utilizing a Maillard type chemistry. The resulting crosslinked (thermosetting) soy protein had enhanced mechanical, thermal and moisture absorption properties. This green resin can be used to replace some of the commercially available petroleum based polymers to produce composites. When reinforced with strong cellulosic fibers they can produce fully sustainable green composites.

Introduction

Polymers are used in diverse applications from disposable plastic bottles to housing and from aerospace and automobile parts to packaging. Most of these plastics are made using petroleum as raw material.⁵⁷⁻⁵⁹ However, petroleum, a fossil resource, is finite and by some estimates we are consuming petroleum at 100,000 times the rate at which the earth can produce.^{60, 61} In addition, petroleum based non-degradable products have significant end of life disposal problems as they cannot be recycled or reused easily and about 95% of them end up in landfills at the end of their life adding to the current environmental pollution problem. As a result, the use of renewable resources, has gained increased attention in the past decade. Other factors contributing to this '*Towards Green*' movement are their abundant availability from the biomass, relatively low cost and enhanced environmental benefits including low carbon footprint.^{293, 294} Soy protein is a less expensive biopolymer, originally introduced by Henry Ford, as a source of plastic in automobile manufacturing.²⁹⁵ Soy protein is commercially available as defatted soy flour (SF), soy protein concentrate (SPC) and soy protein isolate (SPI). SPI, the purest form, contains about 90% protein and 4% carbohydrates, SPC contains about 70% protein and 18% carbohydrates, while SF contains about 55% protein and 32% carbohydrate.²⁶² Of all these varieties, SF is the least expensive (about \$0.2/lb) and was used for the current research.

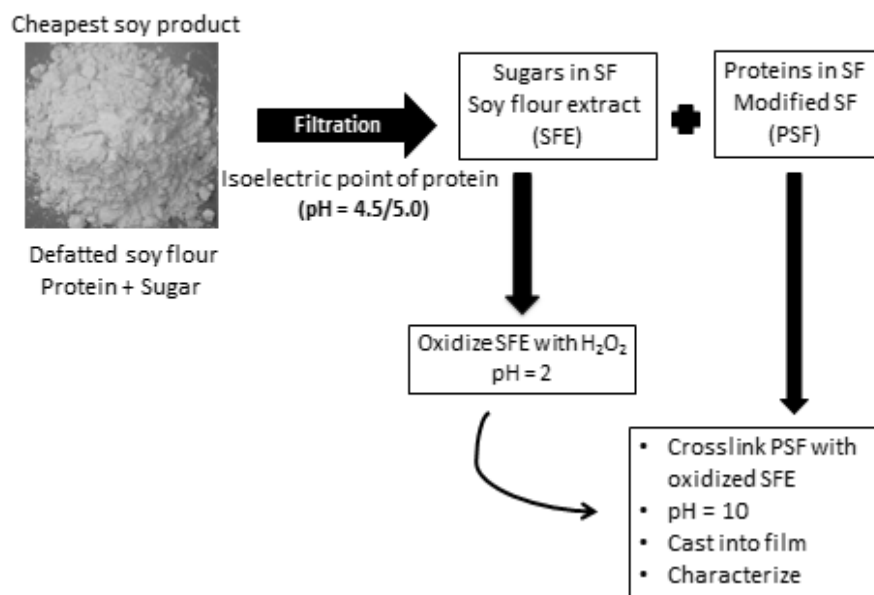
Soy protein is a long chain molecule (polymer) consisting of 18 different polar and nonpolar amino acids. Polar amino acids such as cysteine, arginine, lysine, histidine and others can be used to crosslink the protein to improve mechanical, thermal and physical properties as well as reduce water sensitivity and hydrophilicity.^{262, 276} Such crosslinked soy protein can be used as 'green' biopolymer (resin) in place of currently used petroleum based polymers. Another advantage of the soy protein based resin, besides being green, is that it is inherently fire resistant and can perform better than some petroleum based resins.^{10, 262, 263, 296-298}

It has been reported that soy proteins can be crosslinked using aldehydes including formaldehyde, glutaraldehyde (GA), glyoxal and glyceraldehyde through Maillard-type reactions.²⁹⁹ Park et al.³⁰⁰ crosslinked SPI with GA to produce biopolymers with enhanced

mechanical properties. The tensile strength of the SPI films increased from 8.3 MPa (0% GA) to 14.9 MPa (40% GA) on crosslinking with GA. Chabba et al.^{10, 262, 263, 297-299} crosslinked SF with GA which led to an increase in Young's modulus from 100 MPa (0% GA) to 500 MPa (15% GA) with crosslinking.

Huang and Netravali⁸ have also reported the use of (3-isocyanatopropyl) triethoxysilane (ITES) for crosslinking of SPC. The isocyanate groups react with the amines, hydroxyl and carboxylic acid groups of soy proteins. Once the isocyanate groups have reacted the three silicate groups can condense to form a crosslinked structure utilizing sol-gel chemistry.⁸ However, owing to the low crosslinking density of the proteins with ITES, no significant increase was observed in the Young's modulus and fracture stress of the crosslinked SPC films compared to the native SPC films.

In order, to overcome the cytotoxicity associated with the above mentioned crosslinkers, there has been a continuous search for greener alternatives. Gonzales et al.³⁰¹ crosslinked soy protein using a naturally available crosslinking agent, genipin (Gen). Tensile strength of films increased from 3.2 MPa (0% Gen) to 4.6 MPa (10% Gen) while moisture content decreased from 27.1% (0% Gen) to 26.1% (10% Gen) after crosslinking. SF has also been crosslinked using rutin and quercetin which has resulted in better mechanical properties.³⁰²



Scheme 1. Crosslinking of SF using a novel three step process

As we move towards a ‘greener’ economy, clean syntheses, based on the use of natural renewable reagents, particularly in water and under mild conditions, become highly desirable processes. In the current research SF was crosslinked using a novel 3-step process as shown in **Scheme 1**. In the first step the protein was separated from the soluble carbohydrates consisting of small sugars using a simple lab scale filtration technique. The sugar extract, in water, is termed soy flour extract (SFE) while the separated protein is termed as purified soy flour (PSF). The PSF was confirmed to have over 65% protein, close to that present in SPC. The SFE is usually discarded after extraction of the protein.²⁷⁶ The sugars present in SFE are glucose, fructose, sucrose, raffinose and stachyose.²⁷¹ In our technique, the sugars were converted to aldehydes and carboxylic acids by oxidation using hydrogen peroxide (H₂O₂), a green oxidizing agent, as the second step. Hydrogen peroxide has been used previously as an oxidizing agent for glucose by Velarde et al.³⁰³ and Comottie et al.³⁰⁴, but in the presence of titania or gold nanoparticles as catalyst. Their process, however, yielded carboxylic acids like gluconic acid, glucuronic acid and tartaric acid. In the third step, the oxidized sugars were used as crosslinking

agent to crosslink the PSF, utilizing a Maillard-type chemistry. Thus, no other chemicals were needed to obtain crosslinked soy protein. Besides obtaining better mechanical properties, crosslinking, to some extent, was also advantageous in reducing the moisture sensitivity of the soy protein based resin. Reactions to obtain aldehyde and carboxyl groups in SFE were confirmed separately using commercially available glucose and sucrose (small sugar molecules) and their crosslinking reactions were further confirmed with SPI (90% protein). This technology can be easily extended to flours from other grains where the two components are protein and soluble carbohydrates in the form of sugars and/or low molecular weight starches.

Experimental section

Materials

SF and SPI were obtained from Archer Daniels Midland Co. (Decatur, IL). Sucrose and glucose were purchased from VWR and Sigma Aldrich, respectively. Analytical grade hydrochloric acid (HCl), sodium hydroxide (NaOH) and 30% Hydrogen peroxide (H₂O₂) were obtained from VWR.

Filtration of SF.

As mentioned earlier, the first step involved separating the soy protein from soluble sugars (fructose, glucose, sucrose, raffinose and stachyose) present in SF using a lab based filtration technique. To achieve this, SF was dissolved in water (10 times by weight of SF) by magnetic stirring at room temperature. The solution pH was changed from about 7 to 4.5 using HCl solution. Soy proteins become insoluble in water at pH 4.5 at their isoelectric point. As a result, the protein molecules precipitate but the sugars remain dissolved and thus can be separated easily by filtration. Any type of filter; paper, fabric, etc. can be employed. In our studies both paper and fabric were found to work satisfactorily. The fabric made using microdenier fibers (micro fiber) was preferred because it worked well and could be reused. The retentate (mostly protein) was rinsed twice with deionized water to remove any remaining sugars and used as PSF for further crosslinking reactions. The filtrate, soy flour extract (SFE), consisting of sugars was collected and used for oxidation reaction.

Oxidation of sugars with H₂O₂.

The SFE sugars (≈ 16 g) obtained by the filtration of 50 g SF were oxidized using 50 mL of 30% H₂O₂ at pH 2.0 (using HCl). The reaction was carried out overnight at 60°C to obtain complete oxidation. In the present study separate experiments were carried out to oxidize glucose, sucrose and SFE using acidified H₂O₂ (pH = 2) for comparison and confirmation of reactions.

Preparation of SPI and Crosslinked SPI resin.

SPI, which contains over 90% protein, was crosslinked with oxidized sucrose, as a preliminary study, to understand and confirm the reactions between proteins and oxidized sugars. To fabricate pure SPI films SPI was denatured at 70°C and pH of 10 which led to the formation of a smooth resin due to opening of the protein chains. The denatured protein was cast onto Teflon® coated glass plates to obtain control films. To fabricate crosslinked SPI films it was denatured and crosslinked by reacting the amine and hydroxyl groups with oxidized sucrose. The pH value dropped on adding the acidic oxidized sucrose solution to SPI which was adjusted to pH 10 by adding necessary amount of NaOH to the reaction mixture. Significant effervescence generated on adding the oxidized sucrose to soy protein was allowed to die down to form a smooth crosslinked SPI resin which was cast into films on Teflon® coated glass plates. The films were dried at 40°C for 36 hours, washed thoroughly in water and dried again at 40°C for 24 hrs to remove all the water. This stage is referred to as the precuring of resins when the resins are partially crosslinked. To complete the crosslinking process the films were further cured by heating at 120°C for 20 min leading to complete crosslinking.

Preparation of SF resin and Crosslinked SF resin.

SF was denatured at 70°C and pH 10 and cast into a film following the same procedure as SPI resin based films mentioned in the previous paragraph. To make crosslinked SF resin the protein was first extracted from SF by a filtration technique described before. The purified protein (PSF) obtained from soy flour filtration was denatured at 70°C and pH of 10 to open up the molecules and expose the reactive functional groups. At this pH the denatured protein was

allowed to react with the oxidized SFE, the pH was adjusted to 10 by adding NaOH. As before, the films were cast on Teflon[®] coated glass plates. As explained earlier, this stage is referred to as the precuring of resins when the resins are partially crosslinked. To complete the crosslinking process the films were further cured using a by curing at 120°C for 20 min leading to complete crosslinking. This crosslinked resin will henceforth be referred to as crosslinked SF resin. It had essentially the same constituents as the original SF (protein and sugars), the only change being that the sugars were oxidized to aldehydes and carboxylic acids and reacted with the amine and hydroxyl groups to crosslink the proteins. The SF and crosslinked SF films were fabricated, washed thoroughly in water, dried and conditioned before characterization using the same procedure to compare the properties of SF resin and crosslinked SF resin.

To fabricate films for tensile testing, microfibrillated cellulose (MFC) (5% dispersion in water by wt.) was added to both SF resin and precured SF resin. This was done for ease of film formation and fabrication of relatively defect free, ductile films needed for tensile testing. The precured SF (with 5% MFC) was cured at 120°C and 20 minutes followed by a thorough washing. The washing was important to remove unreacted sugar molecules which can plasticize the films due to moisture absorption. The incorporation of MFC helped in the curing process as well as the washing and drying process by preventing defect formation, wrinkling and curling of the films. Making composites by adding MFC also increases the tensile properties of the resin films by reducing the brittleness and increasing the Young's modulus. Conditioned (at 65% relative humidity, 21°C for 3 days) composite sheets were cut into rectangular specimens of 10 mm × 50 mm dimensions for tensile testing.

Chemical Characterization

Attenuated total reflectance – Fourier transform infrared (ATR-FTIR) analysis: ATR-FTIR spectra were collected using a Nicolet Magna 560 FTIR spectrometer with a split pea accessory for ATR. Each scan was an average of 150 scans recorded from 4000 cm⁻¹ to 550 cm⁻¹ wavenumbers at a resolution of 4 cm⁻¹.

Film Characterization

Film Color. The color of the films, which changed due to crosslinking through Maillard reaction, was measured with Hunterlab Colorimeter (Ultrascan Pro., Hunter Associated Laboratory Inc., Reston, VA) ; L, a and b values were measured. The ranges of the three color coordinates were 0 black to 100 white, – greenness to + redness, and – blueness to + yellowness, respectively. Standard values refer to the white calibration plate (L = 94.47, a = –0.81, b = –0.86).³⁰⁰

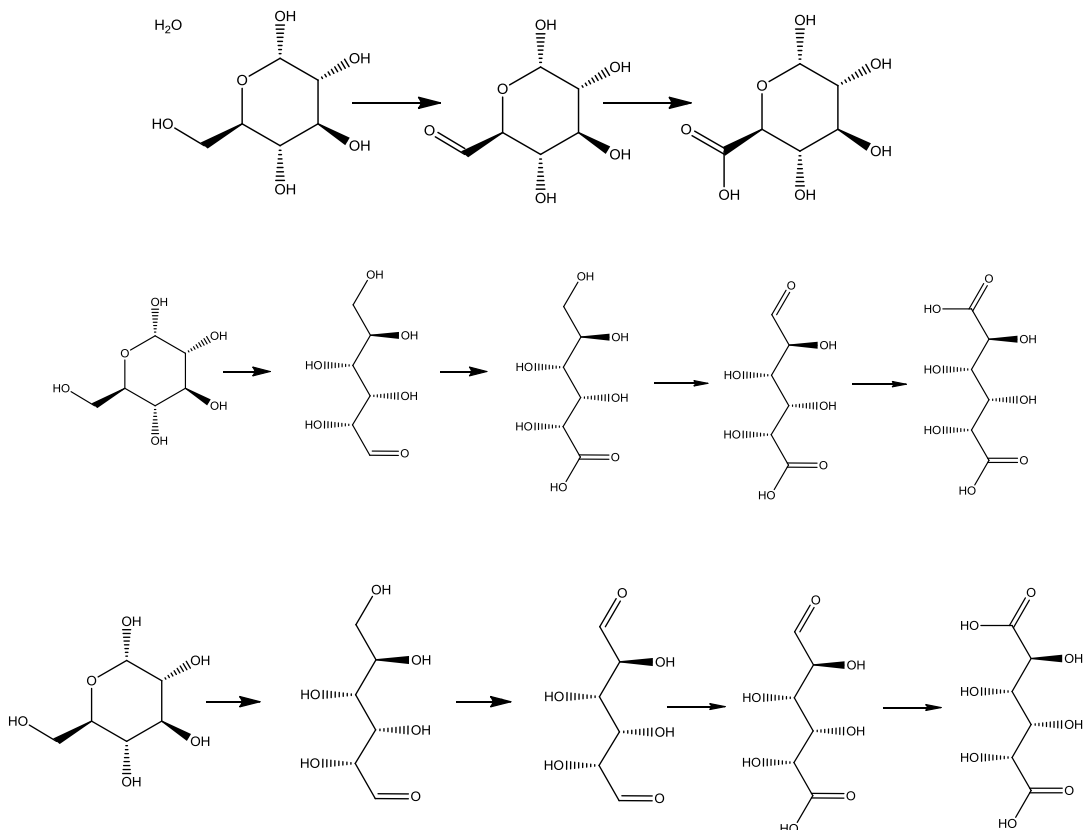
Sol-gel test. A pre-weighed amount of resin (pure and crosslinked) specimens (conditioned at 21°C and 65% RH for 3 days) were immersed separately in 50 ml distilled water in a glass bottle and placed on a platform shaker (Innova™ 2300, New Brunswick Scientific Inc., New Brunswick, NJ) at 80°C and 100 rpm for 3 days. The contents of the bottle were washed/filtered using a microfiber based fabric filter. The gel residue on the fabric filter was then air-dried at 40°C 24 hrs and subsequently conditioned (as per ASTM) at 21°C and 65% RH for 3 days.

Thermogravimetric Analysis (TGA). Pure SF and crosslinked SF resin specimens were scanned from 25°C to 600°C using a thermogravimetric analyzer (TGA-2050, TA Instruments, Inc., New Castle, DE) at a rate of 10°C/min in nitrogen atmosphere to characterize their thermal stability and degradation behavior. At least 3 specimens were tested to obtain average property values.

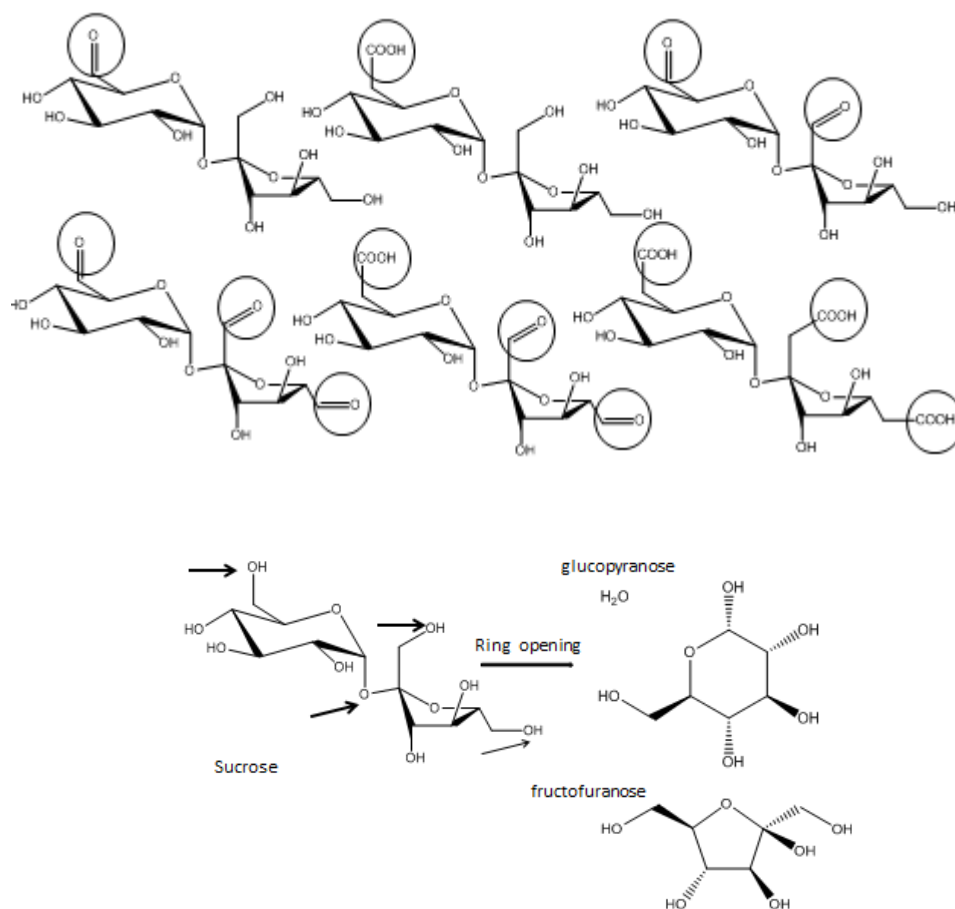
Tensile Properties. Tensile properties of the SF and crosslinked SF resin sheets, both in the form of composites containing 5% MFC, were characterized in accordance with ASTM D 882-97. At least five thickness measurements of the films were made along the length of each specimen and the average of these values was used for calculating the fracture stress and Young's modulus values. The tests were performed on an Instron universal tensile tester, model 5566, at a strain rate of 2 min⁻¹ and a gauge length of 30 mm. At least 5 specimens were tested to obtain average properties.

Results and discussions

Structure, reactions and mechanism



Scheme 2. Proposed reactions for oxidation of glucose.



Scheme 3. Proposed reactions for oxidation of sucrose.

In the present research acidified H₂O₂ (at pH 2), a strong but water based and environmentally benign oxidizing agent, was used for oxidation of sugars present in the SFE. Oxidation of commercially available glucose and sucrose was studied as model reactions prior to the oxidation of SFE. Oxidation of sugars can lead to formation of different oxidation products as proposed in **Scheme 2** and **Scheme 3** for glucose and sucrose, respectively. In fact, previous research on the oxidation of carbohydrates indicate that the oxidation of even simple sugars such as D-glucose can have different reaction mechanisms and products depending on the pH, temperature, concentration and the type of catalyst used in the reaction.³⁰³⁻³⁰⁵ Typical oxidants for carbohydrates (sugars) include CrO₃, KMnO₄, HNO₃, HIO₆ which are highly oxidizing but toxic in nature. Periodates have been used for selective oxidation of the vicinal diols in

sugars.^{305, 306} Often metal catalysts such as gold, titanium or iron are used for clean and efficient oxidation reactions.^{303, 304} Titanium containing zeolites were used by Velarde et al.³⁰³ to catalyze oxidation of D-glucose with 30% H₂O₂ as the oxidant. In their study D-glucose was converted to gluconic acid, glucuronic acid, tartaric acid, glyceric acid, glycolic acid via oxidation of intermediate aldehydes as a result of the catalytic oxidation.³⁰³ Dewit et al.³⁰⁵ oxidized sucrose by using periodate in aqueous dimethyl formamide (DMF). At pH 7 and a temperature of 95°C dialdehydes were selectively formed by double oxidation of the glucose ring. The reaction was thought to proceed via formation of a cyclic ester intermediate. A 1:1 mixture of glucose and fructose were formed at pH of 5 to 7 and 25°C. The pH and temperature as well as presence of water influence the regioselectivity of the sucrose oxidation. TEMPO (2,2,6,6-tetramethylpiperidin-1-yl) oxidanyl mediated hypochlorite oxidation system has been used for sucrose which leads to the selective oxidation of primary alcohol to carboxylic acid group.³⁰⁷ An aqueous solution of sucrose treated with sodium hypochlorite (NaOCl, 2.2 equivalents) in the presence of sodium bromide and TEMPO at pH 10 and 5°C leads to the formation of sodium sucrose tricarboxylate. It has been shown that reaction of isomaltose with H₂O₂ under acidic conditions is hard to control and can lead to partially degraded products due to chain scission.³⁰⁸ Under controlled acidic medium, the reaction of isomaltose with H₂O₂ leads to essentially one product, carboxymethyl α -D-glucopyranoside(α -CMG).³⁰⁸ The reaction of palantiose with excess hydrogen peroxide at pH 2 without any catalyst or at pH 4 with sodium tungstate as catalyst, both reactions carried out at 80°C, resulted in the formation of carboxymethyl α -D-glucopyranoside(α -CMG).³⁰⁹ It was also shown in these studies that the oxidation of fructose was easier than the oxidation of palantiose itself. From the previous researches it was quite clear that a range of oxidation products was possible for oxidation of sugar molecules. It was difficult to predict and characterize all reaction products of the SFE oxidation owing to the wide range of possible reaction products and mechanisms. Characterization of the oxidation products was also not the main intent of this research. However, it was postulated that both aldehydes and carboxylic acids were produced as a result of oxidation of the different sugars present in SFE.

Both dialdehydes and poly carboxylic acids have the potential to react with different functional groups available in soy protein and crosslink them.^{299, 310, 311} Yasir et al.²⁹⁹ showed that soy protein can be crosslinked with formaldehyde, gluteraldehyde (GA) and glyceraldehyde using Maillard type chemistry, which leads to considerable reddish coloration of the crosslinked product. Bifunctional aldehydes such as GA react with the basic amino acids such as lysine, arginine and histidine in soy protein and provide intra- and/or inter-molecular crosslinking.³¹² The tensile strength of the films were found to increase from 8.3 MPa for non-crosslinked soy protein to 14.9 MPa for soy protein crosslinked with 0.4% (w/w with protein) GA.³¹² The value of Hunter L color coordinate decreased from 53 for unreacted soy protein to 42.8 for soy protein crosslinked with 0.3% GA, confirming the darker color and hence the Maillard reaction.³¹² Chabba and Netravali²⁶² prepared biodegradable resin by crosslinking SPC with GA. They found the Young's modulus of the SPC resin increased by 35% after crosslinking. At the alkaline condition (pH 10), the soy protein molecules can be denatured and open (unfolded) form, making it easy to process.²⁷⁶ Adding polycarboxylic acids such as phytigel[®] to SPI have also been shown to improve their tensile properties by forming interpenetrating networks of the two.^{310, 311} However, Phytigel[®] which is composed of glucuronic acid, rhamnose and glucose is also capable of reacting with the amino acids in soy protein.^{310, 311} Glucuronic acid contains carboxylic acid groups which react with the amine, hydroxyl and carboxyl groups present in soy protein to form amide, ester and anhydride linkages respectively.^{310, 311} Similarly, the aldehydes and polycarboxylic acids produced as a result of SFE oxidation react with the polar amino acids in soy proteins (aspartic acid, threonine, serine, glutamic acid, glycine, tyrosine, histidine, lysine and arginine). The most probable reaction products between oxidized sugars and proteins are imines, amides, esters and anhydrides. ATR-FTIR was used to confirm the reactions.

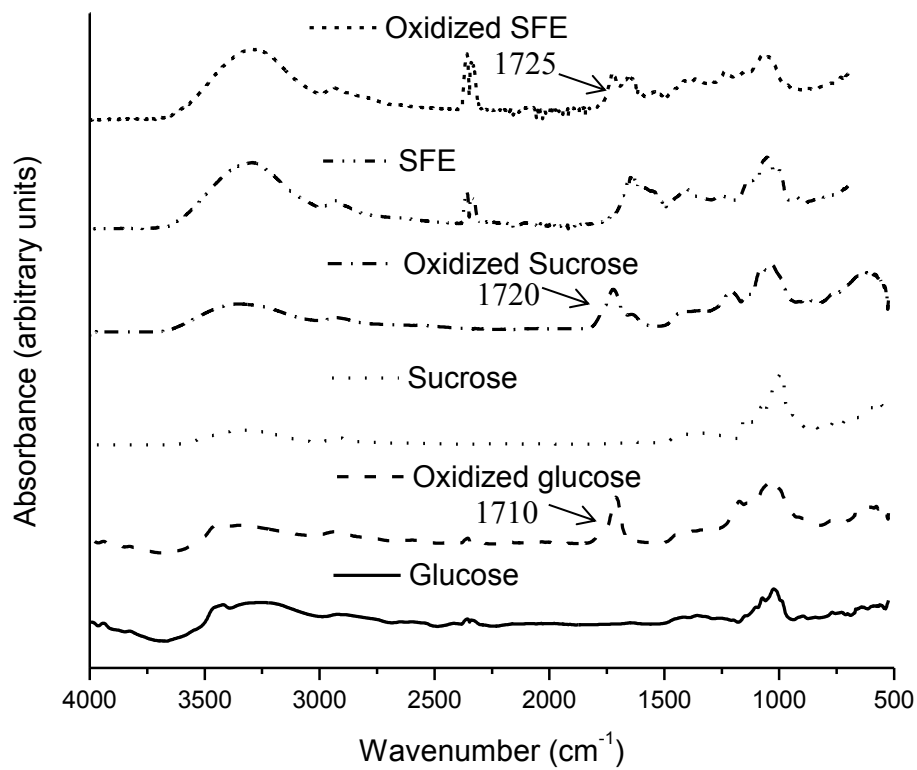


Figure 39. FTIR spectra of sugars (glucose, sucrose and SFE) and oxidized sugars.

Figure 39 shows FTIR spectra of sugars (glucose, sucrose and SFE) and oxidized sugars. In the FTIR spectra all oxidized sugars show a carbonyl peak at 1710 cm^{-1} (glucose), 1720 cm^{-1} (sucrose) and 1725 cm^{-1} (SFE). These peaks correspond to carbonyl peaks from oxidation of the primary alcohols to aldehydes and/or carboxylic acids. These peaks are absent in the unreacted sugars which do not have carbonyl groups. This confirms the oxidation of sugars with acidified H_2O_2 . The exact nature of the carbonyl peak (aldehyde or carboxylic acid or both) could not be identified from the FTIR spectra. The formation of carboxylic acids in sucrose and glucose oxidation was also confirmed by monitoring a sharp change in pH from 2 to below zero as the reaction progressed. However, as mentioned earlier, both aldehyde and carboxyl groups can

react with the amines, hydroxyl and carboxyl groups in the proteins to produce imines, amides, esters and anhydrides and thus crosslink it.

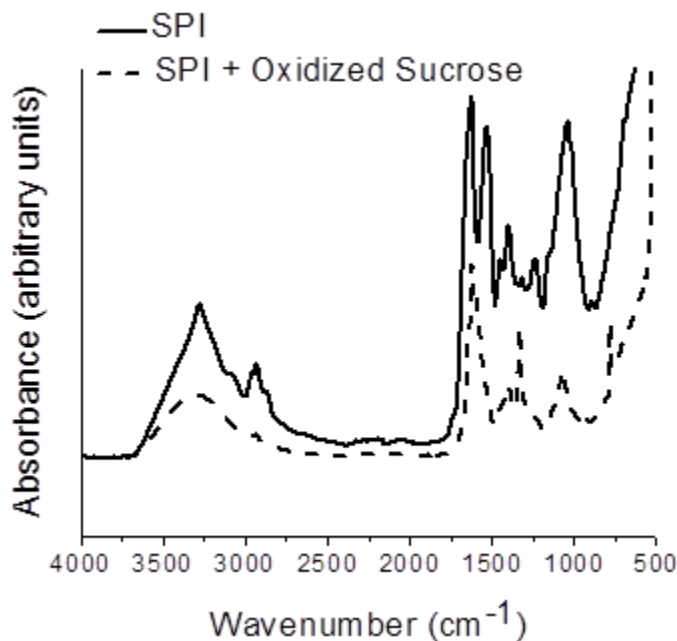


Figure 40. FTIR spectra of SPI and SPI+oxidized sucrose (crosslinked SPI).

Figure 40 shows FTIR spectra of SPI and SPI+oxidized sucrose (crosslinked SPI). A typical soy protein spectrum shows three major peaks at 1638, 1537, and 1238 cm^{-1} , which are assigned to CO stretching (amide I band), N-H deformation (amide II band), and C-N-stretching and N-H vibration (amide III band), respectively, as shown in **Figure 40**.²⁷⁶ The carboxylic acids formed due to oxidation of glucose or sucrose can crosslink proteins via formation of anhydride, ester or amide linkages.^{310, 311} No ester peak was detected at 1720-1730 cm^{-1} for SPI crosslinked with oxidized sucrose indicating that the crosslinking took place without the formation of an ester linkage. Because of the large number of amide linkages already present in the soy protein it was not possible to detect the formation of any additional amide bonds. Formation of imine linkage by the reaction of amine groups with aldehyde (Maillard reaction) is

also hard to detect in the FTIR spectra due to overlap of several peaks in the fingerprint regions. However, the formation of imine linkage can be detected by observing the color change in the specimen as explained later.

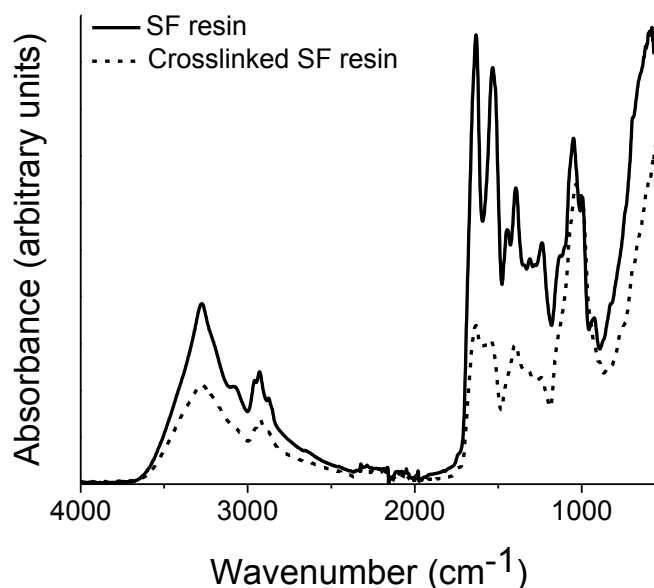


Figure 41. FTIR spectra of SF resin and crosslinked SF resin.

The ATR-FTIR spectra of SF resin and crosslinked SF resin are presented in **Figure 41**. The ATR-FTIR spectrum for SF as presented in **Figure 41** shows another major peak at 1049 cm^{-1} , which is assigned to C-O stretching, indicating the presence of sugar molecules. This peak is not present in the FTIR spectrum for soy proteins (SPI) which do not have significant amount of sugars. As mentioned earlier it was difficult to characterize the different reactions and reaction products using FTIR owing to the wide range of possible reaction products (imines, esters and amides) and some of the groups already present in the protein. Similar difficulties were faced by others as well.^{8, 263, 276, 278, 280, 296-298, 313, 314} However, the crosslinking could be easily confirmed using other characterization techniques including color test, sol-gel analysis and tensile testing.

Characterization of films

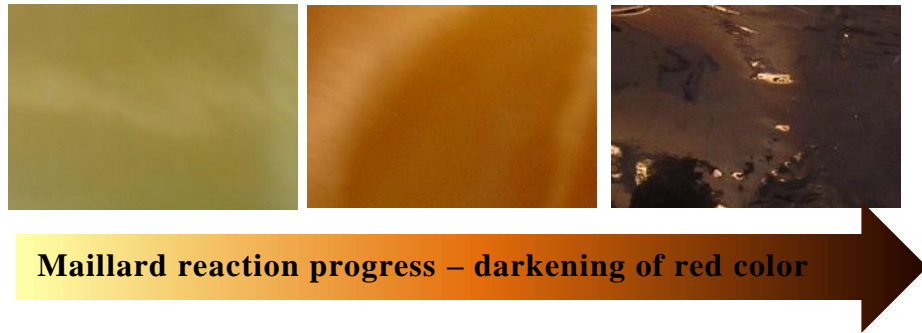
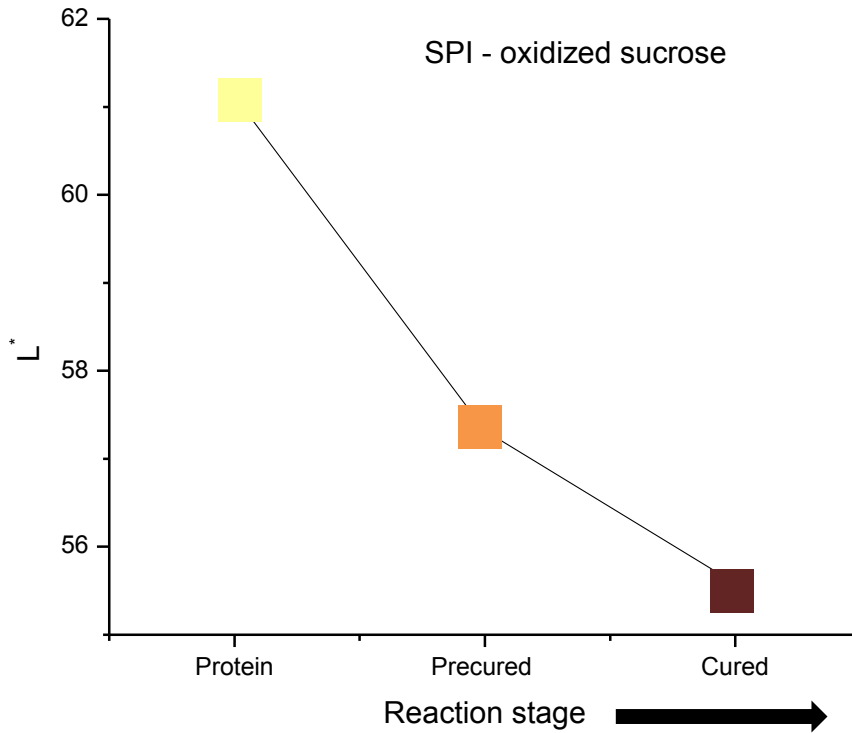


Figure 42. Changing of color from pale yellow (beige) to dark red color with the progression in Maillard reaction between amine groups in amino

Maillard reaction takes place between the amine group in protein and the aldehyde group which is responsible for the red coloration in protein. **Figure 42** shows change of color from pale yellow (beige) to deep red color with the progression in Maillard reaction. This color change has been noted by many other researchers.^{8, 10, 262, 263, 297, 311} In the Hunter color test a

decrease in L value indicates increase in the deepness of the red color of the sample.³⁰⁰ The effect of oxidized sugar reaction with SPI on the Hunter color values of the SPI was significant. As the reaction progressed from the unreacted to the partially cured (precured) and finally cured stage, the L value decreased indicating that the deepness of the red color increased. Identical results were observed for crosslinking of PSF with oxidized SFE (crosslinked SF resin). This confirms that the aldehyde groups produced by the oxidation of SFE were reacting with the denatured PSF obtained from soy flour, i.e., the crosslinking was indeed occurring.

Sol-gel test.

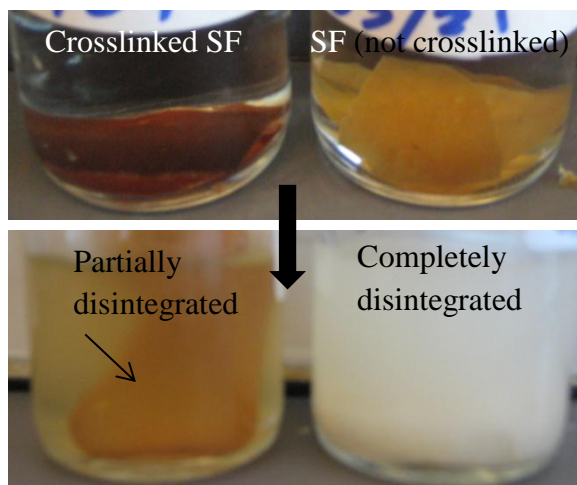


Figure 43. Results of the sol-gel test: SF film, disintegrated, (right) and crosslinked SF, only partially disintegrated, (left).

Sol-gel test for SPI and crosslinked SPI resins showed that SPI completely disintegrated in water while crosslinked SPI resin (with oxidized glucose and sucrose) remained intact. Similar results were observed for SF resin and crosslinked SF resin. **Figure 43** shows sol-gel test results for SF film (top right) and crosslinked SF film (top left). Pure SF resin film completely disintegrated in water (bottom right) while the crosslinked SF resin film remained mostly intact (bottom left) even after being continuously shaken in water at 80°C for 3 days.

The crosslinked SF, however, did show slight disintegration indicating that the specimens were not highly crosslinked. The gel fraction (crosslinked part) of the crosslinked SF resin was calculated to be 42% whereas the gel fraction of the pure SF was 0%. This suggests that there is scope for optimization of the reaction by adjusting time, pH and controlling the oxidation of sugars to aldehydes and carboxylic acids to reach the maximum crosslinking potential. However, optimization studies are not addressed as a part of this paper.

Thermogravimetric analysis (TGA).

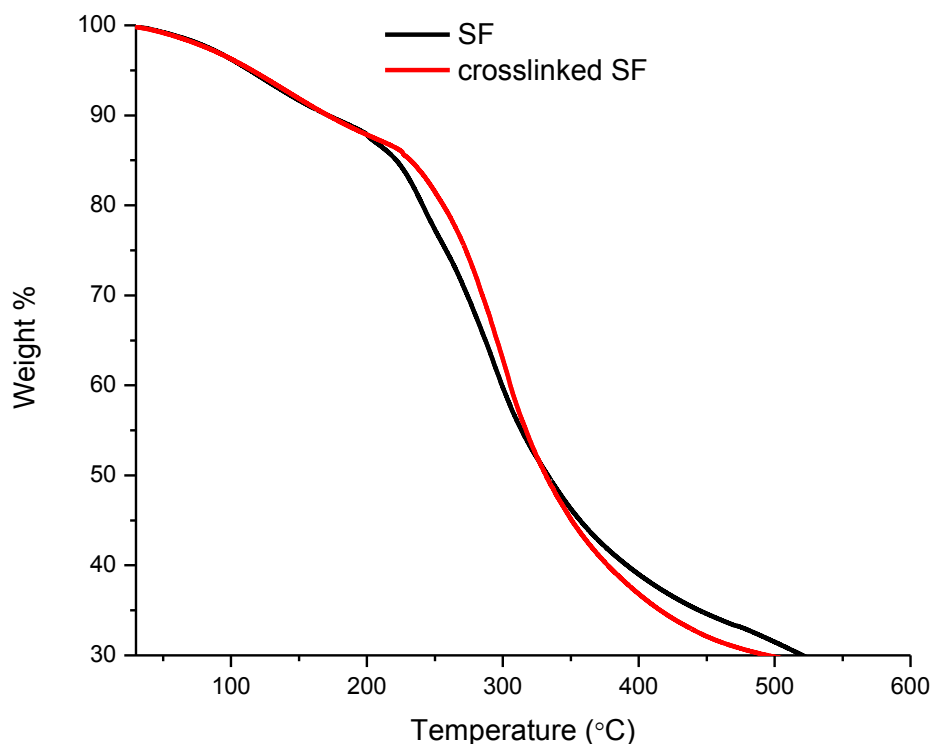


Figure 44. TGA of SF and crosslinked SF.

Table 5. Initial degradation temperatures of SF and crosslinked SF.

Specimen	Initial degradation temperature (°C)
SF	219
Crosslinked SF	233

TGA thermograms of SF and crosslinked SF resin specimens are presented in **Figure 44**. The TGA thermograms of SF and crosslinked SF resins show that there was an increase in the initial degradation temperature of the resin from 219°C to 233°C after crosslinking. **Table 6** presents the initial degradation temperature of SF and crosslinked SF. This indicates an increase in thermal stability of SF resin after crosslinking. Chabba and Netravali²⁶³ also reported an increase in the thermal stability on crosslinking soy protein. The same authors also reported an increase in the initial degradation temperature of SPC from 235°C to 270°C after crosslinking with GA.²⁶²

Tensile properties.

Specimen*	Modulus (MPa)	Fracture Stress (MPa)	Fracture Strain (%)
Soy flour	1106 (17)**	9.2 (28)	1.8 (37)
Crosslinked soy flour	6375 (56)	58 (39)	2.7 (33)

Table 6. Young’s modulus, fracture stress and fracture strain of SF and crosslinked SF resin films.

*5% MFC dispersion was added to both SF and crosslinked SF resin for fabrication relatively defect free film and ease of handling during mechanical testing.

**Numbers in parenthesis are coefficient of variation (%)

Table 6 summarizes the Young’s modulus, fracture stress and fracture strain of SF and crosslinked SF films. The Young’s modulus and tensile strength increase on crosslinking the films as expected. Significantly higher Young’s modulus and fracture stress clearly indicate that the crosslinking was successfully carried out. Also, these results are similar to previous literature on effect of crosslinking on the tensile properties of the polymer films.

A small amount (5 wt%) MFC was added to the specimen instead of plasticizer (glycerol). Incorporation of MFC increased the flexibility and the ease of handling the films during tensile testing without compromising the Young's modulus. **Table 6** presents the Young's modulus, fracture stress and fracture strain data for both SF and crosslinked SF films. It can be seen from these data that both Young's modulus and fracture stress increase after crosslinking the films as can be expected. Significantly higher Young's modulus and fracture stress after crosslinking clearly indicate that the crosslinking was successfully carried out. Also, these results are similar to previous literature^{8, 311, 314 310} on effect of crosslinking on the tensile properties of the polymer films. Huang and Netravali^{8, 278, 311, 313} reported the tensile properties of SPI and SPI reinforced with fillers such as micro/nano fibrillated cellulose (MFC), nanoclay, flax yarns etc. The Young's modulus of SPC (plasticized with 15% glycerol) increased from 3.8 GPa to 4.1 GPa on adding 5% dispersion of nanoclay and further increased to 4.3 GPa on crosslinking with 5% glutaraldehyde. Glutaraldehyde forms inter and intramolecular crosslinking with the protein molecules, especially amino acids like lysine and arginine. The increases in Young's modulus and strength values were shown to be a result of crosslinking.³¹³ In the present case the addition of MFC turns the resin into a nanocomposite making much stronger resin. Never the less, the increase in mechanical properties after crosslinking is significant.

Chabba and Netravali²⁶² reported the crosslinking of SPC with 40% glutaraldehyde and the crosslinked SF showed a Young's modulus of 500 MPa. In another study, gellan which can form interpenetrating network (IPN) by strong hydrogen bonding and ionic interactions with SPC was shown to contribute to higher mechanical properties of Gellan modified SPC.^{263, 310} The SPC composite resin containing 1.5 parts of glycerol, 40 parts of MFC and 0 parts gellan showed Young's modulus of 4.5 GPa and fracture stress of 85 MPa while with 40 parts of gellan, the combination showed impressive Young's modulus of 5.8 GPa and fracture stress of 122 MPa.³⁶ These values are comparable with commercially available epoxy based resins.

Conclusions

The present research discusses a novel reaction scheme for crosslinking of defatted SF, a cheap biomaterial, without the use of any external crosslinker. The sugars in SF are separated from protein, oxidized to sugar aldehydes and carboxylic acids and then reacted with the protein. The resulting crosslinked SF resin shows enhanced thermal and mechanical properties and higher stability (resistance) in water. Similar reactions can also be utilized to crosslink other proteins obtained from plants with commercially available sugars oxidized using acidified H₂O₂. This green and relatively low cost method to crosslink proteins will be useful in making inexpensive biobased materials with enhanced materials properties. This technology can be easily extended to flours from other grains where the two components are protein and carbohydrates in the form of sugars and/or low molecular weight starches.

This SF based resin may be used with natural fibers to form green composites for many applications. The SF based resin may also be used with synthetic fibers such as aramid, graphite and many others to obtain composites with higher mechanical, physical and thermal properties. The resin may also be used as a 'green' adhesive.

APPENDIX
SURFACE FUNCTIONALIZED SILICA AND WAXY MAIZE STARCH BASED
NANOCOMPOSITE

Introduction

Silica in the form of nanoparticles in polymer nanocomposites have recently received wide attention due to their potential attractive applications such as protective coatings, high refractive index films, optical waveguide materials, and flame retardants.³¹⁵ During the past few years, with growing environmental concerns, considerable effort have been focused on the development of biopolymer based nanocomposites or the ‘bionanocomposites’.³¹⁶ Synthetic petroleum based polymers are increasingly being replaced with renewable plant based polymers such as starches and proteins. In a polymer nanocomposite the fillers are particles with at least one dimension in the nanosized regime, i.e., 100 nm or less.³¹⁷ Common nanofillers for starch based resins have been nanoclays or layered silicates. Another widely used nanofiller is silica or silicon dioxide (SiO₂) nanopowders.³¹⁸ Silica nanoparticles are dispersed within the starch based matrix using mechanical shearing and ultrasonication techniques.³¹⁸

It has been shown that the properties of polymer nanocomposites depend on the interfacial interaction between polymer and the nanoparticles. Because of the large surface area of the nanometer sized particles the interface plays a dominant role in the properties of polymer based nanocomposites.³¹⁷ Ciprari et al.³¹⁷ showed that the interfacial interaction depends upon the degree of entanglement of the polymer chains and the actual points of contact between the polymer chains in the resin with the nanoparticles.³¹⁷ Further, by adding the nanoparticles, the tortuosity of the polymer molecules is significantly increased as they have to go around these nanoparticles. The conventional way of just mixing the nanoparticles with the polymer has been shown to lead to serious aggregation problems in many cases as observed by many researchers.^{315, 317} This is particularly true if the surface energies of the polymer and nanoparticles are very different. Surface modification of nanoparticles, to reduce this surface

energy difference, is a good technique to increase the interaction between the polymer and the nanoparticles. A common technique to functionalize silica nanoparticles is the sol-gel process that involves silica precursors such as tetraethyl ortho silicate (TEOS) or tetramethyl ortho silicate (TMOS).³¹⁹ Recently Kim et al.³²⁰ fabricated triacetylcellulose (TAC) polymer-silica nanocomposites with surface modified silica nanoparticles. The silica nanoparticles were surface-modified by reacting with (trimethoxysilyl)propyl-2,3,4,6-tetra-O-acetyl-D-glucopyranoside (TSPAG). The strong interaction between the surface-modified silica nanoparticles (that had groups similar to the polymer repeating units and, hence, similar surface energies) and the TAC matrix resulted in incorporation of nanoparticles without causing any significant aggregation that could result in degradation in the optical characteristics of TAC.

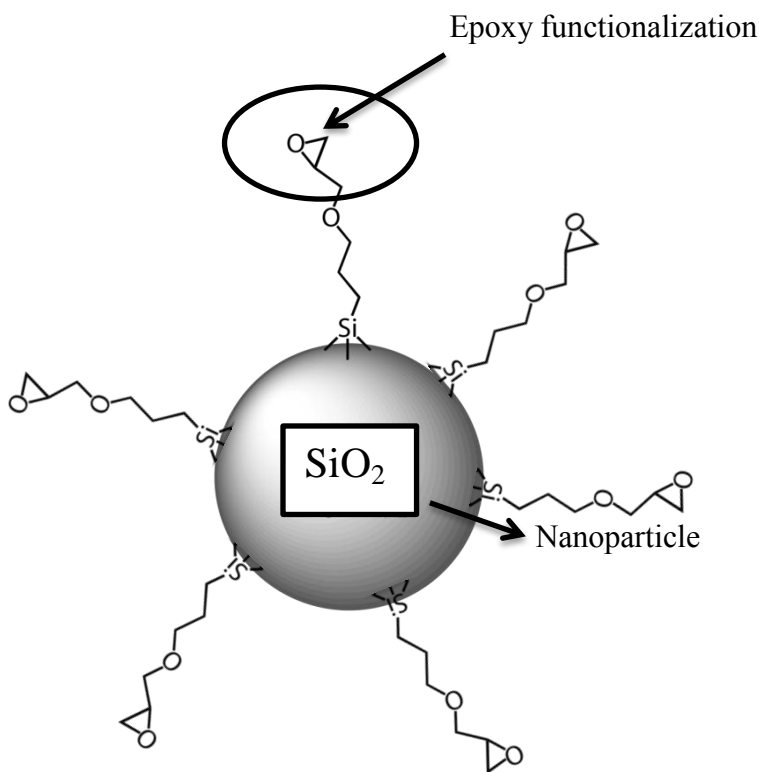


Figure 45. Epoxy functionalized silica nanoparticles

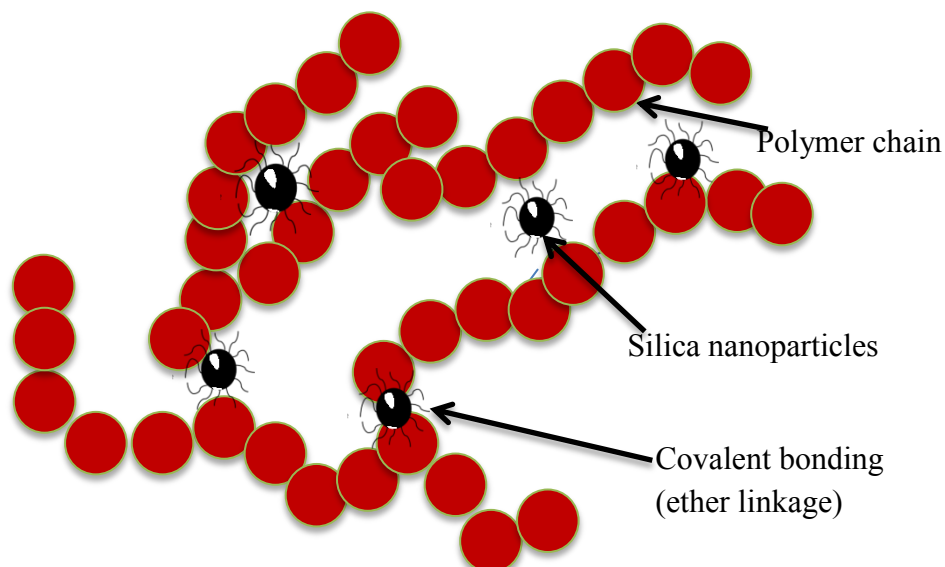


Figure 46. Starch like crosslinking of WMS chains with surface functionalized nanoparticles.

In the current research silica nanoparticles with epoxy functionalization, as shown in **Figure 45**, were synthesized using a simple sol-gel process. Chemical precursor $(\text{CH}_3\text{O})_3\text{Si}(\text{CH}_2)_3\text{OCH}_2\text{CHCH}_2\text{-O}$ or (3-glycidyloxypropyl)trimethoxysilane (GLYMO) was used for synthesis of epoxy functionalized silica nanoparticles.³²¹ The epoxy functionalization on the silica nanoparticles was used to crosslink the starch matrix by an etherification reaction between the epoxy ring and hydroxyl groups on starch chains. A star-like crosslinked network was expected between the nanoparticles and the starch matrix as illustrated in **Figure 46**. This strong chemical interaction between the nanoparticles and starch also prevented the uncontrollable aggregation of the particles.

Experimental methods

Materials:

Industrially pregelatinized, instantized and water soluble, pharmaceutical grade waxy maize starch (WMS) powder was obtained from Nutra Bio (Middlesex, NJ). GLYMO and sodium hydride (NaH) was obtained from Sigma Aldrich (Saint Louis, MO). Anhydrous isopropanol (iPOH), hydrochloric acid (HCl) and DMSO were obtained from VWR (West Chester, PA).

Fabrication of films:

Silica nanoparticles (GlymoNP) were synthesized from GLYMO precursor using a simple sol-gel process with HCl. This method is modified from a synthesis method previously described elsewhere.³²¹ GLYMO (2.65 g) and KCl (0.02 g) were added in a small vial placed in an ice bath and cooled to 0°C. The solution was stirred with a magnetic spin bar. 0.135 mL of 0.1M HCl was added drop by drop and stirred for 15 minutes in the ice bath. The vial was removed from the ice bath and stirred at room temperature for 15 minutes. This was followed by drop by drop addition of 0.1M HCl to the vial and the solution was stirred for another 20 minutes. In order to obtain WMS resin, starch powder (20 g) was added to 50 ml DMSO while stirring using magnetic stirrer. The powder was easily soluble in DMSO and resulted in a low viscosity, homogeneous and transparent solution. This gelatinized WMS will hence forth be referred to as WMS resin. To fabricate nanocomposite (GlymoNP-WMS), sodium hydride (NaH) in anhydrous isopropanol (iPOH) was added to increase the pH of the reaction mixture to 10. Predetermined amount of synthesized GLYMO nanoparticles (GlymoNP) was added drop by drop while mechanically shearing at high speed and pH was continuously adjusted to 10 with NaH solution. It was important to add the GlymoNP in a slow drop by drop manner, with constant shearing to ensure their uniform dispersion without aggregation. The reaction mixture

was sheared overnight, after which the pH was changed to 6 with HCl. The reaction mixture was cast on a Teflon[®] coated glass plate and the solvent was allowed to evaporate by slow drying at 50°C for several (at least 3) days in an air circulating oven. The nanocomposite with 1% GlymoNP (w/w with respect to starch) is termed as (GlymoNP(1%)-WMS) and with 5% GlymoNP was called (GlymoNP(5%)-WMS).

Solid State Nuclear Magnetic Resonance (NMR):

The dry film specimens were ball milled for 5 minutes to grind into fine powder. It was important to make sure there was no lump. Solid state NMR spectra of the specimen were collected to identify any ether bond formation as a result of reaction between starch and epoxy ring in GlymoNP. ¹³C and ²⁹Si CP MAS (cross polarized magic angle spinning) NMR spectra were recorded on a Varian Inova 400 NMR spectrometer, operating at 100.6 and 795.0 MHz for ¹³C and ²⁹Si, respectively.

Attenuated total reflectance–Fourier transform infrared (ATR-FTIR) analysis:

ATR-FTIR spectra of WMS resin, (GlymoNP(1%)-WMS) and (GlymoNP(5%)-WMS) were collected using a Nicolet Magna 560 FTIR spectrometer with a split pea accessory for ATR. Each ATR-FTIR scan was an average of 150 scans recorded from 4000 cm⁻¹ to 550 cm⁻¹ wavenumbers obtained at a resolution of 4 cm⁻¹.

Transmission Electron Microscopy (TEM):

Nanocomposite specimens (films) were microtomed at room temperature using Leica UCT Cryo ultramicrotome (Germany) equipped with a sapphire knife. Ultrathin sections (≈100 nm) were picked up using a copper grid with acetone on the surface. The specimens were examined using FEI Technai G2 T12 Spirit TEM (Hillsboro, Oregon, USA) operating at an acceleration voltage of 120 kV.

Thermogravimetric Analysis (TGA) and Differential TGA (DTGA):

Native WMS resin as well as nanocomposite (GlymoNP-WMS) specimens were scanned from 25°C to 600°C using a thermogravimetric analyzer (TGA-2050, TA Instruments, Inc., New Castle, DE) at a rate of 10°C/min in nitrogen atmosphere to characterize their thermal stability and degradation behavior. Differential TGA (DTGA) plots were constructed from the TGA thermograms.

Differential Scanning Calorimetry (DSC):

Approximately 15 mg specimen was scanned from 0 to 300°C, using DSC (model-Q200, TA Instruments, Inc., New Castle, DE) at a rate of 10°C/min. The heat flow and temperature calibrations were performed according to ASTM E968-99 and E967-97 procedures, respectively, using Indium thermograms. The maximum temperature limit of 300°C for the scans were chosen based on the TGA results.

Film Solubility:

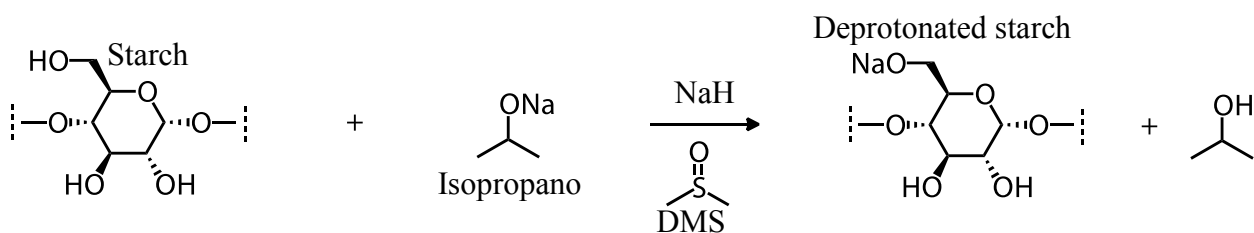
WMS resin and GlymoNP-WMS nanocomposite films were soaked in water at room temperature for 24 hours to characterize their solubility and the change after forming nanocomposite.

Results and Discussions.

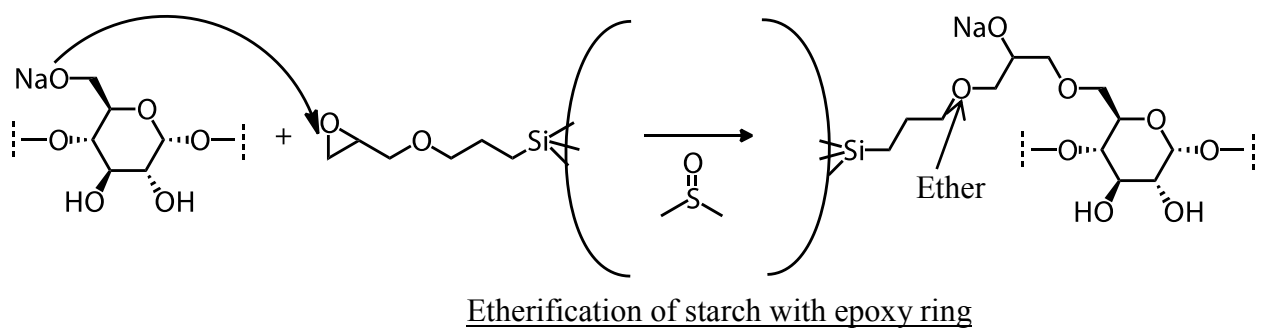
Chemical reaction:

As per **Scheme 4**, in the first step starch solubilized in DMSO is deprotonated by NaH. The deprotonated starch opens the epoxy ring in a nucleophilic attack forming an ether linkage. Since there can be several epoxy groups on a nanoparticle, the crosslinking of starch with nanoparticles can occur easily.

Deprotonation of starch



Etherification of starch



Scheme 4. Crosslinking reaction of WMS with epoxy functionalized silica nanoparticles.

Solid State Nuclear Magnetic Resonance Spectroscopy (Solid state NMR):

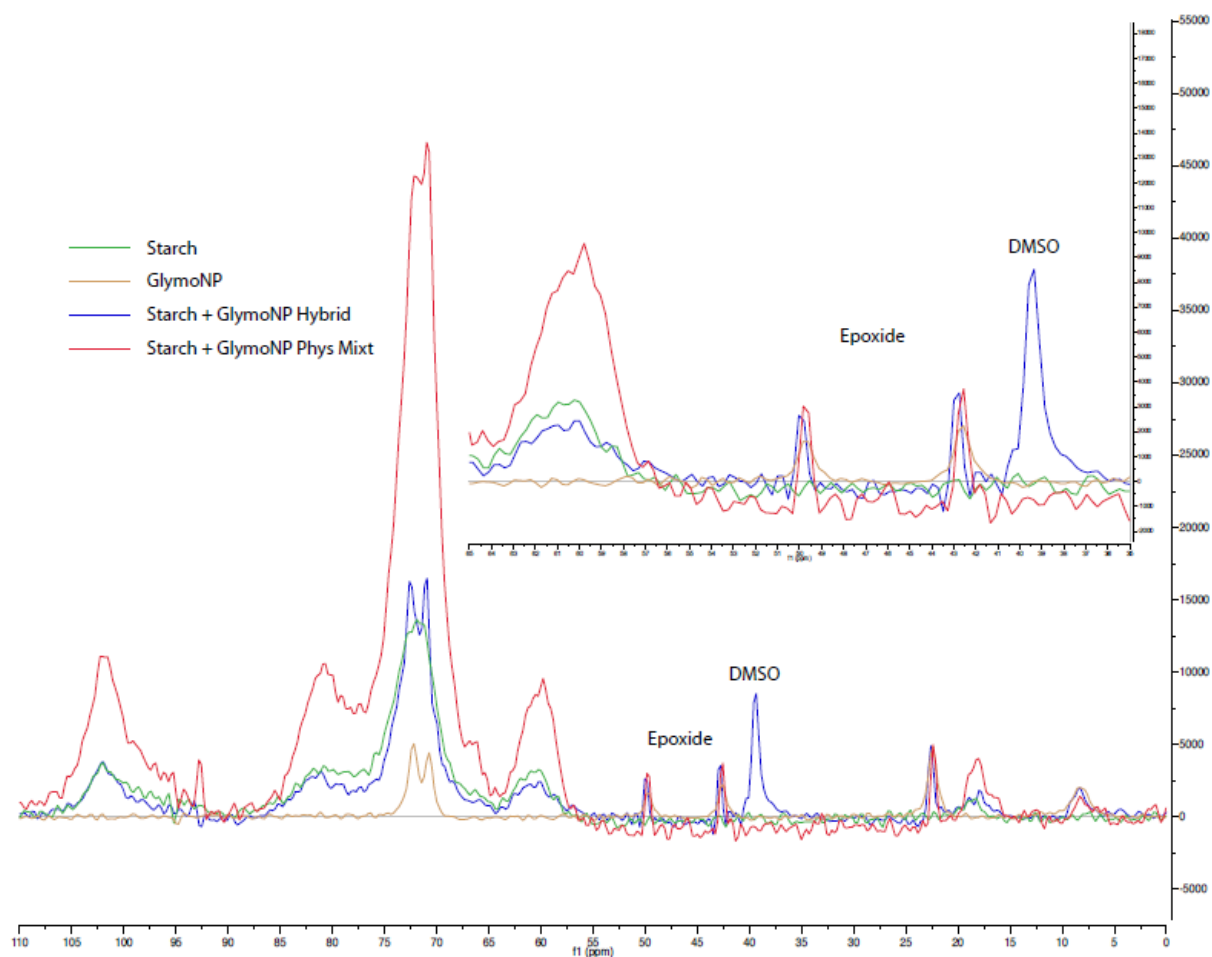


Figure 47. NMR spectra comparing WMS epoxy functionalized silica nanoparticles (GlymoNP), nanocomposite (or hybrid) of WMS and GlymoNP, physical mixture of WMS and glymo NP.

The solid state NMR spectra comparing starch, epoxy functionalized silica nanoparticles (GlymoNP), nanocomposite (or hybrid) of starch and GlymoNP, physical mixture of starch and glymoNP, as shown in **Figure 47**, did not reveal any significant change as a result of GlymoNP incorporation. The nanocomposite spectrum was similar to that of the GlymoNP and WMS physical mixture. It is possible, that formation of ether linkage of epoxy ring with starch was not detected, due to the abundance of ether linkages already present in WMS resin leading to overlapping of spectra.

Attenuated total reflectance–Fourier transform infrared (ATR-FTIR) analysis:

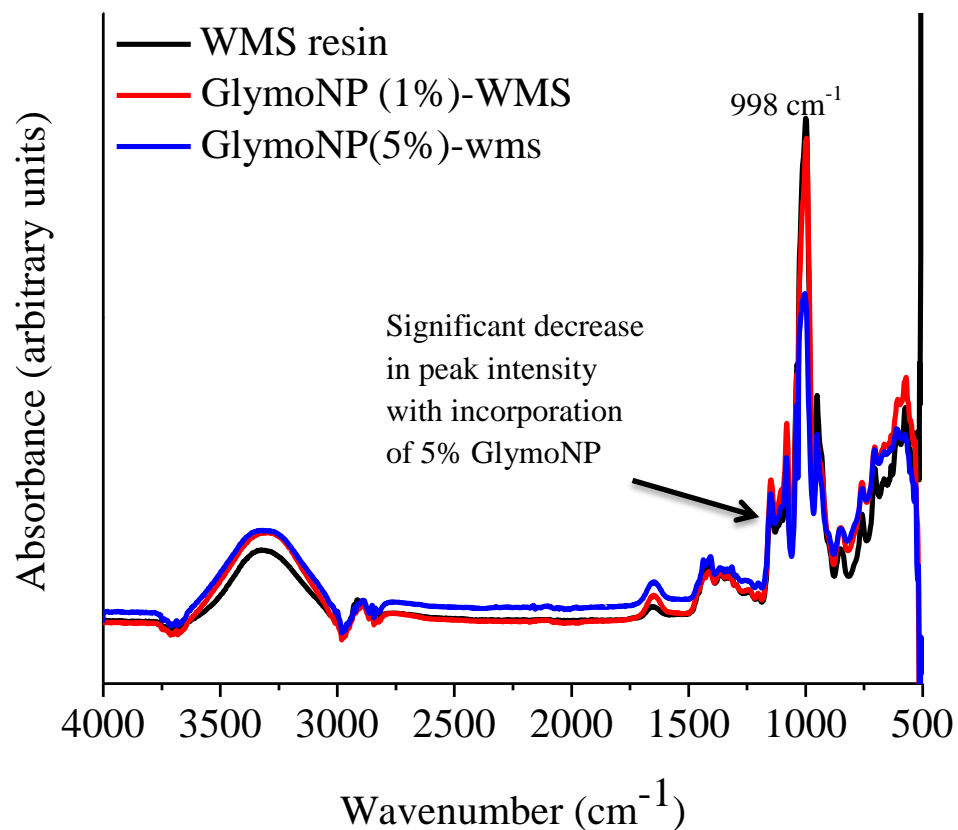


Figure 48. ATR-FTIR spectra comparing neat WMS resin, GlymoNP(1%)-WMS and GlymoNP(5%)-WMS nanocomposites.

In order to confirm the etherification reaction ATR-FTIR spectra of the WMS resin, GlymoNP(1%)-WMS and GlymoNP(5%)-WMS nanocomposite specimens were collected and are presented in **Figure 48**. All the three ATR-FTIR spectra were almost identical except for the peak at 998 cm⁻¹ where the absorbance decreased with increase in GlymoNP loading in the nanocomposite. The peak at 998 cm⁻¹ corresponds to the C-O stretching (C-O-H bond). The decrease in peak intensity of C-O stretching with increase in GlymoNP nanoparticles indicates a decrease in the number of C-O-H bond. This suggests successful etherification reaction of GlymoNP with WMS. However, as mentioned in the case of NMR results, due to the presence

of abundant ether bonds in the WMS resin, it was difficult to characterize the formation of ether bond as a result of reaction with epoxide.

Solution:

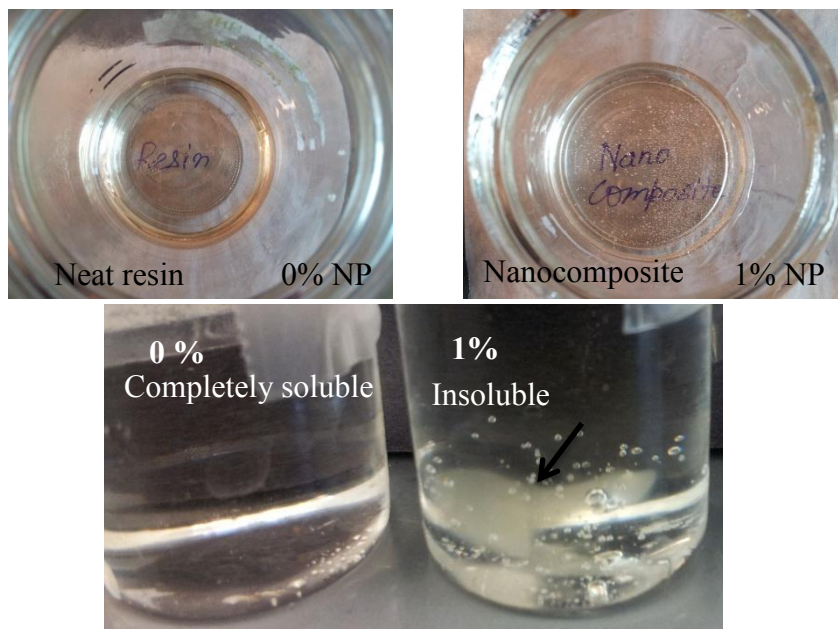


Figure 49. Solution of (A) neat resin (WMS) and (B) nanocomposite: both transparent indicating homogeneous distribution of nanoparticles and no clustering or coagulation (C) WMS resin and GlymoNP(1%)-WMS composite film soaked in water: WMS resin is completely soluble while GlymoNP(1%)-WMS nanocomposite is insoluble indicating crosslinking or formation of strong network structure.

Native starch is inherently hydrophilic and soluble in water. The WMS resin used in this research dissolves in water easily. However, once reacted with the nanoparticles the nanocomposite films do not dissolve in water even after 24 hours at room temperature as is clear from **Figure 49**. This indicates crosslinking of starch through ether linkage. This prevents small molecules including water to enter the starch network and dissolve the polymer.

Transmission Electron Microscopy (TEM):

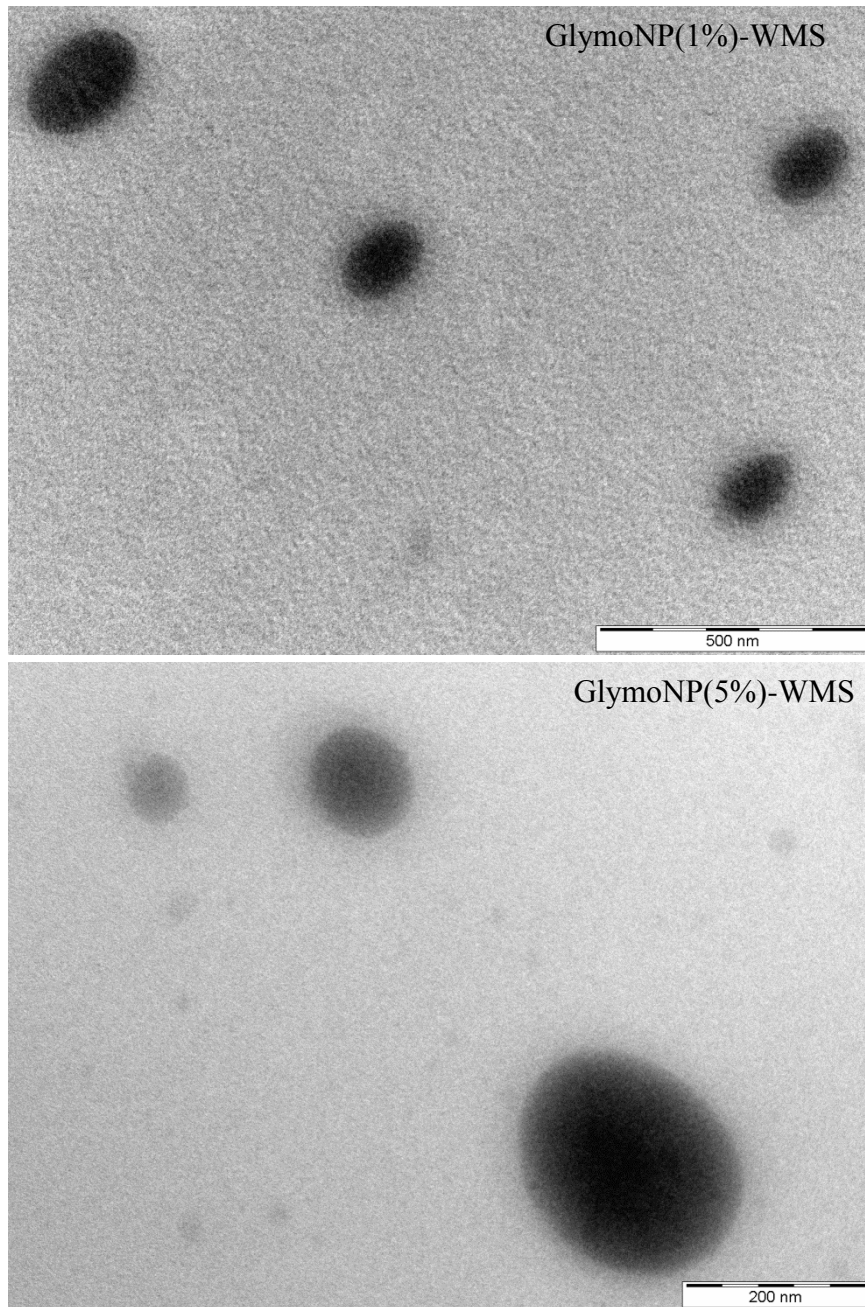


Figure 50. TEM image of GlymoNP(1%)-WMS and GlymoNP(5%)-WMS nanocomposites.

TEM image of GlymoNP(1%)-WMS and GlymoNP(5%)-WMS nanocomposite films are shown in **Figure 50**. No large aggregation or clusters of silica nanoparticles were observed in the TEM images as can be seen in **Figure 50**. The TEM image nanocomposite with 1% silica nanoparticles (GlymoNP(1%)-WMS) showed the average particle size was around 100 nm. The specimen with 5% silica nanoparticles (GlymoNP(5%)-WMS) showed a broader size distribution than the one with 1% GlymoNP. The size of the particles varied from 50 nm to 200 nm. The nanoparticles, however, appear to be homogeneously distributed which is an improvement over previously reported nanocomposites.^{315, 317} It is expected that the anchoring or immobilizing of the functionalized silica particles, due to etherification reaction, in the polymer matrix can prevent large scale aggregation of the particles as observed here. The nanoparticles were uniform and homogeneously distributed in the starch matrix.

TGA and DTG:

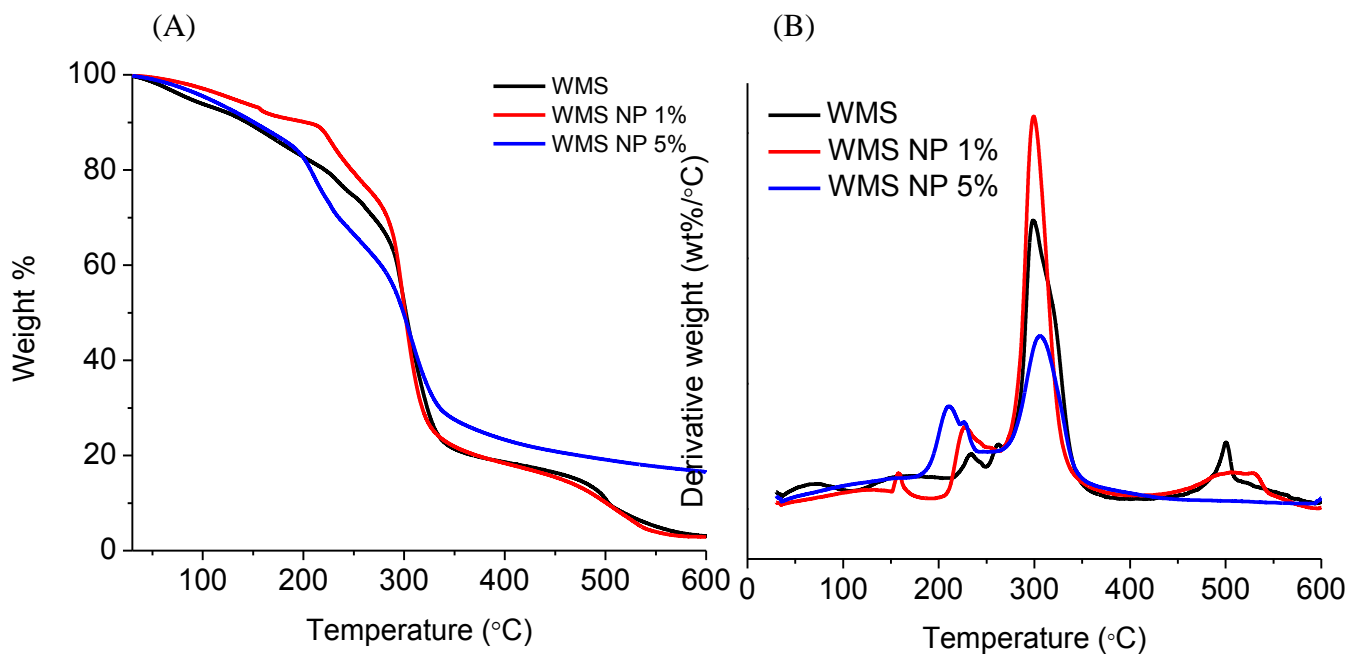


Figure 51. (A) TGA, (B) DTGA for WMS resin and GlymoNP-WMS nanocomposite films.

Figure 51 shows the TGA and DTGA for WMS resin and GlymoNP-WMS nanocomposite films. No increase in initial degradation temperature was observed in **Figure 51** (A), as addition of nanoparticles (GlymoNP) did not significantly alter the degradation mechanism of WMS polymer. Liu et al.³¹⁵ observed an increase in the initial degradation temperature with the incorporation of silica nanoparticles in polymethylmethacrylate (PMMA) polymer. It was reasoned that the increase in degradation temperature was not due to a change in the degradation mechanism or increase in thermal stability of the polymers, rather it was a result of excess inorganic materials in the nanocomposite which did not disintegrate at that temperature. The nanocomposite film contained relatively small amount of organic polymer.³¹⁵ The pure WMS DTGA shows two peaks for degradation. The first peak may possibly be from the evaporation of residual solvent. The peak appears at $\approx 230^{\circ}\text{C}$ for WMS resin and GlymoNP(1%)-WMS nanocomposite, but shifts to 210°C for GlymoNP(5%)-WMS nanocomposite. The reason for this peak shift is not well understood but is definitely related to

the increase in the loading of nanoparticles and possible aggregation. The second weight loss (at $\approx 290^{\circ}\text{C}$) corresponds to the degradation of WMS. From the DTGA it was concluded that incorporation of the nanoparticles (GlymoNP) did not alter the degradation mechanism in the polymers. In other words, the thermal stability of WMS was not enhanced as a result of silica nanoparticle incorporation.

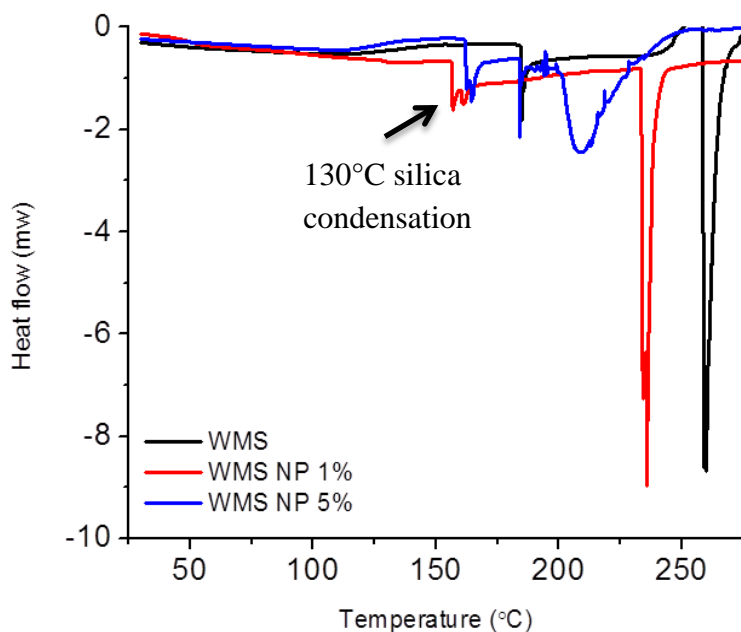


Figure 52. DSC thermograms DSC plots for WMS resin and GlymoNP-WMS nanocomposite films.

Figure 52 shows the DSC thermogram of WMS and GlymoNP-WMS nanocomposite. DSC thermogram indicated silica condensation at 130°C in the nanocomposite specimen.

REFERENCES

1. S. Raimondi, H. Johansson, P. Maisonneuve and S. Gandini, *Carcinogenesis*, 2009, **30**, 1170-1180.
2. P. J. Barham and A. Keller, *J Polym Sci Pol Phys*, 1986, **24**, 69-77.
3. Z. M. Chi, F. Wang, Z. Chi, L. X. Yue, G. L. Liu and T. Zhang, *Appl Microbiol Biot*, 2009, **82**, 793-804.
4. J. Blazek, H. Salman, A. L. Rubio, E. Gilbert, T. Hanley and L. Copeland, *Carbohydrate Polymers*, 2009, **75**, 705-711.
5. J. T. Kim and A. N. Netravali, *J Adhes Sci Technol*, 2010, **24**, 203-215.
6. G. Chen, *Chemical Society Reviews*, 2009, **38**, 2434-2446.
7. D. E. Henton, P. Gruber, J. Lunt and J. Randall, eds., *Natural Fibers, Biopolymers, and Biocomposites*, Taylor and Francis, 2005.
8. X. Huang and A. Netravali, *Compos Sci Technol*, 2009, **69**, 1009-1015.
9. R. E. Rundle, L. Daasch and D. French, *Journal of the American Chemical Society*, 1944, **66**, 130-134.
10. X. Huang and A. N. Netravali, *Compos Sci Technol*, 2009, **69**, 1009-1025.
11. R. Lohmar, J. W. Sloan and C. E. Rist, *Journal of the American Chemical Society*, 1950, **72**, 5717-5720.
12. P. J. Barham, *J Mater Sci*, 1984, **19**, 3826-3834.
13. J. J. G. vanSoest and J. F. G. Vliegenthart, *Trends in Biotechnology*, 1997, **15**, 208-213.
14. T. A. Waigh, I. Hopkinson, A. M. Donald, M. F. Butler, F. Heidelbach and C. Riekel, *Macromolecules*, 1997, **30**, 3813-3820.
15. Y. Poirier, C. Nawrath and C. Somerville, *Bio-Technol*, 1995, **13**, 142-150.
16. N. Reddy and Y. Q. Yang, *Food Chemistry*, 2010, **118**, 702-711.
17. A. N. Jyothi, S. N. Moorthy and K. N. Rajasekharan, *Starch-Starke*, 2006, **58**, 292-299.
18. Z. H. Ao and J. L. Jane, *Carbohydrate Polymers*, 2007, **67**, 46-55.
19. W. M. Kulicke, Y. A. Aggour and M. Z. Elsabee, *Starch-Starke*, 1990, **42**, 134-141.
20. J. D. Gargulak and S. E. Lebo, eds., *Commercial Use of Lignin-Based Materials*, American Chemical Society, 2000.
21. P. T. Martone, J. M. Estevez, F. Lu, K. Ruel, M. W. Denny, C. Somerville and J. Ralph, *Current Biology*, 2008, **19**, 169-175.
22. E. S. Stevens, ed., *Green Plastics: An Introduction to the New Science of Biodegradable Plastics*, 2001.
23. M. Labet and W. Thielemans, *Chemical Society Reviews*, 2009, **38**, 3484-3504.
24. L. Montague, *Lignin Process Design Confirmation and Capital Cost Evaluation*, Report 42002/02, National Renewable Energy Laboratory, Golden, Colorado, 2003.
25. <http://www.matweb.com/reference/tensilestrength.aspx>.
26. K. M. Stridsberg, M. Ryner and A. C. Albertsson, *Adv Polym Sci*, 2002, **157**, 41-65.
27. M. Singh, S. K. S. Patel and V. C. Kalia, *Microb Cell Fact*, 2009, **8**.
28. C. Tappero, S. Barbero, S. Costantino, M. Bergui, R. Ropolo, G. Bradac and G. Gandini, *Radiologia Medica*, 2009, **114**, 595-607.
29. S. Luo, D. T. Grubb and A. N. Netravali, *Polymer*, 2002, **43**, 4159-4166.
30. W. D. Luzier, *Proc. Natl. Acad. Sci.*, 1992, **89**, 839-842.
31. S. Luo and A. N. Netravali, *Polym Composite*, 1999, **20**, 367-378.
32. S. Luo and A. N. Netravali, *Polym Degrad Stabil*, 2003, **80**, 59-66.

33. C. D. Gaudio, E. Ercolani, F. Nanni and A. Bianco, *Materials Science and Engineering A*, 2011, **528**, 1764–1772.
34. S. Luo and A. N. Netravali, *J Adhes Sci Technol*, 2001, **15**, 423-437.
35. R. A. Slepecky and W. T. Starmer, *Mycologia*, 2009, **101**, 823-832.
36. A. C. Albertsson and I. K. Varma, *Adv Polym Sci*, 2002, **157**, 1-40.
37. N. Teramoto, S. Masahiko, J. Kuriowa, M. Shibatar and Y. Yosomia, *Journal of Applied Polymer Science*, 2001, **82**, 2273-2280.
38. S. Dutkiewicz, D. Grochowska-Łapienis and W. Tomaszewski, *FIBRES & TEXTILES in Eastern Europe*, 2003, **11**, 66-70.
39. M. Viljanmaa, A. Soderg and P. Tormalaa, *International Journal of Adhesion & Adhesives*, 2002, **22**, 219–226.
40. V.Herlban, J.SKara, E.Sturdik and J.Ilavsk, *BIOTECHNOLOGY TECHNIQUES*, 1993, **7**, 63-68.
41. M. Tamada, A. A. Begum and S. Sadi, *Journal of Fermentation and Bioengineering*, 1992, **74**, 379-383.
42. A. Södergård and M. Stolt, eds. R. A. Auras, L.-T. Lim, S. E. M. Selke and H. Tsuji, 2010.
43. Y. M. Harshe, G. Storti, M. Morbidelli, S. Gelosa and D. Moscatelli, *Macromolecular Symposium*, 2007, **259**, 116-123.
44. D. K. Yoo, D. Kim and D. S. Lee, *Macromolecular Research*, 2005, **13**, 68-72.
45. K. A. Porter, 2006, pp. 25-32.
46. A. Sodergard and M. Stolt, *Progress in polymer science*, 2002, **27**, 1123-1163.
47. A. Gonzalez, M. C. Strumia and C. I. A. Igarzabal, *Journal of Food Engineering*, 2011, **106**, 331-338.
48. P. R. Gruber, *Journal of Industrial Ecology*, 2004, **7**, 209-213.
49. Y. L. Margaretha Söderqvist Lindblad, Ann-Christine Albertsson, and S. K. Elisabetta Ranucci.
50. J. P. Hogge, T. P. Goodman, S. Alberti, F. Albajar, K. A. Avramides, P. Benin, S. Bethuys, W. Bin, T. Bonicelli, A. Bruschi, S. Cirant, E. Droz, O. Dumbrajs, D. Fasel, F. Gandini, G. Gantenbein, S. Illy, S. Jawla, J. Jin, S. Kern, P. Lavanchy, C. Lievin, B. Marletaz, P. Marmillod, A. Perez, B. Piosczyk, I. Pagonakis, L. Porte, T. Rzesnickl, U. Siravo, M. Thumm and M. Q. Tran, *Fusion Science and Technology*, 2009, **55**, 204-212.
51. M. Rivoire, M. Malerba and A. Gandini, *Bulletin Du Cancer*, 2008, **95**, 1177-1181.
52. <http://en.wikipedia.org/wiki/Chitin>.
53. M. S. Kim, K. S. Seo, G. Khang and H. B. Lee, *Macromol Rapid Comm*, 2005, **26**, 643-648.
54. P. J. Barham, A. Keller, E. L. Otun and P. A. Holmes, *J Mater Sci*, 1984, **19**, 2781-2794.
55. R. P. Martins, P. H. Buschang and L. G. Gandini, *American Journal of Orthodontics and Dentofacial Orthopedics*, 2009, **135**, 182-189.
56. H. J. Jin, B. Y. Lee, M. N. Kim and J. S. Yoon, *J Polym Sci Pol Phys*, 2000, **38**, 1504-1511.
57. R. Bhardwaj, A. K. Mohanty, L. T. Drzal, F. Pourboghraat and M. Misra, *Biomacromolecules*, 2006, **7**, 2044-2051.
58. M. S. Huda, A. K. Mohanty, L. T. Drzal, E. Schut and M. Misra, *Journal of Materials Science*, 2005, **40**, 4221-4229.

59. W. J. Liu, M. Misra, P. Askeland, L. T. Drzal and A. K. Mohanty, *Polymer*, 2005, **46**, 2710-2721.
60. E. S. Stevens, *Biocycle*, 2003, **44**, 24-27.
61. E. S. Stevens, *Biocycle*, 2002, **43**, 42-45.
62. C. S. Pereira, A. M. Cunha, R. L. Reis, B. Vazquez and J. San Roman, *Journal of Materials Science-Materials in Medicine*, 1998, **9**, 825-833.
63. K. D. Pereira, *Ciencia E Tecnologia De Alimentos*, 2007, **27**, 88-92.
64. R. L. Reis, A. M. Cunha, P. S. Allan and M. J. Bevis, *Advances in Polymer Technology*, 1997, **16**, 263-277.
65. A. V. Reis, M. R. Guilherme, T. A. Moia, L. H. C. Mattoso, E. C. Muniz and E. B. Tambourgi, *Journal of Polymer Science Part a-Polymer Chemistry*, 2008, **46**, 2567-2574.
66. P. Tomasik and C. H. Schilling, *Advances in Carbohydrate Chemistry and Biochemistry*, Vol 59, 2004, **59**, 175-403.
67. A. L. Chaudhary, M. Miler, P. J. Torley, P. A. Sopade and P. J. Halley, *Carbohydrate Polymers*, 2008, **74**, 907-913.
68. A. L. Chaudhary, P. J. Torley, P. J. Halley, N. McCaffery and D. S. Chaudhary, *Carbohydrate Polymers*, 2009, **78**, 917-925.
69. J. J. G. vanSoest, S. H. D. Hulleman, D. deWit and J. F. G. Vliegenthart, *Industrial Crops and Products*, 1996, **5**, 11-22.
70. X. Du, J. Jia, S. Xu and Y. Zhou, *Starch - Stärke*, 2007, **59**, 609-613.
71. P. J. Jenkins, R. E. Cameron, A. M. Donald, W. Bras, G. E. Derbyshire, G. R. Mant and A. J. Ryan, *Journal of Polymer Science Part B-Polymer Physics*, 1994, **32**, 1579-1583.
72. S. Simsek, M. C. Tulbek, Y. Yao and B. Schatz, *Food Chemistry*, 2009, **115**, 832-838.
73. S. Mishra and T. Rai, *Food Hydrocolloids*, 2006, **20**, 557-566.
74. J. Blazek and L. Copeland, *Carbohydrate Polymers*, 2008, **71**, 380-387.
75. J. Blazek and L. Copeland, *Journal of Cereal Science*, 2010, **51**, 265-270.
76. T. A. Waigh, A. M. Donald, F. Heidelbach, C. Riekkel and M. J. Gidley, *Biopolymers*, 1999, **49**, 91-105.
77. A. Imberty, H. Chenzy and S. Perez, *J. Mol. Biol.*, 1998, **201**, 365-378.
78. A. Imberty and S. Perez, *Biopolymers*, 1988, **27**, 1205-1221.
79. M. S. Izydorczyk, A. W. MacGregor and C. G. Billiaderis, *Journal of the Institute of Brewing*, 2001, **107**, 119-128.
80. K. Lorenz and K. Kulp, *Starch - Stärke*, 2006, **34**, 50-54.
81. R. Hoover and T. Vasanthan, *Carbohydrate Research*, 1994, **252**, 33-53.
82. R. Hoover, T. Vasanthan, N. J. Senanayake and A. M. Martin, *Carbohydrate Research*, 1994, **261**, 13-24.
83. S. Varavinit, S. Shobsngob, W. Varanyanond, P. Chinachoti and O. Naivikul, *Starch-Starke*, 2003, **55**, 410-415.
84. H. S. Liu, L. Yu, G. Simon, K. Dean and L. Chen, *Carbohydrate Polymers*, 2009, **77**, 662-669.
85. K. Krogars, J. Heinamaki, M. Karjalainen, J. Rantanen, P. Luukkonen and J. Yliruusi, *European Journal of Pharmaceutics and Biopharmaceutics*, 2003, **56**, 215-221.
86. V. M. Leloup, P. Colonna, S. G. Ring, K. Roberts and B. Wells, *Carbohydrate Polymers*, 1992, **18**, 189-197.
87. R. K. Bayer and F. J. Balta-Calleja, *Journal of Applied Polymer Science*, 2007, **104**, 689-696.

88. R. Zullo and S. Iannace, *Carbohydrate Polymers*, 2009, **77**, 376-383.
89. P. Myllarinen, A. Buleon, R. Lahtinen and P. Forssell, *Carbohydrate Polymers*, 2002, **48**, 41-48.
90. D. Lourdin, G. DellaValle and P. Colonna, *Carbohydrate Polymers*, 1995, **27**, 261-270.
91. L. D., V. G.D. and C. P., *Carbohydrate Polymers*, 1995, **27**, 261-270.
92. S. Chillo, S. Flores, M. Mastromatteo, A. Conte, L. Gerschenson and M. A. Del Nobile, *Journal of Food Engineering*, 2008, **88**, 159-168.
93. S. D. Yoon, S. H. Chough and H. R. Park, *Journal of Applied Polymer Science*, 2006, **100**, 3733-3740.
94. Y. H. Yun, Y. H. Na and S. D. Yoon, *Journal of Polymers and the Environment*, 2006, **14**, 71-78.
95. Y. Wu, F. Y. Geng, P. R. Chang, J. G. Yu and X. F. Ma, *Carbohydrate Polymers*, 2009, **76**, 299-304.
96. S. Mathew and T. E. Abraham, *Food Chemistry*, 2007, **105**, 579-589.
97. O. B. Wurzburg, *Nutrition Reviews*, 1986, **44**, 74-79.
98. P. Buwalda, *Abstracts of Papers of the American Chemical Society*, 2008, **236**, -.
99. A. S. Ayoub and S. S. H. Rizvi, *Journal of Plastic Film & Sheeting*, 2009, **25**, 25-45.
100. Y. X. Chen and G. Y. Wang, *Journal of Applied Polymer Science*, 2006, **102**, 1539-1546.
101. G. J. Mao, P. Wang, X. S. Meng, X. Zhang and T. Zheng, *Journal of Applied Polymer Science*, 2006, **102**, 5854-5860.
102. L. Passauer, F. Liebner and K. Fischer, *Starch-Starke*, 2009, **61**, 621-627.
103. C. E. Morris, N. M. Morris and B. J. TraskMorrell, *Industrial & Engineering Chemistry Research*, 1996, **35**, 950-953.
104. C. Q. Yang and X. L. Wang, *Fourier Transform Spectroscopy*, 1998, **753**, 661-664.
105. C. Q. Yang and G. B. Zhang, *Research on Chemical Intermediates*, 2000, **26**, 515-528.
106. Y. A. Aggour, *Starch-Starke*, 1993, **45**, 55-59.
107. L. Kunaik and R. H. Marchessault, *Starch - Stärke*, 2006, **2006**, 110-116.
108. D. Ackar, J. Babic, D. Subaric, M. Kopjar and B. Milicevic, *Carbohydrate Polymers*, 2010, **81**, 76-82.
109. K. P. R. Kartha and H. C. Srivastava, *Starke*, 1985, **37**, 270-276.
110. G. Hamdi, G. Ponchel and D. Duchene, *Journal of Microencapsulation*, 2001, **18**, 373-383.
111. G. E. Hamerstrand, B. T. Hofreiter and C. L. Mehlretter, *Cereal Chemistry*, 1960, **37**, 519-524.
112. I. Simkovic, J. A. Laszlo and A. R. Thompson, *Carbohydrate Polymers*, 1996, **30**, 25-30.
113. G. Hamdi and G. Ponchel, *Pharmaceutical Research*, 1999, **16**, 867-875.
114. C. Katepetch and R. Rujiravanit, *Abstracts of Papers of the American Chemical Society*, 2008, **236**, -.
115. L. Passauer, H. Bender and S. Fischer, *Carbohydrate Polymers*, 2010, **82**, 809-814.
116. L. M. Zhang, G. H. Wang and H. W. Lu, *Journal of Bioactive and Compatible Polymers*, 2005, **20**, 491-501.
117. V. M. Limberger, L. P. da Silva, T. Emanuelli, C. G. Comarela and L. D. Patias, *Quimica Nova*, 2008, **31**, 84-88.
118. A. Blennow, S. B. Engelsen, T. H. Nielsen, L. Baunsgaard and R. Mikkelsen, *Trends in Plant Science*, 2002, **7**, 445-450.

119. P. Deetae, S. Shobsngob, W. Varayanond, P. Chinachoti, O. Naivikul and S. Varavinit, *Carbohydrate Polymers*, 2008, **73**, 351-358.
120. M. Z. Sitohy and M. F. Ramadan, *Starch-Starke*, 2001, **53**, 27-34.
121. M. Z. Sitohy, S. M. Labib, S. S. El-Saadany and M. F. Ramadan, *Starch-Starke*, 2000, **52**, 95-100.
122. M. Gui-Jie, W. Peng, M. Xiang-Sheng, Z. Xing and Z. Tong, *Journal of Applied Polymer Science*, 2006, **102**, 5854-5860.
123. L. Kunlan, X. Lixin, L. Jun, P. Jun, C. Guoying and X. Zuwei, *Carbohydr Res*, 2001, **331**, 9-12.
124. L. Passauer, F. Liebner and K. Fischer, *Starch-Starke*, 2009, **61**, 628-633.
125. L. P. Passauer and K. Fischer, *Abstracts of Papers of the American Chemical Society*, 2008, **235**, 1053.
126. D. Demirgoz, C. Elvira, J. F. Mano, A. M. Cunha, E. Piskin and R. L. Reis, *Polymer Degradation and Stability*, 2000, **70**, 161-170.
127. J. Mulhbacher, P. Ispas-Szabo, V. Lenaerts and M. A. Mateescu, *Journal of Controlled Release*, 2001, **76**, 51-58.
128. J. Mulhbacher, P. Ispas-Szabo and M. A. Mateescu, *International Journal of Pharmaceutics*, 2004, **278**, 231-238.
129. J. Mulhbacher and M. A. Mateescu, *International Journal of Pharmaceutics*, 2005, **297**, 22-29.
130. K. Takahashi, A. Ogata, W. H. Yang and M. Hattori, *Bioscience Biotechnology and Biochemistry*, 2002, **66**, 1276-1280.
131. T. Heinze and A. Koschella, *Macromolecular Symposia*, 2005, **223**, 13-39.
132. T. Heinze, T. Liebert, U. Heinze and K. Schwikal, *Cellulose*, 2004, **11**, 239-245.
133. T. Heinze, K. Pfeiffer, T. Liebert and U. Heinze, *Starch-Starke*, 1999, **51**, 11-16.
134. D. C. Bastos, A. E. F. Santos, M. L. J. da Silva and R. A. Simao, *Ultramicroscopy*, 2009, **109**, 1089-1093.
135. R. L. Whistler and G. E. Hilbert, *Ind Eng Chem*, 1944, **36**, 796-798.
136. I. A. Wolff, D. W. Olds and G. E. Hilbert, *Ind Eng Chem*, 1951, **43**, 911-914.
137. J. H. He, J. Liu and G. Y. Zhang, *Biomacromolecules*, 2008, **9**, 175-184.
138. M. M. Tessler and R. L. Billmers, *Journal of Environmental Polymer Degradation*, 1996, **4**, 85-89.
139. R. L. Billmers and M. M. Tessler, *Abstracts of Papers of the American Chemical Society*, 1996, **212**, 10-Cell.
140. R. L. Billmers and M. M. Tessler, *Abstracts of Papers of the American Chemical Society*, 1995, **209**, 114-PMSE.
141. H. S. Choi, H. S. Kim, C. S. Park, B. Y. Kim and M. Y. Baik, *Carbohydrate Polymers*, 2009, **78**, 862-868.
142. H. Chi, K. Xu, X. L. Wu, Q. Chen, D. H. Xue, C. Song, W. Zhang and P. X. Wang, *Food Chemistry*, 2008, **106**, 923-928.
143. D. L. Phillips, D. H. Pan, H. J. Liu and H. Corke, *Analytical Letters*, 1998, **31**, 2105-2114.
144. S. N. Moorthy, *Starke*, 1985, **37**, 307-308.
145. A. D. Betancur, G. L. Chel and H. E. Canizares, *Journal of Agricultural and Food Chemistry*, 1997, **45**, 378-382.

146. X. Wang, W. Y. Gao, L. M. Zhang, P. G. Xiao, L. P. Yao, Y. Liu, K. F. Li and W. G. Xie, *Science in China Series B-Chemistry*, 2008, **51**, 859-865.
147. H. A. M. Wickramasinghe, K. Yamamoto, H. Yamauchi and T. Noda, *Food Science and Biotechnology*, 2009, **18**, 118-123.
148. A. Boutboul, P. Giampaoli, A. Feigenbaum and V. Ducruet, *Carbohydrate Polymers*, 2002, **47**, 73-82.
149. M. Elomaa, T. Asplund, P. Soininen, R. Laatikainen, S. Peltonen, S. Hyvarinen and A. Urtti, *Carbohydrate Polymers*, 2004, **57**, 261-267.
150. J. M. Fang, P. A. Fowler, J. Tomkinson and C. A. S. Hill, *Carbohydrate Polymers*, 2002, **47**, 245-252.
151. R. L. Shogren, *Carbohydrate Polymers*, 2003, **52**, 319-326.
152. R. L. Shogren and A. Biswas, *Carbohydrate Polymers*, 2006, **64**, 16-21.
153. P. Raatikainen, O. Korhonen, S. Peltonen and P. Paronen, *Drug Development and Industrial Pharmacy*, 2002, **28**, 165-175.
154. M. I. Khalil, A. Hashem and A. Hebeish, *Starch-Starke*, 1995, **47**, 394-398.
155. F. B. Aiyeleye, J. O. Akingbala and G. B. Oguntimein, *Starch-Starke*, 1993, **45**, 443-445.
156. J. Babic, D. Subaric, D. Ackar, M. Kopjar and N. N. Tiban, *Journal of Food Science and Technology-Mysore*, 2009, **46**, 423-426.
157. B. Daramola and G. O. Adegoke, *Journal of Food Agriculture & Environment*, 2007, **5**, 50-54.
158. Y. X. Xu, V. Miladinov and M. A. Hanna, *Cereal Chemistry*, 2004, **81**, 735-740.
159. N. Singh, D. Chawla and J. Singh, *Food Chemistry*, 2004, **86**, 601-608.
160. O. Korhonen, P. Raatikainen, P. Harjunen, J. Nakari, E. Suihko, S. Peltonen, M. Vidgren and P. Paronen, *Pharmaceutical Research*, 2000, **17**, 1138-1143.
161. H. J. Liu, L. Ramsden and H. Corke, *Carbohydrate Polymers*, 1997, **34**, 283-289.
162. P. A. M. Steeneken and A. J. J. Woortman, *Carbohydrate Research*, 2008, **343**, 2278-2284.
163. A. B. Das, G. Singh, S. Singh and C. S. Riar, *Carbohydrate Polymers*, 2010, **80**, 725-732.
164. L. Mirmoghtadaie, M. Kadivar and M. Shahedi, *Food Chemistry*, 2009, **116**, 709-713.
165. K. J. Shon and B. Yoo, *Starch-Starke*, 2006, **58**, 177-185.
166. A. B. Das, G. Singh, S. Singh and C. S. Riar, *Carbohydrate Polymers*, 2009, **80**, 725-732.
167. A. Cizova, A. Koschella, T. Heinze, A. Ebringerova and I. Srokova, *Starch-Starke*, 2007, **59**, 482-492.
168. E. Abdollahzadeh, M. Mehranian and F. Vahabzadeh, *Starch-Starke*, 2008, **60**, 398-407.
169. A. N. Jyothi, K. N. Rajasekharan, S. N. Moorthy and J. Sreekumar, *Starch-Starke*, 2005, **57**, 556-563.
170. J. He, J. Liu and G. Zhang, *Biomacromolecules*, 2008, **9**, 175-184.
171. D. Betancur-Ancona, E. Garcia-Cervera, E. Canizares-Hernandez and L. Chel-Guerrero, *Starch-Starke*, 2002, **54**, 540-546.
172. P. N. Bhandari and R. S. Singhal, *Carbohydrate Polymers*, 2002, **48**, 233-240.
173. J. D. Ntawukulilyayo, C. Vervaet, J. P. Remon, J. P. Gortz and J. A. Berlo, *International Journal of Pharmaceutics*, 1996, **139**, 79-85.
174. J. D. Ntawukulilyayo, S. C. DeSmedt, J. Demeester and J. P. Remon, *International Journal of Pharmaceutics*, 1996, **128**, 73-79.
175. L. F. Wang, R. L. Shogren and J. L. Willett, *Abstracts of Papers of the American Chemical Society*, 1997, **213**, 254-PMSE.

176. Y. S. Jeon, A. Viswanathan and R. A. Gross, *Starch-Starke*, 1999, **51**, 90-93.
177. P. C. Trubiano, *Abstracts of Papers of the American Chemical Society*, 1994, **208**, 151-AGFD.
178. R. L. Shogren, A. Viswanathan, F. Felker and R. A. Gross, *Starch-Starke*, 2000, **52**, 196-204.
179. A. N. Jyothi, K. N. Raiasekharan, S. N. Moorthy and J. Sreekumar, *Starch-Starke*, 2005, **57**, 319-324.
180. L. L. Ren, M. Jiang, J. Tong, X. Bai, X. G. Dong and J. A. Zhou, *Carbohydrate Polymers*, 2010, **82**, 1010-1013.
181. Z. Q. Liu, Y. Li, F. J. Cui, L. F. Ping, J. M. Song, Y. Ravee, L. Q. Jin, Y. P. Xue, J. M. Xu, G. Li, Y. J. Wang and Y. G. Zheng, *Journal of Agricultural and Food Chemistry*, 2008, **56**, 11499-11506.
182. S. D. Zhang, Y. R. Zhang, H. X. Huang, B. Y. Yan, X. Zhang and Y. Tang, *J Polym Res*, 2010, **17**, 43-51.
183. W. Y. Jang, B. Y. Shin, T. X. Lee and R. Narayan, *Journal of Industrial and Engineering Chemistry*, 2007, **13**, 457-464.
184. J. M. Raquez, Y. Nabar, M. Srinivasan, B. Y. Shin, R. Narayan and P. Dubois, *Carbohydrate Polymers*, 2008, **74**, 159-169.
185. J. M. Raquez, Y. Nabar, R. Narayan and P. Dubois, *International Polymer Processing*, 2007, **22**, 463-470.
186. J. M. Raquez, Y. Nabar, R. Narayan and P. Dubois, *Polymer Engineering and Science*, 2008, **48**, 1747-1754.
187. P. Aggarwal and D. Dollimore, *Thermochimica Acta*, 1998, **324**, 1-8.
188. B. Chuenkamol, C. Puttanlek, V. Rungsardthong and D. Uttapap, *Food Hydrocolloids*, 2007, **21**, 1123-1132.
189. A. N. Jyothi, S. N. Moorthy and K. N. Rajasekharan, *Journal of the Science of Food and Agriculture*, 2007, **87**, 1964-1972.
190. W. Vorweg, J. Dijksterhuis, J. Borghuis, S. Radosta and A. Kroger, *Starch-Starke*, 2004, **56**, 297-306.
191. K. N. Waliszewski, M. A. Aparicio, L. A. Bello and J. A. Monroy, *Carbohydrate Polymers*, 2003, **52**, 237-242.
192. C. C. Seow and K. Thevamalar, *Starch-Starke*, 1993, **45**, 85-88.
193. F. O. Onofre and Y. J. Wang, *International Journal of Pharmaceutics*, 2010, **385**, 104-112.
194. M. Wootton and A. Manatsathit, *Starke*, 1983, **35**, 92-94.
195. M. Wootton and A. Manatsathit, *Starke*, 1984, **36**, 207-208.
196. L. E. Butler, D. D. Christianson, J. C. Scheerens and J. W. Berry, *Starch-Starke*, 1986, **38**, 156-159.
197. R. Hoover, D. Hannouz and F. W. Sosulski, *Starch-Starke*, 1988, **40**, 383-387.
198. H. Liu, L. Ramsden and H. Corke, *Carbohydrate Polymers*, 1999, **40**, 175-182.
199. R. A. De Graaf and L. P. B. M. Janssen, *Advances in Polymer Technology*, 2003, **22**, 56-68.
200. L. Kaur, N. Singh and J. Singh, *Carbohydrate Polymers*, 2004, **55**, 211-223.
201. D. Lafargue, B. Pontoire, A. Buleon, J. L. Doublier and D. Lourdin, *Biomacromolecules*, 2007, **8**, 3950-3958.
202. A. Bayazeed, S. Farag, S. Shaarawy and A. Hebeish, *Starch-Starke*, 1998, **50**, 89-93.

203. A. Jonhed and L. Jarnstrom, *Starch-Starke*, 2003, **55**, 569-575.
204. R. E. Wing, W. M. Doane and C. R. Russell, *Journal of Applied Polymer Science*, 1975, **19**, 847-854.
205. P. B. Zamudio-Flores, A. V. Torres, R. Salgado-Delgado and L. A. Bello-Perez, *Journal of Applied Polymer Science*, 2010, **115**, 991-998.
206. Y. S. Wu and P. A. Seib, *Cereal Chemistry*, 1990, **67**, 202-208.
207. C. S. Raina, S. Singh, A. S. Bawa and D. C. Saxena, *European Food Research and Technology*, 2006, **223**, 561-570.
208. O. V. Lopez, M. A. Garcia and N. E. Zaritzk, *Carbohydrate Polymers*, 2008, **73**, 573-581.
209. S. B. Kalambur and S. S. Rizvi, *Polymer International*, 2004, **53**, 1413-1416.
210. Y. L. Chung, S. Ansari, L. Estevez, S. Hayrapetyan, E. P. Giannelis and H. M. Lai, *Carbohydrate Polymers*, 2010, **79**, 391-396.
211. I. Kvien, J. Sugiyama, M. Votrubic and K. Oksman, *Journal of Materials Science*, 2007, **42**, 8163-8171.
212. I. Arvanitoyannis, A. Nakayama and S. Aiba, *Carbohydrate Polymers*, 1998, **36**, 105-119.
213. I. Arvanitoyannis, E. Psomiadou, A. Nakayama, S. Aiba and N. Yamamoto, *Food Chemistry*, 1997, **60**, 593-604.
214. E. M. Teixeira, A. L. Da Roz, A. J. F. Carvalho and A. A. S. Curvelo, *Carbohydrate Polymers*, 2007, **69**, 619-624.
215. A. J. F. Carvalho, A. A. S. Curvelo and A. Gandini, *Industrial Crops and Products*, 2005, **21**, 331-336.
216. D. Thirathumthavorn and S. Charoenrein, *Starch-Starke*, 2007, **59**, 493-497.
217. M. Petersson and M. Stading, *Food Hydrocolloids*, 2005, **19**, 123-132.
218. S. K. Fischer and F. Piller, *Starke*, 1977, **29**, 232-235.
219. H. J. Chung, B. Yoo and S. T. Lim, *Starch-Starke*, 2005, **57**, 354-362.
220. N. N. Hellman, B. Fairchild and F. R. Senti, *Cereal Chemistry*, 1954, **31**, 495-505.
221. C. G. Biliaderis and J. Zawistowski, *Cereal Chemistry*, 1990, **67**, 240-246.
222. Y. J. Kim, T. Hagiwara, K. Kawai, T. Suzuki and R. Takai, *Carbohydrate Polymers*, 2003, **53**, 289-296.
223. Y. Cho, G. Yi, S. Kim, S. Jeon, M. T. Elsesser, H. K. Yu, S. Yang and D. J. Pine, *Chemistry of Materials*, 2009, **19**, 3183-3193.
224. T. Mita, *Carbohydrate Polymers*, 1992, **17**, 269-276.
225. A. Rindlav, S. H. D. Hulleman and P. Gatenholm, *Carbohydrate Polymers*, 1997, **34**, 25-30.
226. H. G. Bader and D. Goritz, *Starch-Starke*, 1994, **46**, 229-232.
227. A. M. Leeman, M. E. Karlsson, A. C. Eliasson and I. M. E. Bjorck, *Carbohydrate Polymers*, 2006, **65**, 306-313.
228. T. Ishigaki, Y. Kawagoshi, M. Ike and M. Fujita, *World Journal of Microbiology & Biotechnology*, 1999, **15**, 321-327.
229. M. Tarvainen, R. Sutinen, S. Peltonen, P. Tiihonen and P. Paronen, *Journal of Pharmaceutical Sciences*, 2002, **91**, 282-289.
230. M. Tarvainen, R. Sutinen, S. Peltonen, H. Mikkonen, J. Maunus, K. Vaha-Heikkila, V. P. Lehto and P. Paronen, *European Journal of Pharmaceutical Sciences*, 2003, **19**, 363-371.

231. S. C. Pang, S. F. Sun, S. H. Tay and F. M. Tchong, *Carbohydrate Polymers*, 2011, **84**, 424-429.
232. S. J. Wang, J. G. Yu and J. L. Yu, *Journal of Polymers and the Environment*, 2006, **14**, 65-70.
233. A. V. Torres, P. B. Zamudio-Flores, R. Salgado-Delgado and L. A. Bello-Perez, *Journal of Applied Polymer Science*, 2007, **106**, 3994-3999.
234. J. F. Zhu, G. H. Zhang and Z. C. Lai, *Polymer-Plastics Technology and Engineering*, 2007, **46**, 1135-1141.
235. D. Lafargue, D. Lourdin and J. L. Doublier, *Carbohydrate Polymers*, 2007, **70**, 101-111.
236. J. A. Kenar, F. C. Felker, G. Biresaw and T. L. Kurth, *Industrial Crops and Products*, 2009, **29**, 45-52.
237. G. Biresaw, A. Adhvaryu and S. Z. Erhan, *Journal of the American Oil Chemists Society*, 2003, **80**, 697-704.
238. G. Biresaw and R. Shogren, *Journal of Synthetic Lubrication*, 2008, **35**, 17-30.
239. G. Biresaw and C. J. Carriere, *Journal of Polymer Science Part B-Polymer Physics*, 2001, **39**, 920-930.
240. F. Bossard, I. Pillin, T. Aubry and Y. Grohens, *Polymer Engineering and Science*, 2008, **48**, 1862-1870.
241. X. D. Cao, P. R. Chang and M. A. Huneault, *Carbohydrate Polymers*, 2008, **71**, 119-125.
242. Y. P. Wu, Q. Qi, G. H. Liang and L. Q. Zhang, *Carbohydrate Polymers*, 2006, **65**, 109-113.
243. Y. X. Xu and M. A. Hanna, *Carbohydrate Polymers*, 2005, **59**, 521-529.
244. M. C. Saha, M. E. Kabir and S. Jeelani, *Materials Science and Engineering A-Structural Materials Properties Microstructure and Processing*, 2008, **479**, 213-222.
245. I. Arvanitoyannis, M. Kalichevsky, J. M. V. Blanshard and E. Psomiadou, *Carbohydrate Polymers*, 1994, **24**, 1-15.
246. J. J. G. vanSoest and P. Essers, *Journal of Macromolecular Science-Pure and Applied Chemistry*, 1997, **A34**, 1665-1689.
247. C. Lan, L. Yu, P. Chen, L. Chen, W. Zou, G. Simon and X. Q. Zhang, *Macromolecular Materials and Engineering*, 2010, **295**, 1025-1030.
248. N. Reddy and Y. Q. Yang, *Biotechnology and Bioengineering*, 2009, **103**, 1016-1022.
249. I. Pashkuleva, H. S. Azevedo and R. L. Reis, *Macromolecular Bioscience*, 2008, **8**, 210-219.
250. I. Pashkuleva, A. P. Marques, F. Vaz and R. L. Reis, *Journal of Materials Science-Materials in Medicine*, 2005, **16**, 81-92.
251. M. I. Santos, I. Pashkuleva, C. M. Alves, M. E. Gomes, S. Fuchs, R. E. Unger, R. L. Reis and C. J. Kirkpatrick, *Journal of Materials Chemistry*, 2009, **19**, 4091-4101.
252. C. Seidel, W. Kulicke, C. He, B. Hartmann, M. D. Lechner and W. Lazik, *Starch*, 2001, **53**, 305-310.
253. S. Garg and A. K. Jana, *Carbohydrate Polymers*, 2011, **83**, 1623-1630.
254. O. Sauperl and K. Stana-Kleinschek, *Text Res J*, 2010, **80**, 383-392.
255. S. Mathew and T. E. Abraham, *Food Hydrocolloids*, 2008, **22**, 826-835.
256. V. Coma, I. Sebti, P. Pardon, F. H. Pichavant and A. Deschamps, *Carbohydrate Polymers*, 2003, **51**, 265-271.
257. Y. H. Yun, Y. J. Wee, H. S. Byun and S. D. Yoon, *Journal of Polymers and the Environment*, 2008, **16**, 12-18.

258. J. Zhou, J. Zhang, Y. Ma and J. Tong, *Carbohydrate Polymers*, 2008, **74**, 405-410.
259. C. Q. Yang, Y. P. Lu and G. C. Lickfield, *Textile Research Journal*, 2002, **72**, 817-824.
260. R. Bhosale and R. Singhal, *Carbohydrate Polymers*, 2006, **66**, 521-527.
261. H. F. Zobel, *Starch-Starke*, 1988, **40**, 1-7.
262. S. Chabba and A. N. Netravali, *Journal of Material Science*, 2005, **40**, 6263-6273.
263. S. Chabba, G. F. Matthews and A. N. Netravali, *Green Chemistry*, 2005, **7**, 576-581.
264. T. Ghosh Dastidar and A. N. Netravali, *Journal of Biobased Materials and Bioenergy*, 2012, **2009**, 1-124.
265. T. Ghosh Dastidar and A. Netravali, *Carbohyd Polym*, Article in press.
266. H. Kumar, M. V. Hosur and A. N. Netravali, *Journal of Adhesion Science and Technology*, 2010, **24**, 217-236.
267. P. Myllarinen, R. Partanen, J. Seppala and P. Forssell, *Carbohyd Polym*, 2002, **50**, 355-361.
268. A. Lopez-Rubio, J. M. Lagaron, M. Ankerfors, T. Lindstrom, D. Nordqvist, A. Mattozzi and M. S. Hedenqvist, *Carbohyd Polym*, 2007, **68**, 718-727.
269. D. Plackett, H. Anturi, M. Hedenqvist, M. Ankerfors, M. Gallstedt, T. Lindstrom and I. Siro, *J Appl Polym Sci*, 2010, **117**, 3601-3609.
270. E. Chiellini, P. Cinelli, V. I. Hieva and M. Martera, *Biomacromolecules*, 2008, **9**, 1007-1013.
271. K. Qiu and A. N. Netravali, *Composites Science & Technology*, In Press, 2012.
272. C. Q. Yang, *J Appl Polym Sci*, 1993, **50**, 2047-2053.
273. C. Q. Yang, Y. F. Xu and D. J. Wang, *Ind Eng Chem Res*, 1996, **35**, 4037-4042.
274. C. Q. Yang and X. L. Wang, *J Polym Sci Pol Chem*, 1997, **35**, 557-564.
275. C. Q. Yang and D. J. Wang, *Text Res J*, 2000, **70**, 615-620.
276. J. T. Kim and A. N. Netravali, *Journal of Agricultural and Food Chemistry*, 2010, **58**, 5400-5407.
277. K. Qiu and A. N. Netravali, *Composites Science & Technology*, 2012, **72**, 1588-1594.
278. X. Huang and A. N. Netravali, *Journal of Macromolecular Science, Part A: Pure and Applied Chemistry*, 2008, **45**, 899-906.
279. C. Q. Yang, *Text Res J*, 2001, **71**, 201-206.
280. P. Lodha and A. N. Netravali, *J. Mater. Sci.*, 2002, **37**, 3657-3665.
281. A. N. Netravali, R. Henstenburg, S. L. Phoenix and P. Schwartz, *Polymer Composites*, 1989, **10**, 226-241.
282. Y. Yamamoto, D. Zahora and A. N. Netravali, *Composite Interfaces*, 2007, **14**, 699-713.
283. K. Li, X. Geng, J. Simonsen and J. Karchesy, *Int J Adhes Adhes*, 2004, **24**, 327-333.
284. Y. Liu and K. C. Li, *Int J Adhes Adhes*, 2007, **27**, 59-67.
285. T. G. Dastidar and A. N. Netravali, *J Biobased Mater Bio*, 2012, **6**, 1-24.
286. *Australia Pat.*, US4272295, 1979.
287. *United States Pat.*, US4297144, 1979.
288. *United States Pat.*, US4424291, 1984.
289. *United States Pat.*, US4687332, 1985.
290. *United States Pat.*, US20110311784, 2011.
291. *United States Pat.*, US 5306749 1994.
292. T. G. Dastidar and A. Netravali, *In preparation*, 2012.
293. A. N. Netravali and S. Chabba, *Materials Today*, 2003, 22-29.

294. N. Supanchaiyamat, P. S. Shuttleworth, A. J. Hunt, J. H. Clark and A. S. Matharu, *Green Chemistry*, 2012, **14**.
295. D. R. Erickson, ed., *In Industrial Uses for Soybeans in Practical Handbook of Soybean Processing and Utilization*, AOCS Press, Champaign, IL, 1995.
296. R. Nakamura, A. N. Netravali, A. B. Morgan, M. R. Nyden and J. W. Gilman, *Fire and Materials*, 2012.
297. S. Chabba and A. N. Netravali, *J. Mater. Sci.*, 2005, **40**, 6275-6282
298. A. N. Netravali, in *Biodegradable Natural Fiber Composites*, ed. R. S. Blackburn, Woodhead Publishing Limited, Cambridge, 2005, pp. 271-309.
299. S. B. M. Yasir, K. H. Sutton, M. P. Newberry, N. R. Andrews and J. A. Gerrard, *Food Chem*, 2007, **104**, 1502-1508.
300. S. K. Park, D. H. Bae and K. C. Rhee, *Journal of the American Oil Chemists' Society*, 2000, **77**.
301. A. González, M. C. Strumia and C. I. A. Igarzabal, *Journal of Food Engineering*, 2011, **106**.
302. S. K. Lingamoorthy, Master of Science, Cornell University, 2010.
303. A. M. Velarde, P. Bartl, T. E. W. Nießen and W. F. Hoelderich, *Journal of Molecular Catalysis A: Chemical*, 2000, **157**.
304. M. Comotti, C. D. Pina, E. Falletta and M. Rossi, *Adv. Synth. Catal*, 2005, **348**.
305. D. Dewit, R. Vandenberg, L. Anders, M. Johansson, F. Vanrantwijk, L. Maat and A. P. G. Kieboom, *Carbohydr Res*, 1992, **226**, 253-260.
306. C. B. Barlow, R. D. Guthrie and A. M. Prior, *Chem Commun*, 1966, 268-&.
307. P. L. Bragda, H. v. Bekkumb and A.C. Besemerc, *Topics in Catalysis*, 2004, **27**, 1-4.
308. S. p. Trombotto, E. Violet-Courtenbs, L. Cottierb and Y. Queneau, *Topics in Catalysis*, 2004, **27**, 1-4.
309. S. p. Trombotto, A. Bouchu, G. r. Descotes and Y. Queneau*, *Tetrahedron Letters*, 2000, **41**, 8273–8277.
310. P. Lodha and A. N. Netravali, *Polymer composites*, 2005 **26**, 647-659.
311. X. Huang and A. N. Netravali, *Biomacromolecules*, 2006, **7**, 2783-2789.
312. S. K. Park, D. H. Bae and K. C. Rhee, *Journal of the American Oil Chemists' Society* 2000, **77**.
313. X. S. Huang and A. Netravali, *Compos Sci Technol*, 2007, **67**, 2005-2014.
314. P. Lodha and A. N. Netravali, *Composites Science and Technology*, 2005, **65**, 1211-1225.
315. Y.-L. Liu, C.-Y. Hsu and K.-Y. Hsu, *Polymer*, 2005, **46**, 1851–1856.
316. M. Darder, P. Aranda and E. Ruiz-Hitzky, *Advanced Materials*, 2007, **19**, 1309–1319.
317. D. Ciprari, K. Jacob and R. Tannenbaum, *Macromolecules*, 2006, **39**, 6565-6573.
318. K. Frosta, J. Barthesa, D. Kaminskia, E. Lascarib, J. Nierea and R. Shanks, *Carbohydrate Polymers*, 2011, **84**, 343–350.
319. H. Zou, S. Wu and J. Shen, *Chemical Reviews*, 2008, **108**, 3893–3957.
320. Y.-J. Kim, S.-W. Ha, S.-M. Jeon, D. W. Yoo, S.-H. Chun, B.-H. Sohn and J.-K. Lee, *Langmuir*, 2010, **26**, 7555–7560.
321. M. Tenzplin, U. Wiesner and H. W. Spiess, *Advanced Materials*, 1997, **9**, 814-817.